AALTO UNIVERSITY SCHOOL OF SCIENCE AND TECHNOLOGY
Faculty of Electronics, Communications and Automation
Department of Electrical Engineering

Manyazewal Tesfaye Fitta

Load Classification and Appliance Fingerprinting for Residential Load Monitoring System

Thesis submitted in partial fulfillment of the requirement for the degree of Master of Science in Technology

Espoo 13.08.2010

Thesis supervisor:
Professor Matti Lehtonen

Thesis instructor:
Professor Matti Lehtonen

AALTO UNIVERSITY SCHOOL OF SCIENCE AND TECHNOLOGY

ABSTRACT OF THE MASTER'S THESIS

AUTHOR: Manyazewal Tesfaye Fitta

TITLE: Load Classification and Appliance Fingerprinting for Residential Load Monitoring System

DATE: 13.08.2010 LANGUAGE: English NUMBER OF PAGES: 100

FACULTY: Faculty of Electronics, Communications and Automation

Department of Electrical Engineering

PROFESSORSHIP: Power Systems and High Voltage Engineering CODE: S-18

SUPERVISOR: Professor Matti Lehtonen

INSTRUCTOR: Professor Matti Lehtonen

Previous work on residential load monitoring has attempted to address different requirements including the systematic collection of information about electric power consumption for load research purpose, the provision of a detailed consumption report to facilitate energy conservation practices and the monitoring of critical loads for fault diagnostics.

This work focuses on developing methods for appliance fingerprinting that is foreseen to be an integral part of an automatic residential load monitoring system. Various approaches outlined in previous research form the basis for the concepts developed in this thesis. In addition, an extensive series of measurement work was performed on several household appliances in order to acquire the necessary operation data for building the technique and also to explore the extent up to which residential loads can be categorized into distinct groups.

The fingerprinting process proposed in this work employs three main phases: feature extraction of electrical attributes, event detection and pattern recognition. Test results obtained at different stages of the work using the measurement data are also discussed in detail.

Such studies are necessary to enable utilities to manage their networks reliably and efficiently, and also to encourage the active participation of consumers in energy conservation programs.

KEYWORDS: load monitoring, appliance fingerprinting, NIALMS, load signature, load classification, energy awareness

PREFACE

The work in this Master's thesis was carried out at the Power Systems Laboratory of Aalto University School of Science and Technology as part of the BeAware project under the supervision of Professor Matti Lehtonen. I would like to express my deep gratitude to him for allowing me to work on this high profile project and also for his constant support during my work.

It was a great pleasure to work with my colleague Solomon Biza, especially during the measurement period; in hindsight, it could have been a difficult undertaking to attempt the measurement work alone as it involved conducting numerous measurements at different locations. I also would like to thank my other colleagues at the laboratory, Tatu Nieminen and Merkebu Degefa, for their interest and helpful feedback throughout the work.

My gratitude also goes to our partners in this project, Dr. Giulio Jacucci and Arto Meriläinen of HIIT (Helsinki Institute for Information Technology) and Topi Mikkola of BaseN Corporation. Our friends at Otaniemi and Espoon keskus who allowed us access to their residences to conduct measurements also deserve big thanks. I appreciate the help William Martin provided in proofreading the final manuscript.

Finally, I would like to thank my whole family, who have always been by my side and provided me with unwavering support throughout my life.

Espoo, August 2010

Manyazewal Tesfaye Fitta

TABLE OF CONTENTS

LIST OF ABBREVIATIONS

A/D	Analog-to-Digital
BeAware	Boosting Energy Awareness with Adaptive Real-time Environments
CF	Crest Factor
DKNN	Dynamic k-Nearest Neighbor
DTW	Dynamic Time Warping
EPRI	Electric Power Research Institute
FFT	Fast Fourier Transform
FPF	Fundamental-frequency Power Factor
HIIT	Helsinki Institute for Information Technology
IALMS	Intrusive Appliance Load Monitoring System
LOOCV	Leave-one-out Cross Validation
NIALMS	Non-intrusive Appliance Load Monitoring System
NN	Nearest Neighbor
PFC	Power Factor Correction
PHS	Personal Handy-phone System
RBFN	Radial Basis Function Networks
SMPS	Switch Mode Power Supply
SVM	Support Vector Machine
THD	Total Harmonic Distortion
TID	Total Inter-harmonic Distortion
TPF	Total Power Factor
VSD	Variable Speed Drive
VTT	Valtion Teknillinen Tutkimuskeskus (Technical Research Center of Finland)

1. INTRODUCTION

The demand for electricity is growing faster than any other form of energy in all parts of the world [1]. This increasing need, coupled with the fact that coal fuels more than 40% of global electric supply, is making electricity generation the single largest and fastest rising contributor to CO_2 emissions [2]. Hence, in order to cope with growing societal and industrial needs whilst contributing less to greenhouse gas emissions, it is of paramount importance to actualize an efficient electric energy supply chain that addresses challenges in the key areas of generation, transmission, distribution and utilization. In fact, projections by the International Energy Agency show that using energy efficiently has a greater potential to curb CO_2 emissions over the next 20 years than all other options put together [1][3].

Efforts in the drive towards achieving this goal include improving the efficiency of fuel combustion in power stations, reducing transmission line losses and optimizing motor-driven systems in industries. However, often excluded from this process are end-users at household level who have traditionally held a passive role in issues related with energy conservation despite the fact that the final influence always rests with them as they decide the amount of energy to consume and in which way to utilize it. In view of this fact, it is quite evident that consumers also need to be active players in this process and research suggests that users are willing and capable to adapt their behavior to energy-saving practices if given the necessary feedback, support and incentives [4][62].

The increasing concern about the impact of energy usage on the environment as well as the rise in energy costs are arguably the main factors that encourage customers to look for ways of consuming less. Nevertheless, the major difficulty is the lack of information about day-to-day activities; for instance, energy bills are usually received at the end of each month from which it is difficult to distinguish the effects of individual actions or obtain meaningful feedback as to the effectiveness of changes [1][65]. Such problems necessitate the creation of innovative feedback mechanisms with greater transparency about the

consumption at any moment of time and the associated cost that can potentially lead to improved energy conservation practices. Current trends in the development and convergence of ICT and energy networks are ushering a range of possibilities in areas such as residential energy monitoring (measuring, processing and providing feedback in near-real-time), context-aware application and activity detection [4][5].

A highly informative aspect of such a monitoring system is the possibility to track the state of operation and corresponding energy consumption of individual household appliances. The availability of appliance operation data at this level of granularity allows utilities to provide detailed information to their customers whenever required as well as in the form of itemized billing. This in turn opens the possibility for consumers to perceive the effects of their individual day-to-day actions, which paves the way for meeting energy efficiency targets through their active participation.

In this regard, the motivation for this work was the requirement to develop a technical solution that shall enable the reliable and accurate tracking of the operation of common end-use appliances in a typical household. The term ‘appliance fingerprinting’ was conceived to express this solution due to the fact that it needs to make use of electrical characteristics (or ‘load signatures’) that each appliance uniquely possesses. With the advent of high-precision sensing devices that are capable of accurately measuring different electrical attributes of appliances [6], it is envisioned to create an innovative system that allows consumers to learn and share energy conservation strategies [4].

While contributing to the creation of such a ‘demand-response’ relationship, through which better options are provided to customers for properly managing their energy expenditures and also to utilities for assuring reliable supply at reasonable costs [7], the appliance monitoring solution can also be applied in power quality monitoring, analysis and mitigation programs. The detailed information collected regarding the electrical attributes of various residential loads, such as harmonics contents, is presumably a key input in devising ways to

tackle power quality issues, which are on a steady rise due to the increasing use of power electronic devices and other non-linear loads in industrial, commercial and domestic applications [52].

In addition to its relevance in energy consumption tracking and power quality control, appliance fingerprinting also helps to realize the following scenarios:

1. Utilities can improve planning and operation; for example, one way is to re-schedule larger loads by offering time-dependent rates to consumers so that they will be encouraged to utilize high-energy appliances at low-rate times [1][8].
2. Equipment manufacturers can improve quality and compliance, thus providing more energy efficient products to the market [9].
3. Aging and abnormally-operating appliances that consume higher amounts of energy can be spotted and remedial action can be taken [8].
4. Monitoring of individuals or systems with specific needs based on their detailed electricity usage patterns; for example, seniors living alone or remotely-operated mission-critical equipments [10].
5. Switching off non-essential loads such as air conditioners in case of emergencies if the power system is in danger of collapse [10].

In order to propose the appliance fingerprinting application, the approach taken in this thesis is as follows:

I. Review of related works in residential load monitoring techniques.

II. Conducting an extensive series of measurements on typical household appliances to attain a taxonomy of residential loads and also to determine relevant electrical attributes for the purpose of fingerprinting (such as phase shifts between harmonic currents and fundamental frequency supply voltage).

III. Development of a methodology for appliance fingerprinting (based on ideas drawn from current methods in load monitoring) within the

framework of the BeAware project (‘BeAware’ is an acronym for ‘Boosting Energy Awareness with Adaptive Real-time Environments’).

IV. Validation of the proposed solution using the available measurement data and identification of potential areas of improvement.

This work is part of the BeAware project, in which European partners from academia and industry are jointly working towards the vision of creating an active and informed consumer who is motivated to utilize energy in an efficient manner. The project has developed a solution called Energy Life to inform consumers about their consumption at the level of individual appliances [11]. As shown in Figure 1.1, the Energy Life architecture comprises three separate logical layers:

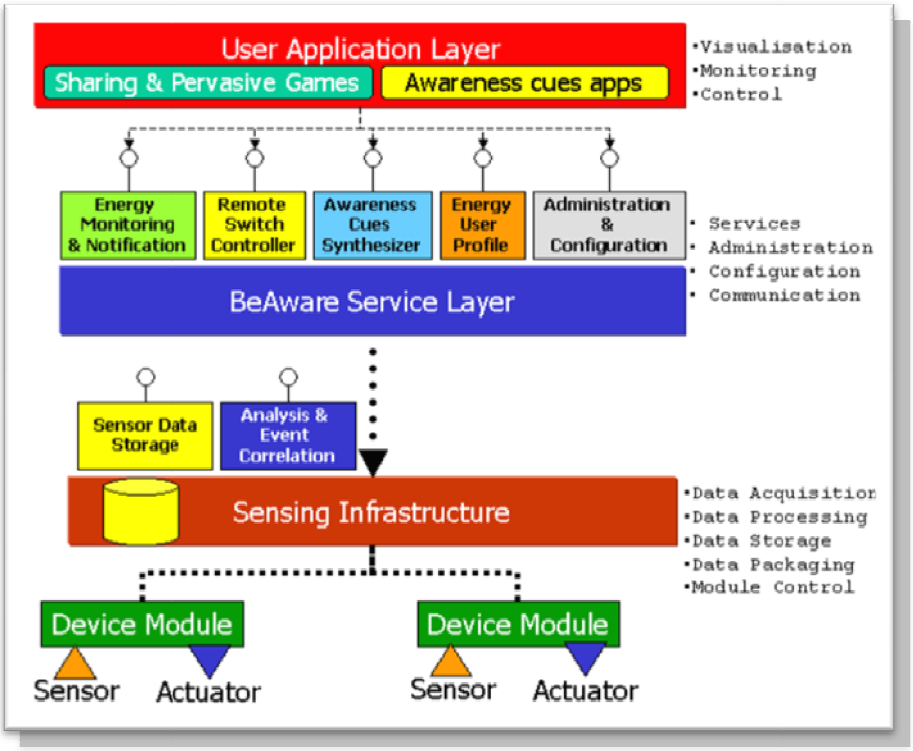

Figure 1.1: BeAware Layers [11]

1. **Sensing Platform –** provides measurement data from a wireless network of sensors and base stations. All household data are processed in the *BeAware base station*, which handles communication to all sensors and serves as a gateway to the Internet. In addition to handling BeAware

equipment, the system is designed to be capable of interfacing with third party products as well [4][11].

2. **Service Layer** – provides an open and distributed web service infrastructure oriented towards consumers and detailed analysis of consumption in households [4].
3. **User Application Layer** – provides information to the consumers and makes them an active stakeholder in the energy conservation chain [4].

The appliance fingerprinting application resides in the Sensing Platform. The basis of its operation is measurement data received from the *BeAware sensor*, which is presented in more detail in Chapter 4.

It is hoped that the solution proposed in this work will assist in the actual implementation of the fingerprinting application within the BeAware system and hence contribute its own share in the development of energy conservation services.

2. RELATED WORKS IN LOAD MONITORING

Pioneering works in load monitoring were mainly driven by the need to collect information about electric energy consumption patterns of different groups of consumers so that utilities would be able to manage their network more *efficiently*. Analysis of such gathered data allows the prediction of possible future scenarios and their effect on the network, which in turn creates the opportunity to enhance *system reliability* and *security*. There were also other areas of interest such as providing a *detailed consumption report* to facilitate efforts to reduce energy consumption and monitoring of the state of appliances for *fault diagnostics* [12][13].

2.1 TYPES OF LOAD MONITORING TECHNIQUES

Load monitoring techniques at the household level can be broadly classified as Intrusive Appliance Load Monitoring (IALM) and Non-intrusive Appliance Load Monitoring (NIALM) systems [14]. IALM refers to standard sub-metering techniques, which are able to track the operation of appliances more precisely and thus provide highly accurate data by employing a network of sensors or meters attached to individual appliances. However, the precision of sub-metered data is achieved at the expense of high installation cost, complexity and customer discomfort [14][15][56][58][62][64].

The lowest layer of the present BeAware system can be perceived as a *semi-intrusive* monitoring scheme for two reasons:

1. Its intrusiveness lies in the fact that the Sensing Platform comprises a set of wireless sensors and meters to monitor a typical household.
2. On the other hand, in contrast to conventional sub-metering techniques, it does not involve significant sensor wirings, which simplifies the installation process. A sample conventional sub-metering circuit is shown in Figure 2.1.

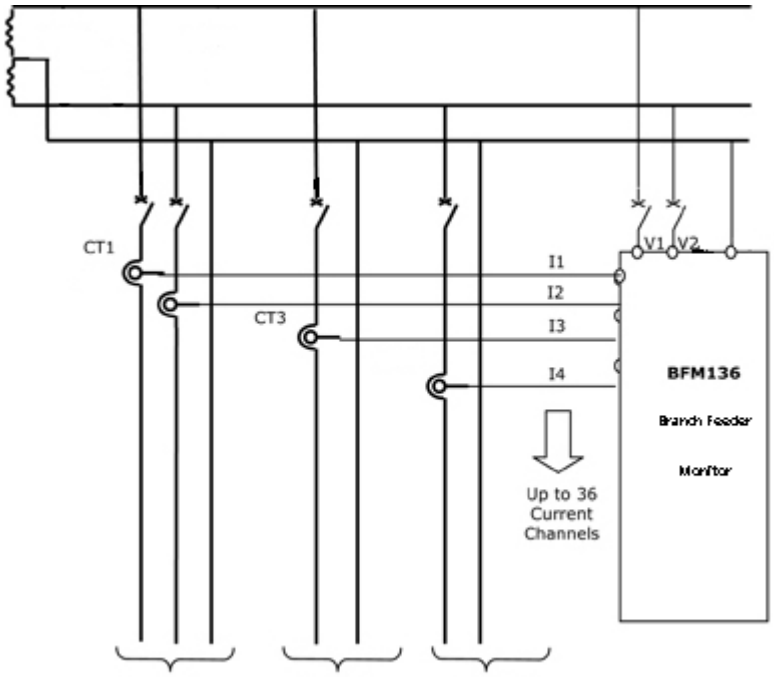

Figure 2.1: Schematic circuit of multi-channel sub-metering [16]

The future plan for the BeAware Sensing Platform is to migrate towards a whole-house sensing system that monitors the total consumption at the power entry point, which will be similar to a NIALMS operation. For this reason, the concept behind NIALMS and a number of research works related to this system were studied that are presented in the following sections.

2.2 THE NIALMS CONCEPT

Non-intrusive methods are intended to offer installation simplicity and the ability to distinguish important load changes via measurement at a central monitoring point [15]. Researchers at MIT were the early users of this technology to monitor residential and commercial end-use loads [17][18].

By analyzing measured current and voltage waveforms, NIALMS disaggregates the total load and estimates the operational states of individual loads and their energy consumption. In general, factors that affect NIALMS performance are its power measuring range, sampling rate, resolution of A/D conversion, electrical

noise in the premises and the operational variation and quantity of individual loads being monitored [15]. The system has evolved over the years through enhancements of its hardware features (such as higher sampling rates to handle transients) and improved algorithms to recognize a variety of appliances in residential as well as commercial buildings.

Central to NIALMS is the concept of *load signature* or *appliance fingerprint*, which is a characteristic that every appliance intrinsically possesses [19][58]. It is a measureable parameter of the total load that gives information about the nature and operating state of an individual appliance in the total load. Parameters which can be used as load signature include active power, harmonics content, reactive power and load transient shape [20].

Figure 2.2 illustrates different types of load signatures applied in NIALMS [21]. The choice of a particular method depends on the measuring and processing capacity of the NIALMS hardware. This choice in turn determines the algorithm to be developed for NIALMS operation.

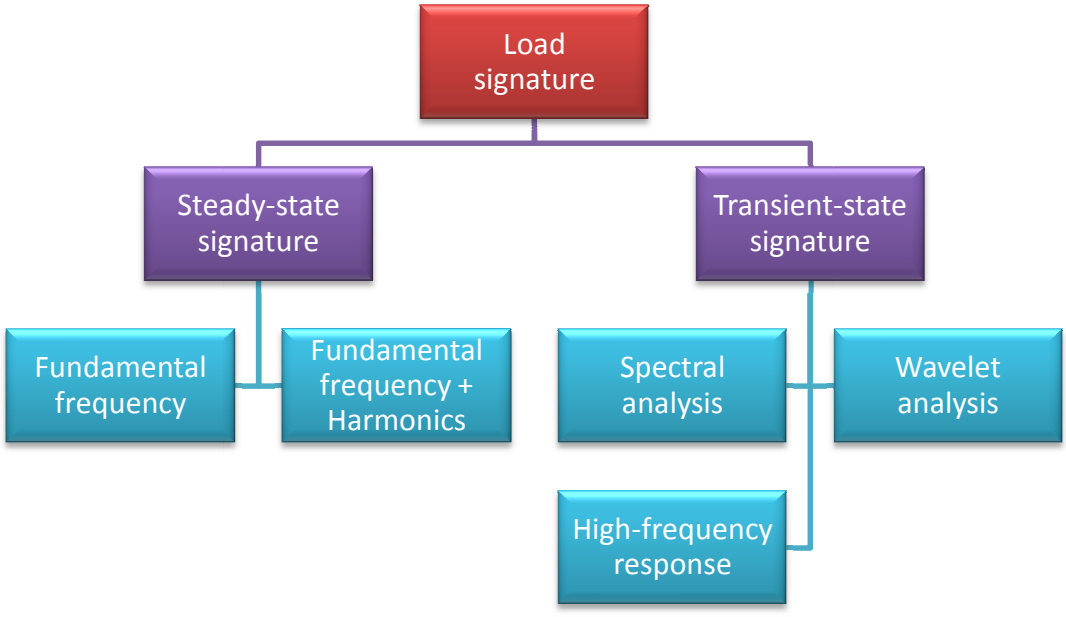

Figure 2.2: Classification of load signatures [21]

2.2.1 STEADY-STATE SIGNATURE

A. Fundamental frequency analysis

In this method, the operating states of an individual appliance are determined by identifying moments at which its active and/or reactive power consumption measurements change from one nearly constant or steady-state value to another [21]. These steady-state changes normally correspond to the appliance either turning on or turning off and are characterized by the magnitude and sign of changes in active and/or reactive power (±ΔP, ±ΔQ).

Figure 2.3 shows an example of steady-state changes of a composite load consisting of two individual appliances A and B [21]. Load identification starts with the detection of steady-state transitions of each load, which are called *events*. Previously recorded *switch-on* and *switch-off events* belonging to different appliances are stored in a *load register* and are used for matching purposes when the operation of a certain load is detected on the power line.

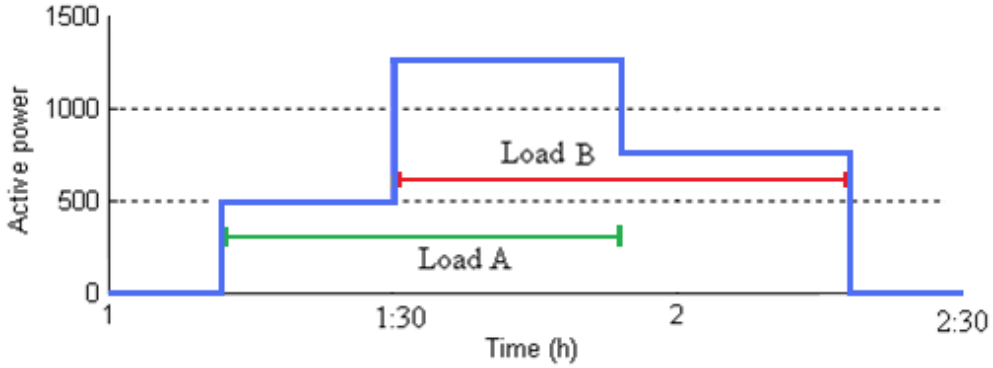

Figure 2.3: Active power changes during appliances operation [21]

The exactness of this matching technique depends on the measured system voltage. Usually, standards allow supply voltage to vary within ±10% of the nominal value [22], which in turn can cause the current to vary by ±10%. Because power (P or Q) is defined as the product of current and voltage, it can possibly vary by a further ±20%.

To overcome this variation, power is normalized according to Eq. 2.1 and 2.2:

$$P_{norm}(t) = [V_{ref}/V(t)]^2 . P(t) \quad (2.1)$$

$$Q_{norm}(t) = [V_{ref}/V(t)]^2 . Q(t) \quad (2.2)$$

Where $V(t)$, $P(t)$ and $Q(t)$ are system voltage, active power and reactive power values measured during appliance operation and V_{ref} is the nominal value of supply voltage [13]. In fact, the normalized values $P_{norm}(t)$ and $Q_{norm}(t)$ are products of admittance components and the fixed voltage V_{ref} (note that *conductance* is $P(t)/V(t)^2$ and *susceptance* is $Q(t)/V(t)^2$). Hence, power normalization allows the tracking of changes in admittance values, which are more independent of voltage variations as compared to power and current measurements [23].

The main limitations of this method are its inability to cope with rapid sequences of events generated by continuously-varying loads and lack of preciseness to distinguish between appliances with similar power consumption profiles (overlapping ±ΔP, ±ΔQ) [62].

B. Harmonic analysis

The number of appliances containing power electronic components is rising considerably in domestic applications due to the additional energy efficiency and flexibility they offer [24]. Power electronic devices are the main sources of harmonic currents [25], and this makes harmonic current signatures quite useful to identify appliances that are too similar to distinguish looking only at the fundamental frequency active and/or reactive power signatures [23].

Harmonic content is calculated by using the Fast Fourier Transform (FFT) of the input current [21][24][26][27]. A sample harmonic pattern from one of the power electronic-based appliances measured in this work is shown in Figure 2.4. As can be seen, odd-numbered harmonics at the lower end of the pattern constitute a significant share of the total harmonic current.

By combining harmonic current and fundamental frequency signatures, better identification can be achieved specially for appliances with large harmonic contents. However, harmonic analysis is less effective for highly resistive loads because their harmonic content is very small and thus difficult to discriminate. Besides, it requires steady-state measurement which means it also cannot deal with rapid sequences of events generated by continuously-varying loads.

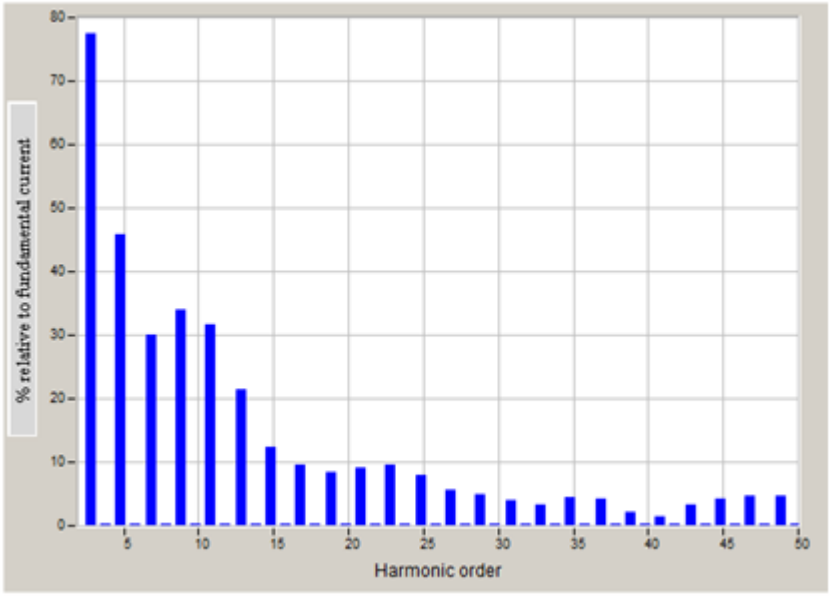

Figure 2.4: Harmonic pattern up to 50th order (15 W compact fluorescent lamp)

2.2.2 TRANSIENT SIGNATURE

Transient signatures are useful to identify appliances that exhibit similar steady-state signatures (but with unique transient turn-on characteristics) and also in situations where rapid activation of loads is common such as in commercial and industrial facilities [20]. Figure 2.5 shows the simultaneous activation of 4 loads, within 1.2 seconds of each other, and how these loads can be discerned by detecting their switch-on transients [21].

Transient profiles tend not to be eliminated even in loads which employ active wave-shaping or power factor correction [30]; in contrast, steady-state signatures are affected by harmonic mitigation and power factor correction

circuits, which homogenize steady-state behaviors, thus masking the nature of the load [31].

One way to implement transient analysis is demonstrated in [28], in which each *detected transient* is compared to a *database of known transients* using least squares criterion. In [30] it is stated that transients belonging to loads in a specific group can be detected using a single prototype transient shape as a reference and by applying appropriate scaling in *amplitude* and *duration* in order to find the best fit.

Major limitations of transient analysis are the need for high sampling frequency to handle the transient state, which in turn leads to the processing of large amount of data, and the need for relatively unique and reasonably repeatable transient patterns that may not be attainable in all cases [21]. One reason given is that transient measurement often depends on the exact point in the voltage cycle at which the turn-on or turn-off occurs and this causes transients to exhibit variability in parameters like duration, shape and size [34].

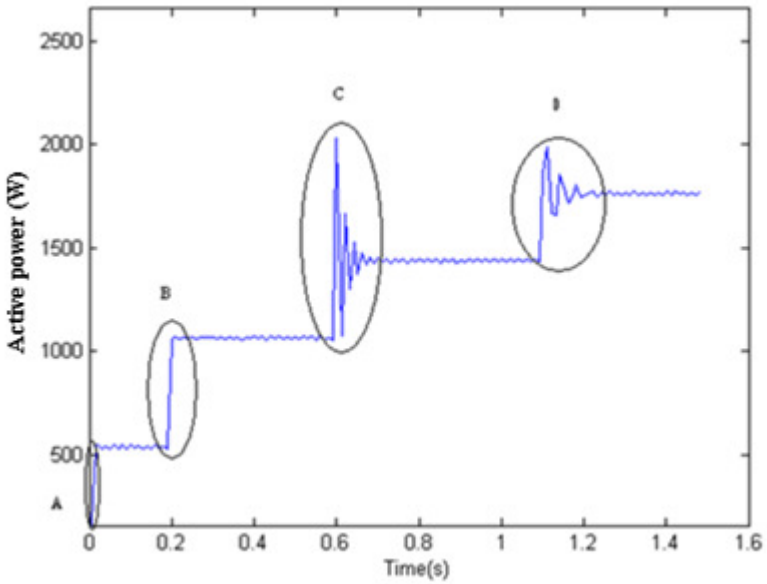

Figure 2.5: Simultaneous activation of appliances (A, B, C and D) – transient demarcation on active power consumption [21]

2.3 EARLY NIALMS WORKS

One of the earliest approaches to NIALMS was developed in the 1980s at MIT by George Hart for two-state appliances [21]. A collar-mounted recorder was designed that was installed between the existing utility meter and existing socket, with the NIALMS recorder providing a new socket into which the existing meter was plugged in [29]. An upper level system consisting of processing units and the NIALMS software suite was also designed to process the data collected by the NIALMS recorders. The work was mainly driven by the need to simplify the process of data collection of energy consumption required for load research by utilities [21].

Following this invention [32], the NIALMS prototype was further developed and put into a beta-test program supervised by the Electric Power Research Institute (EPRI) [12]. The NIALMS product available at that time consisted of the following three components:

I. Recorder

The NIALMS recorder uses current and voltage sensors and it records step changes in active and reactive power. This is achieved by periodic measurement of voltage and current from which RMS values of voltage and current as well as active and reactive power are calculated. The sampling rate is set at 2 kHz, and computation of active and reactive power is done three times per second [33].

The recorded data contain *interval data* (whole-house measurement) as well as *event data* consisting of the time and magnitude of specific load changes. Either on automatic user-defined schedule or on demand, the recorder transmits the data to the Master Station over public telephone network [12].

II. Master Station

The Master Station is a personal computer running the NIALMS Master Station software. Using the time-stamped data received from recorders and a database of known loads as reference, it generates the respective

appliance-specific consumption data. The NIALMS database contains a library of load models that are used for semi-automatic identification whereby the operator first selects the appliances in a specific building from the library list and then the NIALMS algorithm processes the event data and tries to identify loads with matching profiles [12].

The Master Station also handles the configuration of each recorder and information related to recorder physical location.

III. Analysis Station

The Analysis Station software is a relational database application that performs processed data query and presentation functions [33]. Upon user request, it retrieves the specified information from the Master Station database and presents it in the form of reports and graphs for review and further analysis [12].

Load disaggregation process

Load disaggregation starts with the ***detection of events*** (edges) in the recorder. A power transition will be recorded as an event if it exceeds a threshold for longer than a predefined time. Typical setting used during the EPRI beta test program was an increment or decrement of 150 W or 150 VAr [12].

The recorded events are then transmitted to the Master Station and ***cluster analysis*** is performed. In this step, similar sets of events are grouped together based on their magnitudes giving positive clusters (turn-on) and negative clusters (turn-off). For instance, if there are five operations of a single toaster in the batch of data being analyzed, then the five switch-on events will most likely be grouped into a *single positive cluster* and similarly the five switch-off events will be grouped into a *single negative cluster*.

The next step is ***cluster matching***, in which each positive cluster is matched with a possible negative cluster as shown in Figure 2.6, thus making it ready for appliance identification. The ***anomaly resolution*** part of the NIALMS software

handles any cluster matching problems that may arise from situations such as *missed events* or *simultaneous activation of loads*.

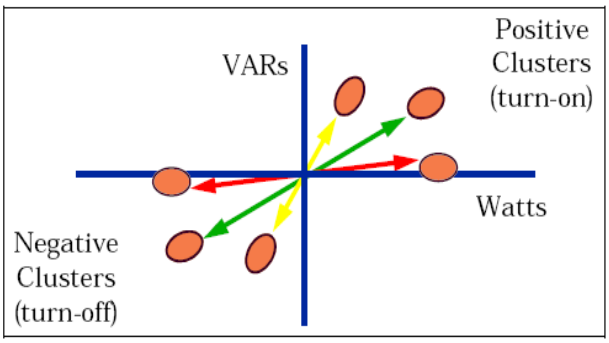

Figure 2.6: ΔP/ΔQ plane - cluster matching of turn-on and turn-off events [12]

In the ***appliance identification*** step, the matched clusters are associated with known load profiles; the comparison is based on fundamental frequency signatures (ΔP/ΔQ changes). In addition, the time-stamped clusters are useful to derive information such as *total energy consumption, operating power* and *usage duration* of a specific appliance and its *frequency of use*, all of which are calculated in the ***interval data computation*** step. It also monitors the balance (residue) between the *measured aggregate premises power* and the *computed total power* of all identified appliances at a specific instance. This residual power, if found to be significant, triggers a repeat of the *anomaly resolution* step to verify if any events were missed or were happening at the same instance.

Table A-1 in Appendix A summarizes overall performance of the system at the end of the beta test period as published in [12]. In addition to encountering the main limitations of fundamental frequency analysis, it is also reported that this NIALMS did not detect small loads due to the higher setting of event threshold and also it was not able to track appliances which are in continuous operation all the time. In the case of multi-state appliances, which possess a number of distinct switch-on states, NIALMS was able to detect some or all of the individual transitions but it did not aggregate them into a single appliance [12].

While this EPRI project was in progress in the mid 1990s, other researchers were also working on different NIALMS approaches to monitor residential and industrial loads. Some of these works include NIALMS actualized by means of neural networks for pattern identification [34], prototype implementation of a transient event detector [30][37], novel NIALMS algorithms based on fundamental frequency analysis as illustrated in [35][36] and NIALMS developed at VTT (Finland) using a 3-phase integrated power-quality and energy meter for recording events [13].

2.4 IMPROVEMENTS USING HARMONIC AND TRANSIENT ANALYSIS

An improved NIALMS that addresses the limitations of fundamental frequency signature by employing harmonic and transient analysis is presented in [20]. It computes harmonic contents up to 7th harmonic by using phase-locked short-time Fourier Transform of current waveforms collected at a sampling rate of 8 kHz.

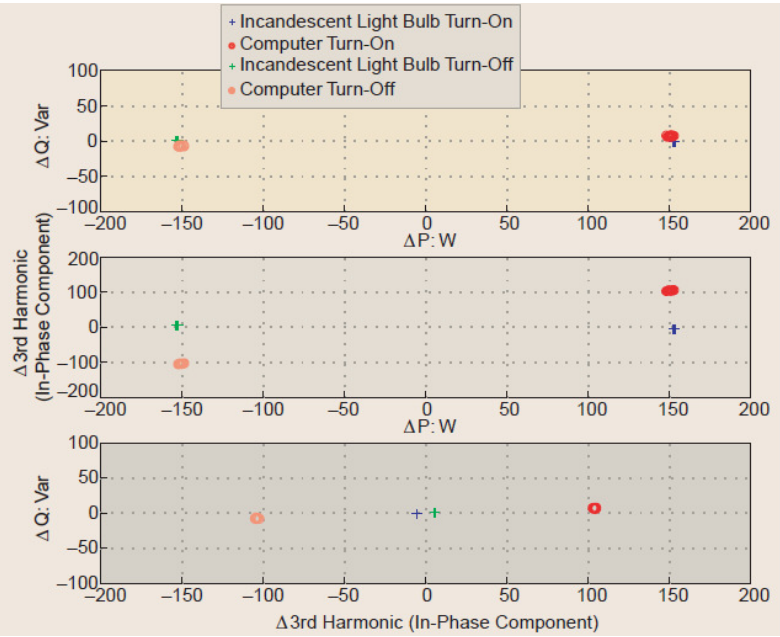

Figure 2.7: Identification using ΔP, Δ 3rd harmonic and ΔQ signatures [20]

The advantage of harmonic analysis is elaborated via the disaggregation of a sample load composed of personal computer and incandescent lamp as shown in Figure 2.7. In this example, both appliances consume nearly identical active and reactive power (refer to the first ΔP/ΔQ plane in the figure). However, the analysis of higher harmonics reveals that the computer power supply draws 3rd harmonic current, which distinguishes it from the linear incandescent lamp load (refer to the 2nd and 3rd planes in the figure). If required, the monitoring system proposed in [20] is customizable to examine higher harmonic contents beyond the 7th harmonic.

In addition to the implementation of *harmonic contents* method, [20] also offers a transient event detection system with the assumption that transient characteristics are closely related to the physical task a particular load performs, which leads to distinct transient load shapes. In contrast to the limitations mentioned in [21] and [34] regarding the applicability of transient analysis, it is stated in [20] that most appliances observed during its test period possessed repeatable transient profiles (or at least sections of their transient profiles were found to be repeatable).

Besides its application in *improving load disaggregation*, the work identifies transient analysis to be suitable also for *near-real-time identification* via the recognition of transients that occur during *switch-on events*. Another benefit obtained from transient detection, as explained in detail in [20], is the ability to *monitor continuously variable loads* such as Variable Speed Drives (VSDs) by tracking transient behaviors that are repeatable during their operation.

2.5 NOVEL APPROACHES TO LOAD DISAGGREGATION

Various research works continue to propose novel approaches to NIALMS [53], mainly focusing on improving its identification accuracy and increasing its scope of application in residential as well as industrial load monitoring. A summary of some of these works is presented next.

2.5.1 FUZZY LOGIC-BASED PATTERN RECOGNITION

A method based on fuzzy logic theory for pattern recognition that attempts to identify the type of connected individual appliances from an aggregate load is presented in [38]. The proposed algorithm makes use of operations from fuzzy logic theory (inner product and outer product of vectors) to build relationships between a database of known transients and a newly recorded transient.

Its output yields the pattern that closely resembles the unknown load transient. Tests were limited to a few sample waveforms and the work claims that satisfactory results were obtained.

2.5.2 DYNAMIC TIME WARPING FOR NIALMS

A load recognition technique based on Dynamic Time Warping (DTW) is proposed in [40]. DTW is an algorithm used for pattern matching of any two time series, mainly in automatic speech recognition.

The approach starts with measuring electric power consumption of selected appliances. These measurements are then processed to extract feature vectors and thus create a set of templates for identification; two attributes, namely *energy consumption* and *rising edge count* (from switch-on transitions), are extracted from the measurement data. After forming the templates, subsequent actual measurements are matched to the reference set in order to find out the identity of connected loads; DTW is applied here for matching purpose.

The basic concept of the DTW algorithm is to eliminate the *timing difference* between two vectors by *warping the time axis* of a new sample in such a way that maximum coincidence with a stored template is achieved. It starts with the calculation of *local distances* between elements of these two vectors. Distance calculation can be performed using different metrics such as Euclidean or Manhattan distance (Euclidean distance was used in [40]). The result of this operation is a *local distance matrix* from which a *minimal distance matrix* is then derived by applying *dynamic programming algorithm*.

The *warping path* or optimal path is finally determined by identifying the *minimal distance path* from the start element up to the end element of the minimal distance matrix. This computation is repeated for all stored templates; i.e., feature vector of the new sample is compared with feature vectors of the stored templates using the DTW algorithm to find their optimal paths and thus their respective overall distances. Finally, the algorithm selects the template vector that closely matches with the new sample. In [40], this step is accomplished by using the nearest neighbor rule.

Tests were performed on feature vectors collected over several days from a small group of household appliances (refrigerator, computer, microwave oven, dish washer, coffee machine and printer). The identification of a sample refrigerator using rising edge count and energy consumption attributes is elaborated in [40].

2.5.3 SVM & RBFN-BASED INFERENCE MODELS FOR NIALMS

A research conducted in Japan proposed a NIALMS solution using harmonic pattern recognition from the total load current measured at the entrance of a residence [39]. The developed system consists of *measuring terminals* installed at households ('slave stations'), a *communication system* and a *master station*. The measuring terminal at the power entry point measures odd-numbered current harmonics up to 13^{th} order. The respective phase shift of each harmonic current from the fundamental frequency voltage is also extracted from the measurement. The communication between the two stations is handled either by a Personal Handy-phone System (PHS) or the Internet.

At first, harmonic characteristics of individual appliances are separately recorded. The obtained training data are then used to build *inference models* that allow the monitoring of individual appliances' actual operation. Since NIALMS cannot single out permanently-connected loads through event detection, it was necessary for the inference models to take into account this condition, which was attained by attaching measuring devices to this group of loads.

Support Vector Machine (SVM) is used in [39] for *inferring whether the appliance is switched-on or switched-off* and Radial Basis Function Networks (RBFN) for *inferring power consumption*. The individual harmonic measurements (magnitudes and respective phase shifts) and power consumption are provided as inputs to SVM and RBFN to build a set of inference models. The next step is to evaluate these inference models and select the *optimal model* for field operation. In the actual implementation phase, the operating conditions of appliances are inferred by applying aggregate harmonic and power consumption measurements (received from measuring terminals at households) to the selected optimal model.

The performance of this model was evaluated by comparing its outputs with the values individually measured for training purposes. The results obtained from tests conducted at four households are provided in [39].

2.5.4 NIALMS BASED ON INTEGER PROGRAMMING

This work introduces a new NIALMS technique by treating the estimation of operating conditions of electrical loads as an integer programming problem [41].

The electrical attribute used as an input to this optimization approach is current waveform, which is recorded for a length of *one cycle* from each appliance of interest. The estimation of operating conditions is proposed for two groups of loads: two-state appliances, discussed in detail next, and multi-state appliances.

Procedure outlined for two-state appliances identification [41]:

- Assume that **N** kinds of appliances $\mathbf{L_1, L_2 \ldots L_N}$ are connected to the power line in a household.
- For each appliance type $\mathbf{L_n}$ (**n** from **1… N**), $\mathbf{C_n}$ number of appliances are also assumed to be connected to the power line, i.e., $\mathbf{C_n}$ is the quantity of a specific appliance $\mathbf{L_n}$.
- One cycle of current waveform, $\mathbf{i_n(t)}$, is measured independently at a sampling rate of *40 kHz* and stored in a database (**t** from **0…T−1**).

The total number of samples, **T**, obtained in one cycle is 666 (60 Hz power line in [41]) and **t=0** is the time when the voltage switches from negative to positive (voltage is also measured simultaneously to serve as reference when extracting one cycle of the current waveform).

- Next the *overall load current* is represented by using integer variable $\mathbf{c_n}$ ($\mathbf{c_n}$ from $\mathbf{0 \ldots C_n}$) as:

$$\hat{i}(t) = \sum_{n=1}^{N} c_n(m) i_n(t) + \boldsymbol{\varepsilon} \tag{2.3}$$

Where **m** is the number of distinct operating states of an appliance (useful in the analysis of multi-state appliances) and **ε** represents the disturbance due to noise or unknown appliances.

- The proposed NIALMS is realized by estimating the number of operating appliances $\{\mathbf{c_1 \ldots c_n}\}$ from the overall load current waveform. This is achieved by formulating the above scenario as an integer quadratic programming problem, which can be solved with the help of commercially available optimization software:

$$\begin{aligned} &\text{Find } \mathbf{c}^* = \{c_n | n \in \{\mathbf{1}, \cdots, N\}\} \\ &\text{which minimize} \\ &E = \sum_{t=0}^{T-1} \left(\hat{i}(t) - \sum_{n=1}^{N} c_n(m) i_n(t) \right)^2 \\ &\text{subject to} \\ &c_n \in \mathbb{Z},\ 0 \le c_n \le C_n \quad \forall n \in \{1, \cdots, N\} \end{aligned} \tag{2.4}$$

- Hence, NIALMS is actualized by finding the most probable operating conditions, **c***, that minimize the square error between the *measured aggregate load current* and the *estimated sum of individual currents*. ILOG CPLEX 10.2 optimization software was used in [41].

This procedure is extended to cover a second group of loads comprising multi-state appliances. Experiments performed at a single household, which receives power supply from two lines L1 and L2, are explained in detail in [41].

A partial list of appliances used for the tests in [41] (those appliances connected to line L1) and the derived constraint conditions are provided in Appendix A of this thesis (refer to Table A-2 and Equation A-1). The average identification success rates achieved after 6 days of testing were 79.0% and 96.8% for L1 and L2 respectively. It is mentioned that these tests did not include continuously-varying loads [41].

The paper suggests that this NIALMS technique is suitable for application in *real-time load monitoring* thanks to the high-speed processing of data that are extracted from a single-cycle current measurement [41].

Types of load monitoring techniques, the concept behind NIALMS and different research works conducted on NIALMS were discussed in this chapter. Based on the ideas derived from this review, an appliance fingerprinting solution was outlined for the BeAware project. The first activity in this process, which was to perform a series of measurements on typical household appliances, is discussed in detail in the next chapter.

3. MEASUREMENT WORK ON COMMON HOUSEHOLD APPLIANCES

The measurement work was carried out on different household appliances with the following main objectives –

- To explore the extent to which household appliances can be categorized based on their electrical attributes
- To select the electrical attributes that will be used for the fingerprinting application
- To study the contribution of individual appliances towards harmonic production, which is a major power quality concern nowadays

3.1 MEASURING EQUIPMENT

TOPAS 1000 Power Quality Analyzer (Figure 3.1), a product of LEM NORMA GmbH, was used for performing the measurement work in this thesis. The equipment has several fields of application including power quality analysis as per EN 50160 standard and is also capable of measuring harmonics up to 50^{th} order [43]. It has 8 electrically isolated analog input channels for current and voltage measurement. Each channel is equipped with a 16-bit analog-to-digital converter. The sampling rate is synchronized with the line frequency and is typically 6400 Hz on a 50 Hz line. Specifications of its voltage and current sensors are given in Appendix B.

TOPAS measurement data mainly used for analysis were:

- *RMS values computed every second* – important for studying switch-on and switch-off behaviors and detecting *events* (state transitions of appliances).
- *Average values from 3-second and 10-minute measuring intervals* – required for extracting steady-state operating values (such as harmonic content and power factor) that will be used for building load signatures.

– *Digital oscilloscope measurement* – sampled values of voltage and current waveforms that will be applied in *harmonic phase angles* and *crest factor* calculation.

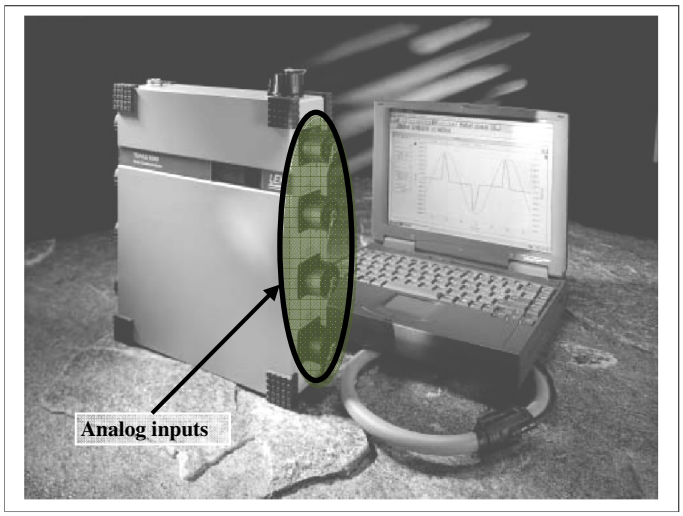

Figure 3.1: TOPAS 1000 Power Quality Analyzer (adapted from [43])

3.2 MEASUREMENT PROCEDURE

The actual measurement work was carried out for a period of eight weeks mainly at Aalto University Power System Laboratory and a few other premises. During this period, the following general measurement procedure was adopted:

1. TOPAS is initialized with an appliance-specific *configuration file* (for example, **appliance001.vdf**) – this step ensures that the recording mode and types of measuring sensors used are compatible with the power rating of the appliance and its duration of operation.
2. The appliance to be measured is disconnected and TOPAS is electrically inserted between the appliance and supply point as shown in Figure 3.2.
3. If applicable, the desired mode of operation is selected (for instance, a microwave oven operating at 'keep warm' mode) and then the appliance is switched-on; TOPAS starts to record the electrical operation of the appliance.

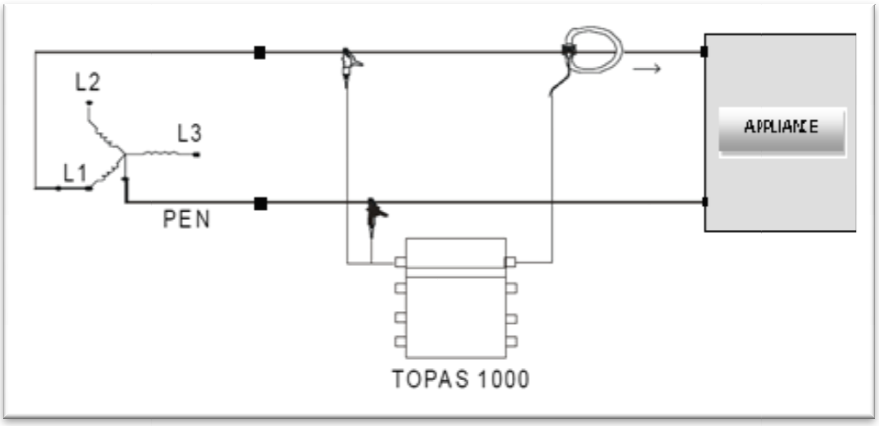

Figure 3.2: Measurement set up (adapted from [43])

4. Every measurement is aimed at recording *switch-on*, *steady-state* and *switch-off* characteristics of the appliance. Hence, the duration of measurement is determined by the function of the appliance:
   - A minimum of 10-minute data are recorded for continuously operating appliances (such as television).
   - In the case of appliances that perform sequential operation to complete a given task (such as washing machine), the entire cycle of operation is recorded.
   - For appliances with long-cyclic operation (such as refrigerator), a minimum of two-hour data are recorded in order to capture some of the switched-on cycles (e.g. compressor operation cycles).
5. At the end of each measurement activity, the recorded data are retrieved from TOPAS and documented for later analysis (data are fetched in the form of a TOPAS *definition file* – for example, **appliance001.def**).
6. If available, manufacturer's nameplate information is recorded for documentation with the corresponding measurement file.

Note that transient measurement is not included in the design of the current BeAware sensor version. Hence, load transients are not recorded as part of this measurement work.

3.3 ANALYSIS OF MEASUREMENT DATA

Measurement reports were prepared per appliance after analyzing the corresponding data retrieved from TOPAS. The types of appliances and number of samples covered in this measurement work are provided in Appendix B.

Each measurement report consists of:

1. **Appliance rating data** (from name plate information).
2. **Average steady-state operating data** (for instance, Table 3.1 shows average operating values of a refrigerator). The contents are briefly explained next.

10 MINUTE AVERAGE DATA (UNDER NORMAL OPERATION)							
No	Measurment	Unit	Fridge 1 - MODE 1 (cycle during a sample steady operation)	Fridge 1 - MODE 2 (first cycle during switch on)			
1	Active Power	W	10,95	100,69			
	Normalized P	*W*	*11,20*	*99,50*			
2	Reactive Power	VAr	8,90	93,26			
	Normalized Q	*VAr*	*9,10*	*92,16*			
3	Apparent power	VA	14,17	137,73			
4	Current	A	0,06	0,60			
	Normalized I	*A*	*0,06*	*0,59*			
5	System voltage	V	227,41	231,37			
6	FPF	-	0,776	0,734			
7	Total PF	-	0,773	0,731			
8	THD (I) %	-	8,1	8,1			
9	TID (I) %	-	4,8	2,1			
10	ON Cycle	min:sec	9:37	10:01			
11	**Crest factor**	-	**1,51**	**1,49**			

Table 3.1: Average operating values (from refrigerator measurement report)

Active power, *reactive power* and *current values* are normalized to get rid of the effect of *system voltage* variation (normalization was discussed in Subsection 2.2.1).

FPF is fundamental frequency (*displacement*) power factor given by:

$$FPF = \cos\left(\tan^{-1}\left(\frac{Q}{P}\right)\right) \tag{3.1}$$

Total PF is *true* power factor given by:

$$PF = \left(\frac{P}{S}\right) \tag{3.2}$$

Where, P, Q and S are active, reactive and apparent power values respectively. The relationship between these quantities is given by:

$$S = \sqrt{P^2 + Q^2 + D^2} \tag{3.3}$$

D is the *distortion power*, which is linked to the presence of current harmonics [44][57]. The operation of appliances with higher harmonic content causes significant distortion power to prevail in the system.

THD_I is *total current harmonic distortion* – a frequently used measure of harmonic levels in power system given by the ratio of RMS value of harmonics (above fundamental) to RMS value of the fundamental [45]:

$$THD_I = \frac{\sqrt{\sum_{k=2}^{\infty} I_{k,RMS}^2}}{I_{1,RMS}} \tag{3.4}$$

Where, $I_{k,RMS}$ (k>1) are harmonic currents existing at frequencies that are *integral multiples* of the fundamental frequency.

TID_I is *total current inter-harmonic distortion*, which is similar to THD_I but deals with frequencies that are *non-integral multiples* of the fundamental frequency.

ON-cycle duration is the width of switched-on cycle (in this example it is the length of compressor operation).

Crest factor is the ratio of peak amplitude of current waveform to its RMS value. It is equal to √2 in a pure sinusoidal waveform [57].

3. **Current harmonic data up to 25th order** (*actual values* and also *values relative to the fundamental frequency current*, $I_{1,RMS}$). Table 3.2 shows average current harmonic data of the refrigerator from the previous example.

Harmonic	Relative to H01 (%)	Value [A]
1		0,0572
2	1,3	0,0007
3	**7,5**	0,0043
4	0,3	0,0002
5	**2,0**	0,0012
6	0,3	0,0002
7	**1,4**	0,0008
8	0,2	0,0001
9	0,4	0,0002
10	0,2	0,0001
11	0,3	0,0002
12	0,2	0,0001
13	0,4	0,0003
14	0,2	0,0001
15	0,2	0,0001
16	0,2	0,0001
17	0,2	0,0001
18	0,2	0,0001
19	0,2	0,0001
20	0,2	0,0001
21	0,1	0,0001
22	0,2	0,0001
23	0,1	0,0001
24	0,2	0,0001
25	0,2	0,0001
THD (upto 25th)	8,1	

Harmonic	Relative to H01 (%)	Value [A]
1		0,5792
2	1,3	0,0074
3	**7,6**	0,0441
4	0,2	0,0012
5	**2,1**	0,0123
6	0,1	0,0005
7	**1,4**	0,0083
8	0,0	0,0003
9	0,4	0,0024
10	0,0	0,0002
11	0,2	0,0014
12	0,0	0,0001
13	0,4	0,0026
14	0,0	0,0001
15	0,2	0,0010
16	0,0	0,0001
17	0,0	0,0003
18	0,0	0,0001
19	0,1	0,0003
20	0,0	0,0001
21	0,0	0,0002
22	0,0	0,0001
23	0,0	0,0001
24	0,0	0,0001
25	0,0	0,0002
THD (upto 25th)	8,1	

Table 3.2: Average current harmonic data of the two cycles (from refrigerator measurement report)

H01 refers to the fundamental frequency current, $I_{1,RMS.}$ The distortion up to the 25th order is also computed, which is comparable to the *THD_I (up to the 50th order)* directly obtained from TOPAS.

Some of the values in the measurement reports such as TID_I are not directly applicable in this thesis. However, the belief is that the availability of such

detailed measurement reports will benefit other research works, especially in the areas of load monitoring and power quality studies.

3.3.1 LOAD TAXONOMY

At the start of this work, it was presumed that a given type of load, for example desktop computer, may exhibit a set of electrical characteristics that makes it distinctly identifiable from a larger group of appliances. Load identification based on this assumption, i.e., by merely observing operating values without prior knowledge about the particular load, can potentially lead to erroneous results. This is attributable to variations in design philosophy among manufacturers producing the same type of appliance, the impact of power factor correction [46] and harmonic mitigation techniques, and specific operating mode of the appliance due to user selection or automatic process (for instance, a cloth washing machine exhibits markedly different load signatures when operating first in *water heating mode* and then *washing/spinning mode*).

Such variations within a given class of appliances have led to the categorization of loads in a more generalized manner. Based on field tests, [47] classifies household appliances into six groups: *resistive*, *pump-operated*, *motor-driven*, *electronically-fed*, *electronic power control* and *fluorescent lighting*. Another study focusing on harmonic analysis [48], identifies three types of residential loads: *resistive*, *motive (inductive)* and *nonlinear*. In [49], appliances are broadly divided into *linear loads*, which, if supplied by a sinusoidal source at fundamental frequency, produce only pure sinusoidal current and *nonlinear loads*, which produce nonlinear current that is rich in harmonic content. The study further classifies appliances into the same six categories as in [47].

A similar NIALMS study [50], makes reference to the proposed categories in [47] and discusses a methodology for constructing load taxonomy based on shape features extracted from V-I trajectories as shown in the example of Figure 3.3. The study discusses the formation of 13 groups of loads using these shape features as classifiers. Appliance examples and elaboration on the

characteristics pertaining to each category can be referred to further in [47]–[50].

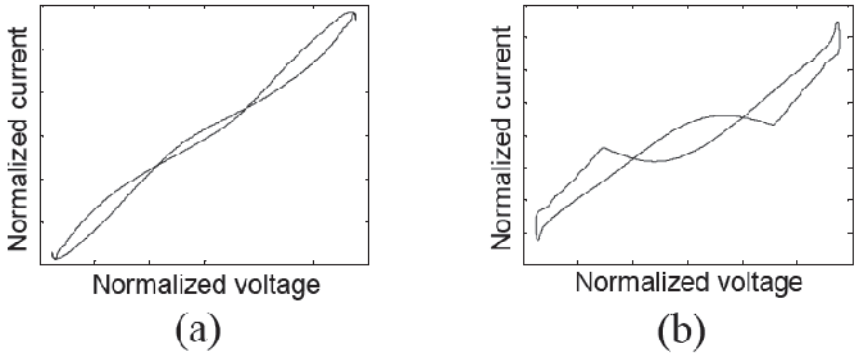

Figure 3.3: (a) V-I trajectories of a window-type air conditioner, and (b) a microwave oven [50]

Based on the findings of the measurement work, the load classification proposed in this thesis is similar to the preceding works. Some of the classes in [47] can be merged and a classification equivalent to that of [48] and [54] can be attained. *Motor-driven*, *pump-operated* and *fluorescent lighting* fall under *motive (inductive) loads* whereas *electronically-fed* and *electronic power control* can be grouped into *electronic loads*. Hence, it is possible to categorize the majority of household appliances into the following three main classes:

A. Resistive load

This category encompasses appliances that are mainly used for heating and lighting purposes such as panel heaters and incandescent lamps. Heating elements of other appliances like washing machines and dishwashers also belong to this category [47]. Their *reactive power* consumption is comparatively quite small, which means they regularly operate close to unity *power factor* (both *FPF* and *total PF*). Their *harmonic content* is usually negligible and in general THD_I does not exceed **5%**. Results of the measurement work also show that the *crest factor* of appliances in this group normally falls in the range **1.38** to **1.44,** which is close to the crest factor value of a *pure sinusoidal current*.

Figure 3.4 depicts total PF and FPF values during a coffee maker operation (both values are almost equal to unity) and Figure 3.5 shows the level of harmonic distortion up to 50th order of the same appliance.

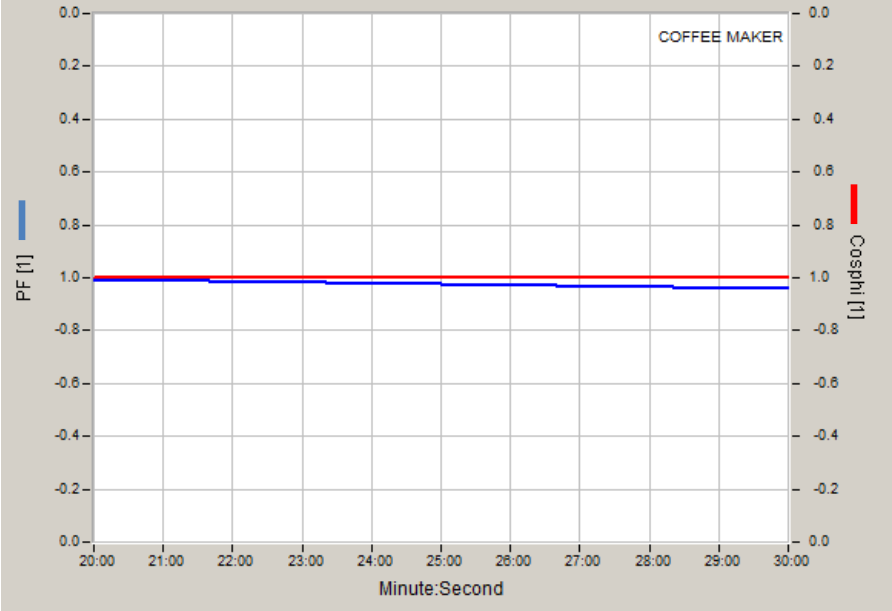

Figure 3.4: *Total PF* and *FPF* (Cosphi) during coffee maker operation

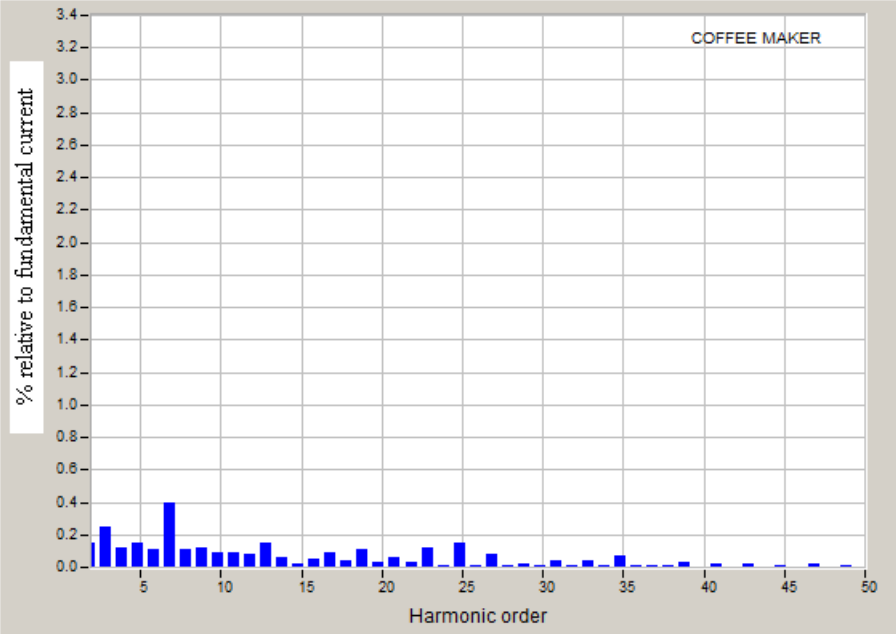

Figure 3.5: Current harmonic pattern during coffee maker operation

(from coffee maker measurement report)

In this example, the magnitudes of all harmonic orders are below **0.5%** of the fundamental frequency current and THD_I is only **1.4%**.

B. Power electronic load

Majority of modern electronic equipments use switched-mode power supplies (SMPS). These differ from older units in that the traditional combination of a step-down transformer and rectifier is replaced by direct-controlled rectification [51][52]. The benefits are improved load efficiency, better controllability, and reduced size, weight and cost [51][25]. However, the undesirable effect is an increase in the propagation of harmonic currents back to the utility grid [53], with amplitudes at times exceeding that of the fundamental frequency current [27]. Appliances such as computers, television sets and compact fluorescent lamps belong to this category.

As can be seen in Figure 3.6, these appliances contain significant levels of harmonic distortion. For instance, THD_I values of 230% (laptops) and 175% (next generation LEDs) were recorded during the measurement work. Due to the high level of harmonic content and hence the existence of distortion power, *total PF* is notably smaller than *FPF* (Figure 3.7).

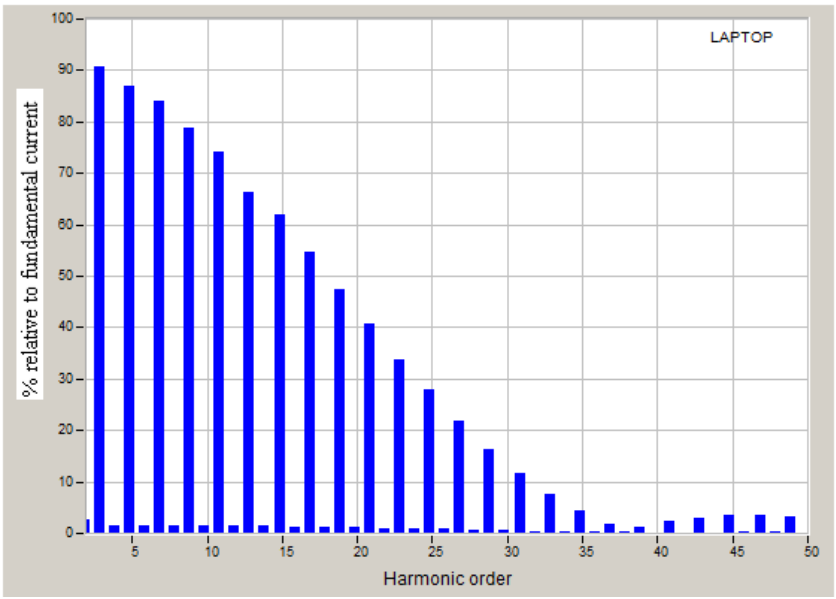

Figure 3.6: Current harmonic pattern of laptop

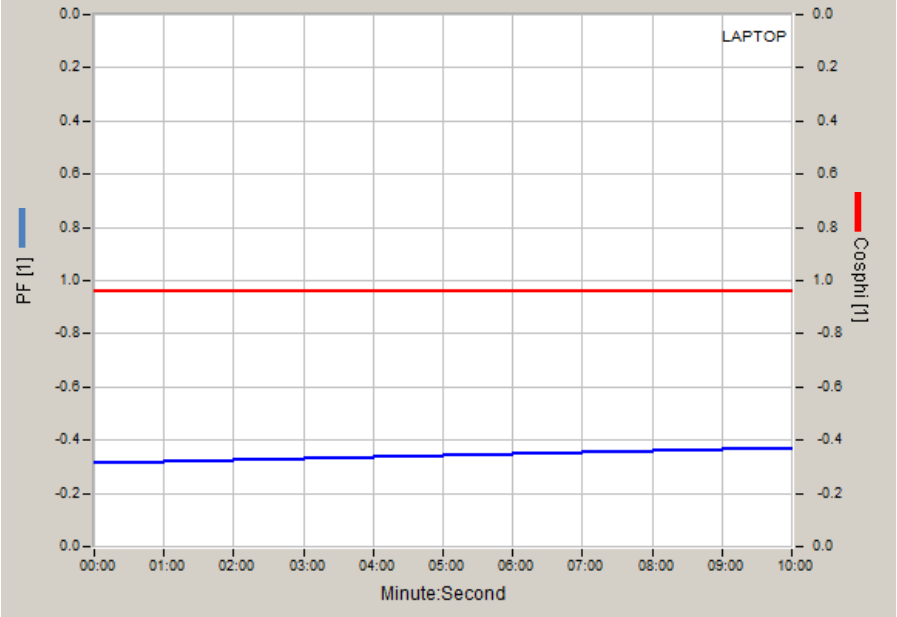

Figure 3.7: *Total PF* and *FPF* (Cosphi) during laptop operation (from laptop measurement report)

Results of the measurement work indicate that electronic loads possess high *crest factors*; for the appliances included in this work, the range above **1.65** is assigned to electronic loads, i.e., a crest factor value greater than **1.65** shall signify the nature of the load to be electronic. The highest crest factor measured was that of a sample LED lamp (**CF=4.96**), with CFLs and laptops also exhibiting high crest factors.

C. Motive (inductive) load

This class consists of motor-driven, pump-operated and other inductive loads such as refrigerators, microwave ovens and fluorescent lamps (without PFC). The operation of these loads results in the production of substantial *reactive power* and it also causes *harmonic distortion* but at a lesser level as compared to electronic appliances. Figure 3.8 shows total PF and FPF values during the operation of a freezer. Due to significant reactive power consumption, such loads do not operate close to unity power factor. However, the addition of a PFC circuit, as observed in the case of fluorescent lamps, improves the condition.

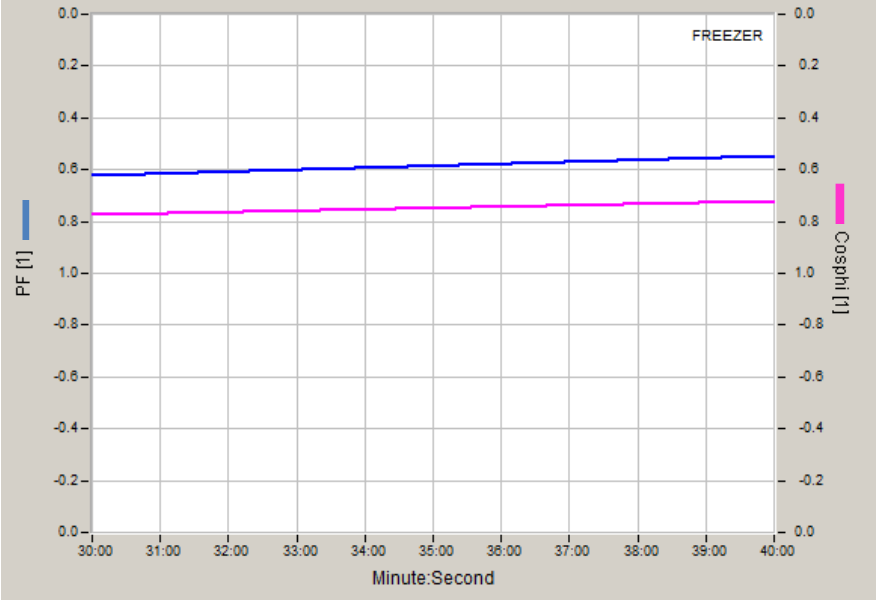

Figure 3.8: *Total PF* and *FPF* (Cosphi) during freezer operation

Figure 3.9 shows the level of harmonic distortion of the freezer sample. In this group of loads, the *3rd harmonic current* is dominant over the other harmonic orders. Regarding *crest factor* values of appliances in the scope of this work, it was noted that most of the loads in this category fall in the range **1.45** to **1.65**.

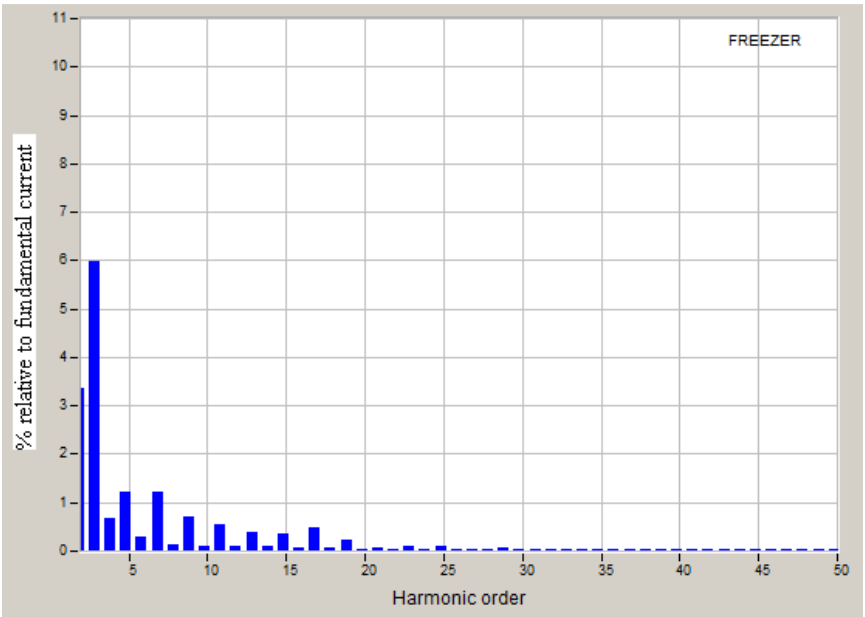

Figure 3.9: Current harmonic pattern of freezer
(from freezer measurement report)

In addition to the load classification discussed above, it is also possible to categorize household appliances according to their operational nature:

- *Depending on the duration of ON-cycle:*
  continuous (e.g. television), **long-cyclic** (e.g. refrigerator) or **short-cyclic** (e.g. microwave oven).
- *Depending on the sequence of tasks performed:*
  multi-mode (e.g. dish washing machine) or **single-mode** (e.g. toaster).
- *Depending on the number of distinct switch-ON states:*
  multi-state (e.g. table fan) or **two-state** (e.g. coffee maker).

This approach can be utilized to create conditions for appliance idetification in the fingerprinting process, which will be discussed in the next chapter.

3.3.2 OBSERVATIONS ON MEASUREMENT RESULTS

I. Odd-order harmonic content

Total current harmonic distortion is virtually composed of *odd-order harmonics* as the levels of even-order harmonics are negligible (even-order harmonics are nowadays relatively rare but were common when half wave rectification was widely used [52]). In particular, the contribution of odd-order harmonics at the lower end of the frequency spectrum is significant. It was observed among the measured appliances that the first three odd-order harmonics (3^{rd}, 5^{th} and 7^{th} harmonics) are the most dominant and they provide distinction between *electronic loads* and *motive (inductive) loads* – in the case of electronic loads, although the 3^{rd} harmonic is higher in magnitude, the 5^{th} and 7^{th} harmonics are also significant whereas in the case of motive (inductive) loads, the 5^{th} and 7^{th} harmonics do not have significant contributions comparable to that of electronic loads, which means the 3^{rd} harmonic is responsible for most of the total harmonic distortion.

II. Active and reactive power at higher frequencies

Measurement results show that almost all the active and reactive power consumptions occur at the fundamental frequency. Figure 3.10 depicts the *active power harmonic pattern* of a CRT television set. As can be seen, the power flow at higher frequencies is in the order of mW. Hence, measurement of active and reactive power flows at higher frequencies does not yield detectable load signatures.

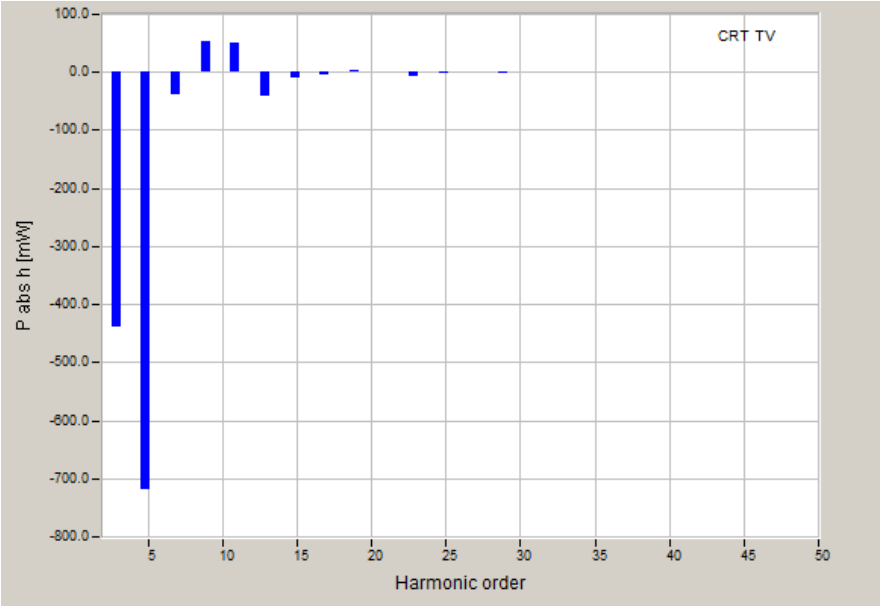

Figure 3.10: Active power harmonic pattern of CRT TV

III. Harmonics and power factor

Current harmonics and power factor are closely related; as indicated earlier, the presence of distortion power due to harmonic current sources reduces power factor. In other words, the harmonic distortion of load current decreases the average power transferred to the load. This relationship helps to impose limitations on current harmonics by using the *widely-accepted concept of power factor* (TPF), as highlighted in [45] with some examples:

Desired Limit on THD_I - %	Corresponding Limit on pf_{true}
20	0.981
50	0.894
100	0.707

Each THD_I corresponds to a maximum TPF; thus, a limit on TPF automatically invokes a limitation on THD_I.

In addition to the above points, other observations include – the masking effect of *PFC* and *harmonic filters* on load signatures, the directly-proportional relationship between THD_I and *crest factor* and the effect of consumer interaction on the *ON cycle length* of cyclic appliances such as refrigerators.

3.4 CURRENT HARMONICS PHASE SHIFT

At the start of this work, it was intended to investigate the possible application of *current harmonic phase shifts* as a load signature in the fingerprinting process. Since TOPAS does not record the phase shifts of harmonic currents (with reference to the fundamental frequency voltage), it was necessary to make use of its digital oscilloscope measurement that furnishes sampled values of voltage and current waveforms for calculating the phase shifts.

The instrument was set to record 8 cycles (total 160 ms length) at an interval of 60 seconds, i.e., 8 cycles every minute. Figure 3.11 shows the voltage and current waveforms of a sample CFL that were recorded during its steady-state operation. The sampling rate of the instrument is 6400 Hz [43], which means the digital oscilloscope measurement is capable of supplying *128 samples per cycle* for each wave form.

After extracting a total of *1024 samples* for the 8 cycles (from the respective TOPAS ***.def** file per appliance), the data series was fed to a MATLAB code to compute *current harmonic phase shifts from the fundamental frequency voltage* up to the 25th order for every cycle. The results are then averaged over the eight cycles to give the *mean phase shift of each harmonic order* during a *single measuring instance*.

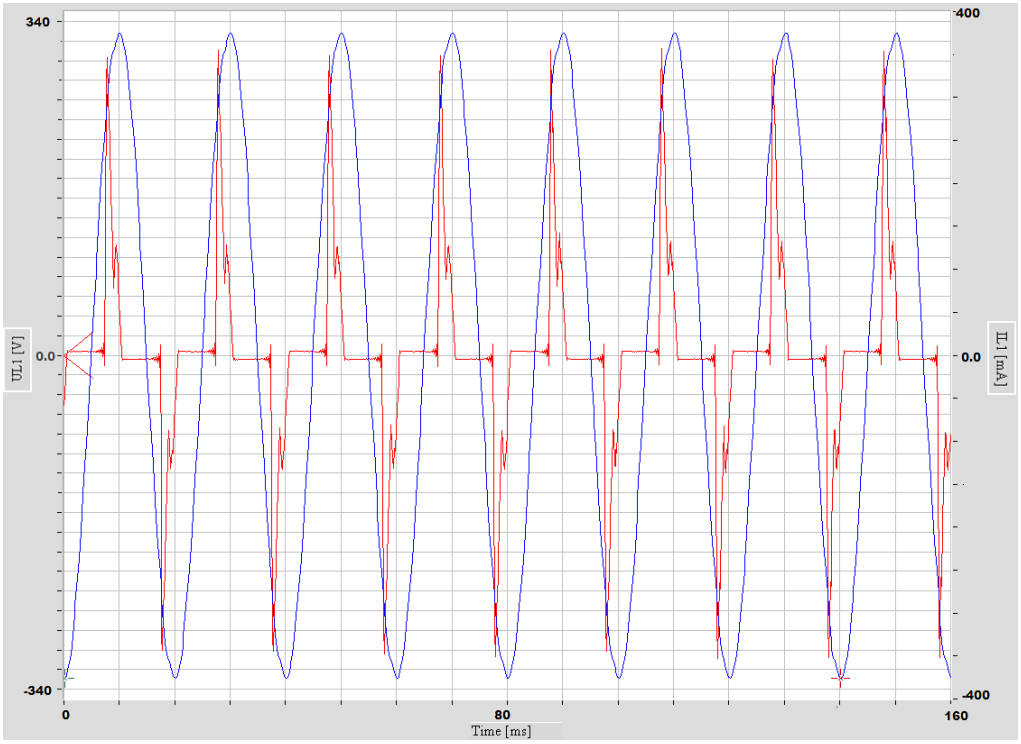

Figure 3.11: Instantaneous voltage and current waveforms of a CFL (8 cycles) (--- voltage [V], --- current [mA] and time [ms])

Since the instrument records the 8 cycles every 60 second, a set of *new samples* is obtained every minute. For the purpose of comparison, *ten consecutive measuring instances* were extracted from the steady-state operation region and harmonic phase shifts were computed.

The flow chart in Appendix C outlines the steps followed to compute the phase shifts. It uses Eq. 3.5 and Eq. 3.6 below to calculate the Fourier series coefficients, from which phase angles are calculated according to Eq. 3.7.

$$a_n = \left(\frac{2}{N}\right)\left(\sum_{k=1}^{N} i[k]\cos\left(n\,\frac{2\pi k}{N}\right)\right) \tag{3.5}$$

$$b_n = \left(\frac{2}{N}\right)\left(\sum_{k=1}^{N} i[k]\sin\left(n\,\frac{2\pi k}{N}\right)\right) \tag{3.6}$$

Where $\mathbf{a_n}$ and $\mathbf{b_n}$ are the Fourier series coefficients, **i[k]** is the current sample series, **N** is the total number of samples in a cycle (N=128) and **n** is the harmonic order. Similar equations are applied for voltage sample series **v[k]**.

$$\theta = \left(\tan^{-1}\frac{b_n}{a_n}\right)\left(\frac{180}{\pi}\right) \tag{3.7}$$

Where $\boldsymbol{\theta}$ is the phase angle expressed in degrees.

Results obtained for *vacuum cleaner* and *LCD television samples* are partially shown in Figure 3.11 and Figure 3.12 (phase shifts of fundamental frequency, 3rd and 5th harmonic currents from the fundamental frequency voltage over a 10-minute interval are shown). The full lists of results of the *25 harmonic orders* are given in Appendix C (for the same appliance samples).

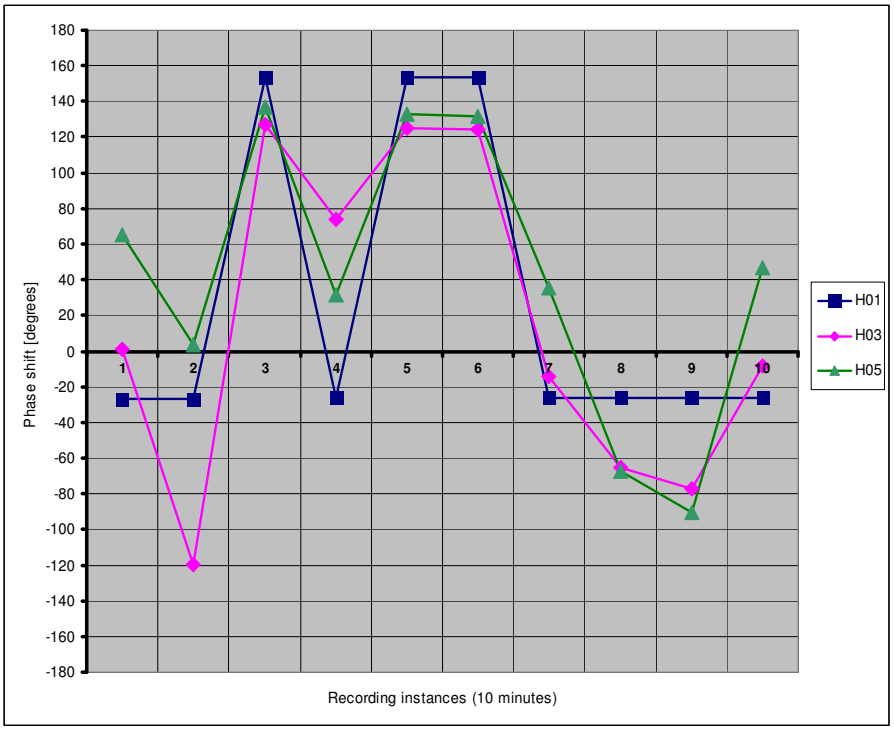

Figure 3.12: Phase shift variations (sample vacuum cleaner)

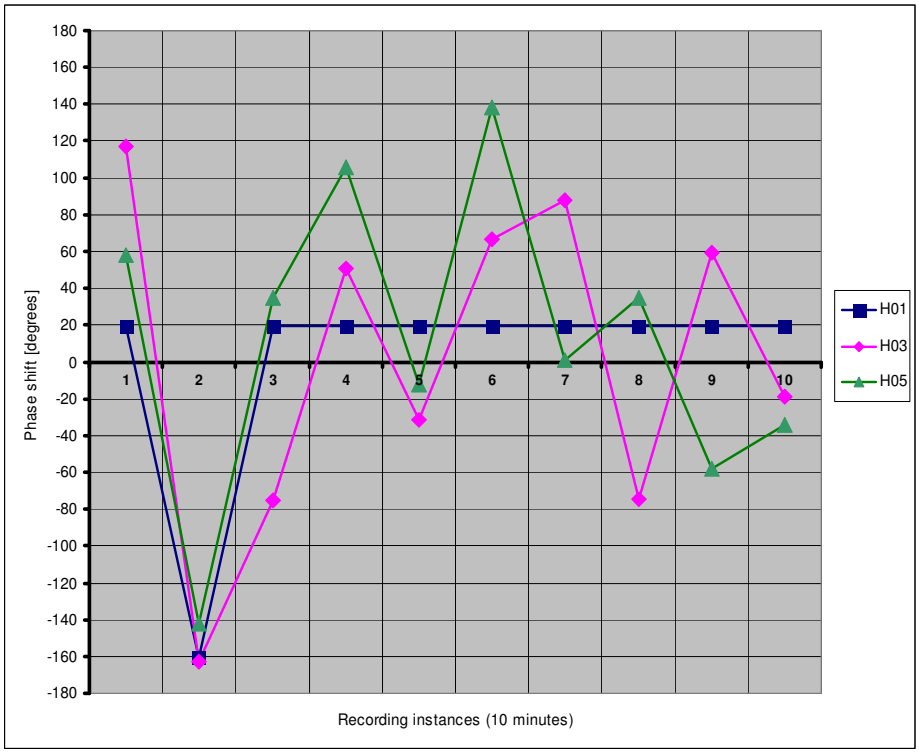

Figure 3.13: Phase shift variations (sample LCD television)

As can be seen, the phase shifts at fundamental frequency exhibit better level of stability. While keeping in mind the two specific conditions under which the above results were obtained, i.e., *the selected TOPAS measurement setting* and *the method applied for phase angle computation*, it can be deduced that **as the measuring instances change, the phase shift of the respective harmonic current from the fundamental frequency voltage also changes**. In [55] it is mentioned that waveform distortion varies widely in practice and is dependent on both load level and system conditions. It is typical to assume that a steady-state condition exists at the instant at which the measurement is taken, *but the next measurement at the next time could be markedly different*.

Nevertheless, as mentioned earlier in Subsection 2.5.3, other works such as [39] have applied harmonic current phase shifts as load signatures for appliance identification. Hence, it will be interesting to investigate the approach used in this thesis further and also examine alternatives to verify if indeed there is the possibility to make use of this attribute in the fingerprinting process.

4. PROPOSED METHODOLOGY FOR APPLIANCE FINGERPRINTING

Based on the outputs of the measurement work and the methods studied in the literature, a first phase fingerprinting technique is proposed in this thesis for the BeAware project; the steps involved in this process are discussed in subsequent sections of this chapter.

The fingerprinting process illustrated in Figure 4.1, for application in a next-to-real-time processing environment, shall consist of the following three main steps:

I. **Feature extraction** – different attributes such as active power and current harmonics are extracted from voltage and current waveforms. The feature extraction is performed by the *BeAware sensor* [6].

II. **Event detection** – changes in the extracted features are *detected* and *classified as events* based on static or dynamic thresholds [56].

III. **Appliance type identification** – a set of attributes, captured after the occurrence of a corresponding event, is processed to find its match from a *load library* consisting of known appliance signatures by using *pattern recognition* [34][50][56] or *optimization* [41][42] techniques.

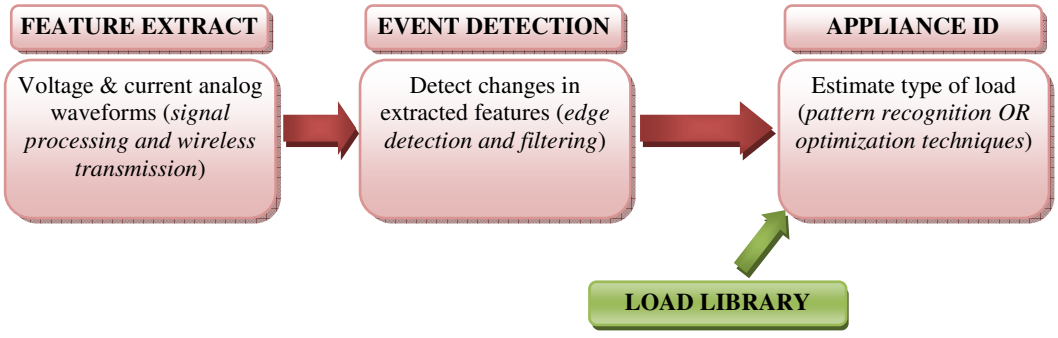

Figure 4.1: Proposed fingerprinting process

The solution proposed in this work is different from several conventional appliance identification systems in two areas:

- As being a first phase implementation in the BeAware project, it utilizes measurement data received from *a sensing device that monitors a single appliance*. In contrast, previous and contemporary works in this field operate by disaggregating the total load current that is measured at the main power entry point.
- Such works usually analyze measurement data accumulated over a longer duration; for instance, a 24-hour period or in certain cases up to several days. On the contrary, the fingerprinting system in this project attempts to furnish the desired information, i.e., *appliance identification*, *duration of operation* and *amount of energy consumption*, using the constant stream of data available from the sensing device in near real-time intervals.

4.1 BEAWARE SENSOR FOR FEATURE EXTRACTION

The BeAware sensor measures an appliance's energy consumption and sends measurement data wirelessly [6]. Line voltage and current drawn by the connected appliance are continuously measured and sampled at a rate of *900 Hz* and accuracy of *16 bits* (this is the specification of the latest model at the time of writing this report). This sampling rate allows measurement up to the 7^{th} harmonic current, which has a frequency of 350 Hz on a 50 Hz line. The sensor consists of three functional parts:

- Analog measurement connection and analog-to-digital conversion.
- Sensor program running on main micro-controller.
- Radio communication (wireless link) [6].

The sensor transmits two types of Binary Coded Decimal (BCD-coded) messages to the base station: *average power message*, which is sent every 2 seconds and *cumulative energy message* that is sent every 15 seconds.

The *average power message* is composed of *8 average values* – active power, total power factor, crest factor, total harmonic distortion, fundamental power factor and 3rd harmonic, 5th harmonic and 7th harmonic currents. The last three attributes were included in the power message following the observations on measurement results in this work as discussed in Subsection 3.3.2. The *energy message* contains two values – one for the total duration the sensor is connected (E_{tot}) and the other for energy consumed in the last 24 hours (E_{24h}).

Energy consumption and *active power measurements* are used for EnergyLife purposes whereas the other *more specialized measurements* are meant for appliance fingerprinting. The sensor takes its power supply from the line it is measuring and its nominal consumption is 0.3 W.

Figure 4.2: BeAware sensor (plugged into a wall socket)

4.2 EVENT DETECTION

The information obtained from the event detection stage is required for:

- Triggering the *appliance identification phase* in the fingerprinting process
- Computing the appliance's *duration of operation* and *frequency of use*
- Estimating the *energy consumed* in that period

There are several ways in which events can be defined. For example, events can be changes in average active power exceeding a certain threshold,

the appearance of a known start up transient shape or any other suitable criterion. It is possible to select a single method or to have a combination of different methods for detecting events [56]. After selecting a suitable method, it is necessary to define an appropriate threshold. Previous works such as [12][13][17][19] and [35] utilized changes in average active and/or reactive power for defining events based on *static thresholds*. For instance, changes were classified as events if they exceeded 100 W in [19] and 200 W in [35].

Opting for a static threshold presents its own challenges: choosing a large setting means it will not be able detect the operation of small appliances and on the contrary, a small setting means it becomes too sensitive for appliances with large power consumptions. The event detection method proposed in this work is based on *dynamic threshold*, which allows the detection of events of different appliances over a wide range of active power consumption. The advantage is that the threshold adjusts itself according to the power consumption level of the appliance connected to the sensor, thus avoiding the need to define equipment-specific settings.

Figure 4.3 shows the power consumption curve of a sample desktop computer during 30 minutes of operation. In this particular example, only the *switch-on* and *switch-off* transitions (marked with arrows) shall be classified as events whereas the fluctuations shall be rejected to prevent inadvertent activation of subsequent functions in the fingerprinting process. Hence, event detection involves searching for stable transition points (edges) that correspond to an appliance turning on or turning off and filtering out the noise created due to operational nature of the appliance or disturbances in the electrical network.

The method used here is based on event detection techniques discussed in [58]. The difference between each pair of adjacent points in a fixed time interval is calculated and then the *standard deviation of all the differences* is used as the *dynamic threshold*. Next, the changes between adjacent points are classified as *events* if they fulfill a set of criteria based on the calculated threshold.

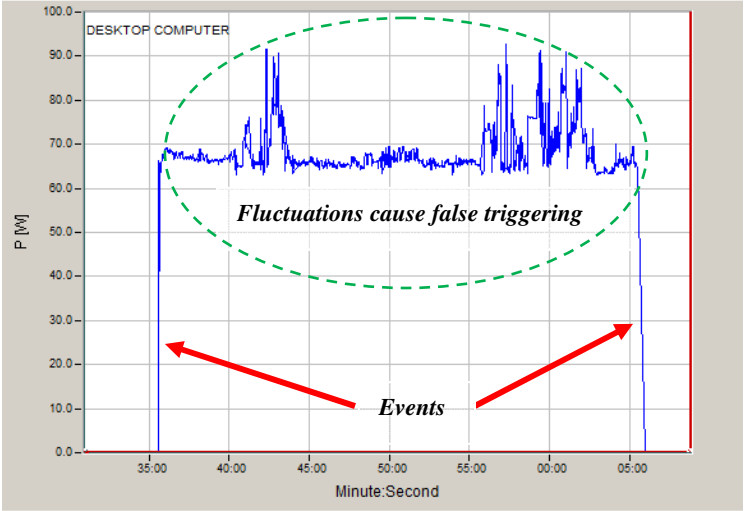

Figure 4.3: Active power consumption during half-hour operation
(from desktop computer measurement report)

The change in active power shown in the example of Figure 4.4 will be classified as an *event* if both the following conditions are fulfilled:

1. The differences *[(i+1)-i]* AND *[(i+2)-i]* are greater than twice the standard deviation.
2. The differences *[(i+3)-(i+2)]* AND *[(i+4)-(i+2)]* are smaller than twice the standard deviation.

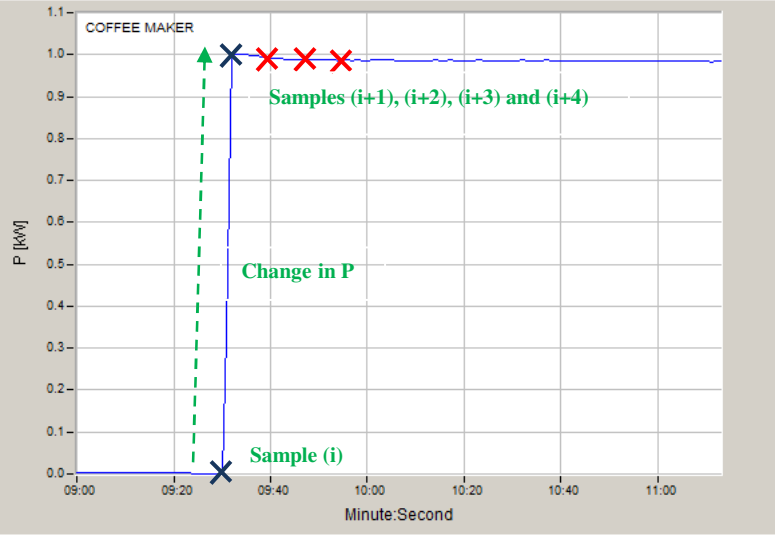

Figure 4.4: Active power change during switch-on transition
(from coffee maker measurement report)

Hence, by considering the sample points ***i+2***, ***i+3*** and ***i+4***, in addition to the first two adjacent points ***i*** and ***i+1***, it is possible to reduce sensitivity to fluctuations, which are further filtered by using a hard-defined threshold. The flowchart in Appendix D provides the details of the proposed method.

This flowchart was coded in MATLAB and its performance was checked using active power data extracted from the measurement files. The test done on the available *two-state, single-mode appliances* resulted in the correct detection of 87.50% of the total possible *switch-on events* and 90.63% of the total *switch-off events*. However, the event detector did not work reliably on multi-state appliances. Table D-1 in Appendix D gives detailed results obtained from this test [*actual (observed)* vs. *detected values* for both switch-on and switch-off transitions are provided].

The following points were observed during the event detection test:

- Switch-on events belonging to appliances with *large starting current* (such as refrigerators) were not detected. Besides, the falling edge of such initial spike (the instant just before settling into steady-state operation) can be wrongly detected as a switch-off event. Hence, an improvement is needed to search for the first stable transition point.
- In the case of multi-state appliances (such as a table fan operating at different speeds), improvement is needed to detect *intermediate state transitions*. Note that it is possible to have in-between state changes other than the *initial* switch-on and *final* switch-off events.
- By tracking the number of switch-on and switch-off event pairs (especially if they occur within a short period of time as in the case of microwave oven), it is possible to substantiate the output of the pattern recognition algorithm.

Improved event detector

Following this initial attempt to trace state changes of appliances, a *signal smoothing scheme* was added to the event detector, as illustrated in Figure 4.5, in order to attenuate the frequent fluctuations and switch-on spikes.

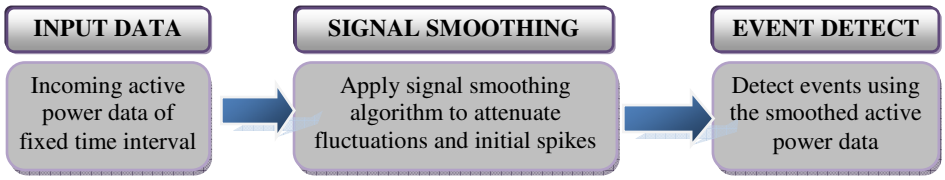

Figure 4.5: Additional signal smoothing to improve event detection

Multiple-point-averaging is mentioned in [15] as a means to remove much of the noise from a power signal and also to smooth the signal so that significant events are easier to identify. An array of raw data, for instance $\mathbf{[y_1, y_2 \ldots y_N]}$ from active power measurement, can be converted to a new array of smoothed data in which the 'smoothed point' $\mathbf{(y_k)^{sm}}$ is the average of consecutive 2n+1 (n=1, 2, 3, ..) points of the raw data $y_{(k-n)}$, $y_{(k-n+1)}$, …, $y_{(k-1)}$, y_k, $y_{(k+1)}$, …, $y_{(k+n-1)}$, $y_{(k+n)}$.

$$(y_k)^{sm} = \sum_{i=-n}^{i=n} \left(\frac{y_{k+i}}{2n+1}\right) \qquad (4.1)$$

The odd number (2n+1) is the *filter width*; the greater the filter width, the more intense the smoothing effect becomes [59].

The MATLAB code in [60] was directly used to execute the signal smoothing function shown in the above block diagram. Figures 4.6 and 4.7 illustrate the signal smoothing that can be achieved when active power data from sample appliances are passed through the filter provided in [60].

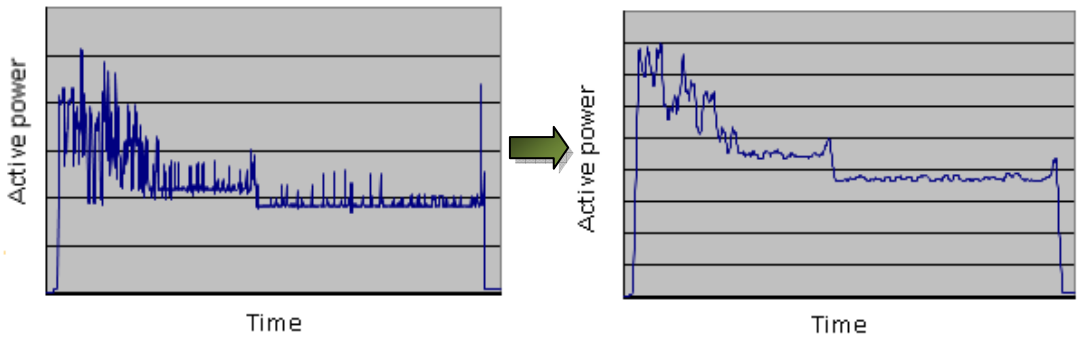

Figure 4.6: Reducing fluctuations allows easier identification of events (from laptop measurement report)

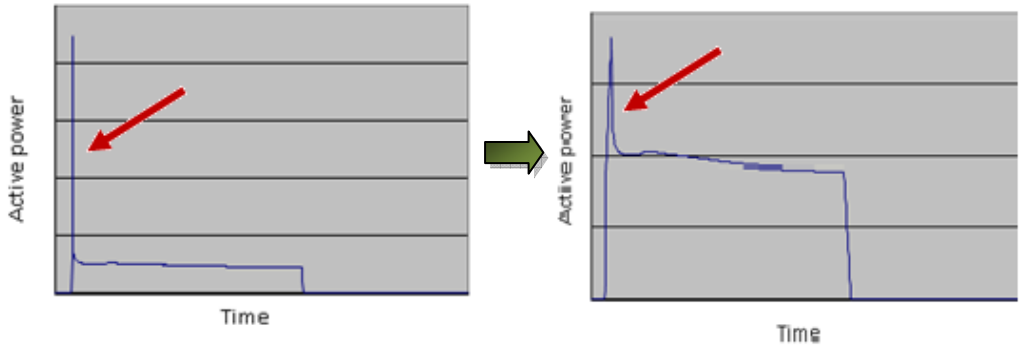

Figure 4.7: After the reduction of the level of switch-on spike, significant events tend to be dominant and detectable (from freezer measurement report)

Another round of testing with the improved event detector was then performed on the appliances whose events were not properly detected during the previous test (refer to Table D-1 in Appendix D for the previous test results).

The results from the second test are summarized next in Table 4.1.

1	Desktop PC #2	Both switch-on and switch-off events detected within 7 seconds deviation from actual events
2	CRT PC monitor #2	Both switch-on and switch-off events detected within 8 seconds deviation from actual events; Additional switch-off event wrongly detected
3	Refrigerator (cycle 1)	Switch-on event not detected again; Switch-off event detected within 9 seconds deviation from actual event
4	Laptop #2	Both switch-on and switch-off events detected within 8 seconds deviation from actual events; Additional switch-off event wrongly detected
5	Freezer (cycle 3)	Both switch-on and switch-off events detected within 8 seconds deviation from actual events

Table 4.1: Additional test results for events that were not correctly detected

The application of signal smoothing improved the detectability of events that were missed in the previous test. On the other hand, the unwanted detection of additional switch-off events and more importantly the failure to detect the switch-on event of the refrigerator are the shortcomings of the improved detector. The filter width used was $\boldsymbol{n = 5}$; by increasing this width, it is possible to further reduce the level of spike and thus permit the recognition of the missed switch-on event. However, as already mentioned above, larger filter widths tend to 'flatten' the signal curve and may result in the masking of other significant events, especially for multi-state appliances with intermediate transitions.

The BeAware project team at HIIT also developed an event detection technique using *median filter* and *gradient edge detection* [61]. It uses time-stamped active power data series as input and constitutes the following three main steps –

1. **Data preprocessing** – this step employs median filter to remove noise from the input data.
2. **Detection of stable states** – the stability of the transition between two *filtered adjacent samples* is checked in this step; this allows to further reduce noise level by removing fluctuations that are

momentary in nature (and hence do not represent actual state changes).

3. **Classification of events** – changes between *adjacent stable states* are classified as events if their difference satisfies a set of criteria.

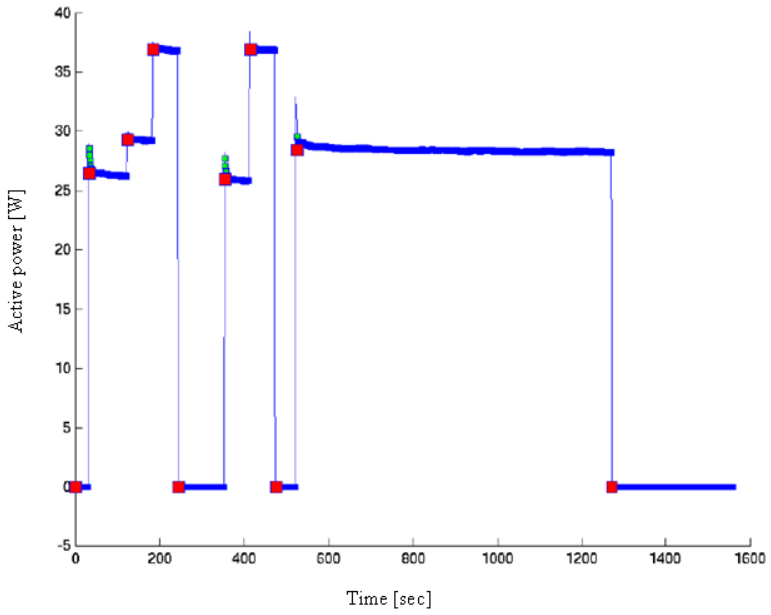

Figure 4.8: State transitions and stable states of a multi-state table fan [61]

In Figure 4.8, the bold parts of the curve represent *clusters of stable states* and the red markings indicate the *beginning of a stable state after the occurrence of an event* [61]. In this particular example, even though the user-selectable sequences varied during the entire operation, the algorithm was able to properly detect the four different states of the appliance (three different operation sequences: 0-1-2-3-0, 0-1-3-0 and 0-2-0, as can be observed from the figure).

The algorithm was tested on 7 appliances to validate its performance [61]. Although the overall detection success rate was not quantified, it is evident from the individual test results published in the report that it performed reasonably well for two-state as well as cyclic appliances within the test domain.

It also worked correctly for the more complex multi-state appliances (table fan and dishwasher in this case), which were not included in the previous two event-detection tests.

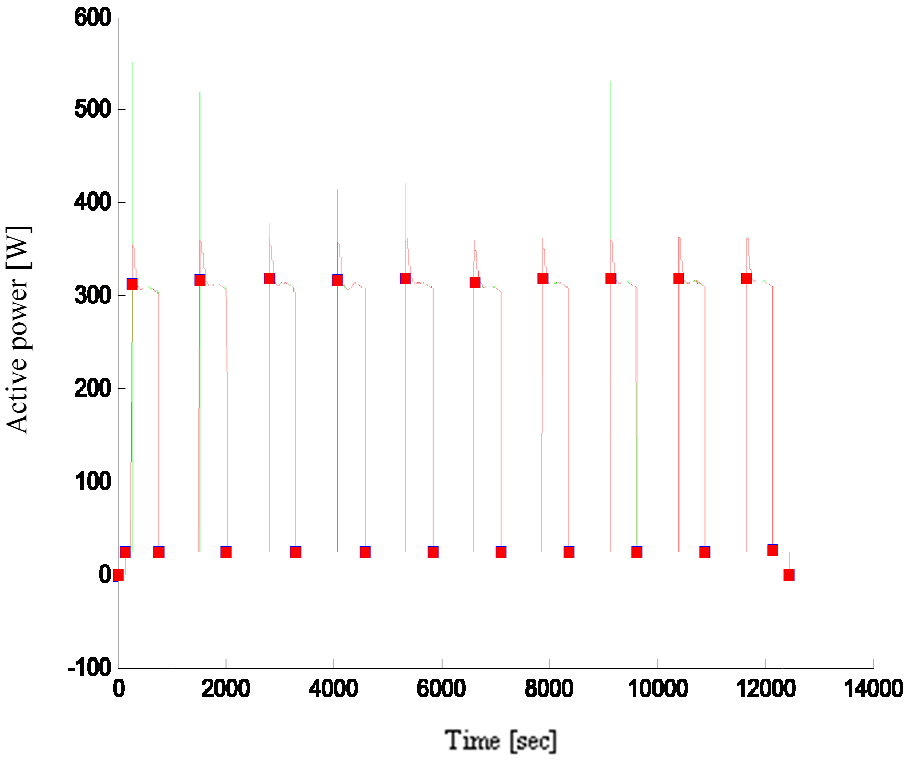

Figure 4.9: Detected switch-on and switch-off events (shown in red markings) of refrigerator sample

The missing switch-on event of the refrigerator sample ('Refrigerator-cycle 1' in Table 4.1) was tested using this algorithm. As shown in Figure 4.9, it is correctly detected as are the other switch-on and switch-off events belonging to subsequent cycles. Although this algorithm worked well for appliances with large switch-on spikes and also for complex multi-state appliances, it was observed from the test results in [61] that the presence of noise even after filtering still affects the accuracy of the event detector due to the generation of false events.

4.3 APPLIANCE TYPE IDENTIFICATION

The experiments in the previous section demonstrated different methods for detecting the occurrence of events, which are the inputs for the next step in the fingerprinting process, namely *appliance type identification*.

Referring back to Figure 4.1, the appliance type identification step can be actualized by using *pattern recognition* (which is used in this work) or *optimization techniques*. Irrespective of the method applied, the basis for this step is the creation of a *load library (database)* that consists of known appliance signatures [50].

Taking into account the parameters being measured and transmitted by the BeAware sensor and based on observations from the measurement work, a given appliance can be characterized by the following 8 selected features, which were discussed in detail in Section 3.3:

***Active power** (P) | **Fundamental power factor** (FPF)*

***Total power factor** (TPF) | **Total harmonic distortion** (THD_I) | **Crest factor** (CF)*

3rd harmonic current | 5th harmonic current | 7th harmonic current

After forming the load library, the detected events from the previous step are classified by a pattern recognition algorithm as belonging to one appliance type or another [56].

APPLIANCE NAME	*ID*	P [W]	FPF	TPF	THD_I	CF	3RD H	5TH H	7TH H
Space heater	***709***	1196.09	0.999	0.999	0.9	1.41	0.2	0.4	0.5
PC LCD monitor	***711***	33.93	0.937	0.500	156.9	3.51	90.5	80.9	68.9
Freezer	***723***	334.27	0.684	0.681	10.2	1.54	8.7	1.7	1.4

Table 4.2: Appliance samples characterized by the selected attribute values

The above table shows three sample entries in the load library; each appliance sample is tagged with an identification number (ID) and then characterized by the 8 steady-state attributes that were recorded during the measurement period. Note that THD_I and the odd harmonics are percentage values.

4.3.1 PATTERN RECOGNITION USING *k*-NN ALGORITHM

A study conducted at Carnegie Mellon University in relation to residential load monitoring compared the performances of four different training classifiers in noise free (laboratory) as well as real world situations [63][65]. The tested training classifiers were Gaussian Naïve Bias, 1-Nearest Neighbor (1-NN), Multiclass AdaBoost (MultiBoost) and Decision Tree by using 449 recorded events as training dataset that formed a signature database.

According to experimental results in [65], each algorithm performed differently and the best results were obtained using 1-NN. During laboratory testing on 8 appliances, the average accuracy of this classifier using Fourier regression coefficients was 79%; in a real world test, conducted at an occupied residential building on 17 appliances, the classifier performed with 80% accuracy [63]. For the sake of its simplicity and adequate performance, the *k*-NN algorithm was studied in further detail so as to explore its applicability in the BeAware fingerprinting process.

The algorithm was originally suggested by Cover and Hart [66] and nowadays it is the most widely applied classification method [74]. Its operation is based on comparing a new record with a set of training records in order to find the ones that are similar to it [67]. The training phase of this algorithm consists of storing the *training records* and *their class labels*.

Each record with n attributes represents a point in an n-dimensional space. When given a new record, the *k*-NN algorithm searches the space for the k training records that are nearest to the new record and then predicts the class label of the new record using the class labels of these nearest neighbors [67].

In this algorithm, nearness is defined in terms of a distance metric such as Euclidean distance [68]. For any two records consisting of n continuous attributes or two points in an n-dimensional space, $\mathbf{p} = (p_1, p_2 \ldots p_n)$ and $\mathbf{q} = (q_1, q_2 \ldots q_n)$, the Euclidean distance is defined as:

$$d(\boldsymbol{p}, \boldsymbol{q}) = \sqrt{\sum_{i=1}^{n} (p_i - q_i)^2} \tag{4.2}$$

On the other hand, if the records are composed of discrete attributes, then *hamming* or *edit distance* is applied to define nearness [75]. After calculating the distances between the new record and the respective training records, the resulting values are then *sorted* and *k* nearest neighbors are *selected*. A training record will qualify as nearest neighbor if its distance from the new record is less than or equal to the k^{th} smallest distance.

The next step is to provide a *classification decision* for the new record based on the class labels of the selected *k* nearest neighbors. Generally, two methods exist: *unweighted voting*, in which the class label most frequent among the neighbors is simply selected as the class label of the new record without considering the preference of the neighbors, and *weighted voting*, in which more weight is given to the neighbors that are closer to the new record [67].

A common weighting scheme is to give each neighbor a weight of ***1/d***, where ***d*** is the distance to the neighbor. Thus, the nearer neighbors will have more influence on determining the class label than the more distant ones [68]. After weighting the neighbors, the sum of weights of neighbors with the same class label is calculated. Finally, the class label corresponding to the neighbors with the largest sum of weights is selected as the class label of the new record.

If the features of records, for instance, $x_1, x_2 \ldots x_n$ of **x** are on different scales, then it is necessary to remove scale effects [69]. A common way to do this is to transform the records by applying *Z-score standardization*. A raw feature value x_{ij} is transformed using the *mean* and *standard deviation* of all feature values, given by the relationship [70]:

$$\frac{x_{ij} - \mu_j}{\sigma_j} \tag{4.3}$$

Where x_{ij} is the j^{th} feature/attribute (e.g., *total power factor*) of the i^{th} record (e.g., *desktop PC sample #3*), μ_j is the arithmetic mean and σ_j is the standard deviation of the entire values under the j^{th} feature. The distance calculated using these transformed values is called *Standardized Euclidean Distance*.

For the i^{th} record $\mathbf{x_i}$ and new record $\mathbf{y}$, the standardized Euclidean distance can be written as:

$$d(\boldsymbol{x_i}, \boldsymbol{y}) = \sqrt{\sum_{j=1}^{n} \left(\frac{1}{\sigma_j^2}\right)\left(x_{ij} - y_j\right)^2} \tag{4.4}$$

Since the j^{th} *mean* cancels out when computing the differences between the corresponding feature values, the standardized Euclidean distance is in effect the ordinary Euclidean distance with a weight attached to the respective squared differences, which is the *inverse of the* j^{th} *variance* ($1/\sigma_j^2$) [69].

Unlike other classification algorithms such as Decision Tree that use only one subset of attributes for classification, the *k*-NN algorithm utilizes all attributes equally. However, all attributes may not have the same effect on the classification process, a phenomenon commonly known as 'the curse of dimensionality'. One approach to overcome this problem is to weight attributes differently and compute the distances accordingly [67]. In this way, similarity with respect to important attributes becomes more critical than similarity with respect to irrelevant attributes [69]. Attribute weighting techniques include *dynamic k-nearest neighbor algorithm* (DKNN) [67] and *quadratic programming* [72] [73].

Another important aspect is validation of classification accuracy of the algorithm, which is usually performed by using *leave-one-out cross validation* (LOOCV) or *k-fold cross validation* (*k* is often equal to 5 or 10). The result obtained is indicative of the classification accuracy for that particular dataset, which is characterized by:

- *The number of attributes* – e.g., 8 attributes used in this work,
- *The number of records* – i.e., the total number of sample entries in the load library,
- *The number of class label types* – e.g., how many different types of household appliances in the dataset

4.3.2 APPLIANCE TYPE IDENTIFICATION TESTS

A procedure developed in this work for *predicting the class label* of a new record using the *k*-NN algorithm that employs distance-weighted voting is given in Appendix E (Figure E.1). Another procedure for *validating classification accuracy* based on LOOCV is also provided in Appendix E (Figure E.2). In the LOOCV procedure, one of the ***n*** training records is temporarily removed and is used as a validating record on the remaining ***n-1*** records. This process is repeated for all training records and finally the *percentage of classification accuracy* is calculated.

The load library created for testing purpose consists of only those appliances with a minimum of two measured samples from the same appliance family so that at least the accuracy of classification at k=1 can be checked. Besides, ID number is given to each appliance sample in the library so as to simplify the computation process. Thus, appliances in the same family will have identical ID numbers. Table E.1 in Appendix E gives the classification results obtained using 1-NN (k=1) approach. The 8 steady-state attributes are also shown in the table for each appliance (or for *each operating state*, in the case of appliances that perform sequence of tasks and multi-state appliances).

It should be noted that the *62.30%* overall identification accuracy obtained is in effect the result of a first-time classification because the temporary removal of a specific record means that there is no stored information about the corresponding appliance at the time of class prediction. It is expected that subsequent re-classifications of the same set of appliances using data acquired from new measurements will have a much improved accuracy owing to the fact

that the data obtained from these new measurements will closely match with the respective steady-state features already available in the load library. This is assuming that newer measurements are conducted while the appliance is operating under *normal condition* and also assuming that there is *no significant degradation* in the performance of the appliance through time.

Regarding the relevance of each attribute, it was observed for the dataset considered here that all attributes have comparable contribution towards accuracy of class prediction. This was validated by applying *backward elimination* [76] to check whether improvement in accuracy can be achieved or not by discarding one attribute at a time (for example, removing THD_I values from the library) and then running the classification algorithm using the remaining *n-1* attributes.

A second round of measurement[1] was done on a selected group of appliances to test the performance of the algorithm in the situation when the information about a particular appliance is already available in the load library from a previous measurement.

The steady-state values extracted from the new measurement and the obtained result are given in the table below.

APPLIANCE NAME	*ID*	P [W]	FPF	TPF	THD_I	CF	3^{RD} H	5^{TH} H	7^{TH} H	RESULT (k=3)
Microwave oven 1 (at 500W)	***727***	781.77	0.989	0.722	28.1	1.65	23.8	12.5	5.2	**727**
Vacuum cleaner 1	***721***	825.53	0.896	0.774	56.4	2.03	53.1	17.9	6.8	**721**
Desktop PC 1	***718***	64.90	0.831	0.821	15.1	1.61	13.1	1.4	3.05	**718**
Coffee maker 1	***708***	825.21	0.998	0.910	1.4	1.41	0.2	0.4	0.7	**709**
Refrigerator 1	***723***	94.32	0.724	0.691	7.7	1.49	7.2	1.9	1.5	**723**

Table 4.3: Steady-state values of appliances from the second measurement

[1] First measurement period was January - February 2010. The second round of measurement (on a few selected appliances) was done in June 2010; it was also done using TOPAS power quality analyzer.

As can be observed from Table 4.3, the pattern recognition algorithm identifies appliances[2] with better precision when the information about the particular appliance is already available in the load library.

4.3.3 BUILDING THE FINGERPRINTING PROCESS

One possible scheme for assembling the different steps discussed in the preceding sections is proposed next. It should be noted that the approach needs to be modular in order to facilitate necessary modifications for the present scenario and also to allow possible migration to fingerprinting at aggregate current measurement level.

The steps are explained next (with reference to the flowchart in Figure 4.14):

- The sensor monitors the consumption at a specific socket point and transmits measurement data periodically.
- Received Power Messages are temporarily accumulated, say ΔT=300 sec, for event detection (NOTE - length of accumulation time can be adjusted). For instance, in [77] the appliance recognition program tries to recognize an appliance one minute after it is turned on.
- The event detection system then searches for events related to appliances switching-on, switching-off or changing their operating states.
- The detected events are classified as *switch-on* or *switch-off events* and temporarily stored with their respective time-stamps.
- Events analysis starts with switch-on events. Even if both types of events are detected during a single search (ΔT=300 sec), as shown in Figure 4.10, events analysis shall start with switch-on events. For the purpose of analysis, an 8-element vector '*switch-on profile*' is created using attributes from the $(n+3)^{th}$ Power Message (i.e., assuming the first switch-on event was detected in the n^{th} Power Message).

[2] The numbered appliance samples in the first column of Table 4.3 refer to the corresponding appliance samples in the test results of the previous measurement (Table E.1 in Appendix E).

- A delay of *3 Power Message steps* (equivalent to 6 seconds) is introduced here in order to allow the appliance enter its steady-state operation.

– The *switch-on profile* is then fed to an appliance identification system (e.g. a pattern recognition algorithm) to find its match from a load library.

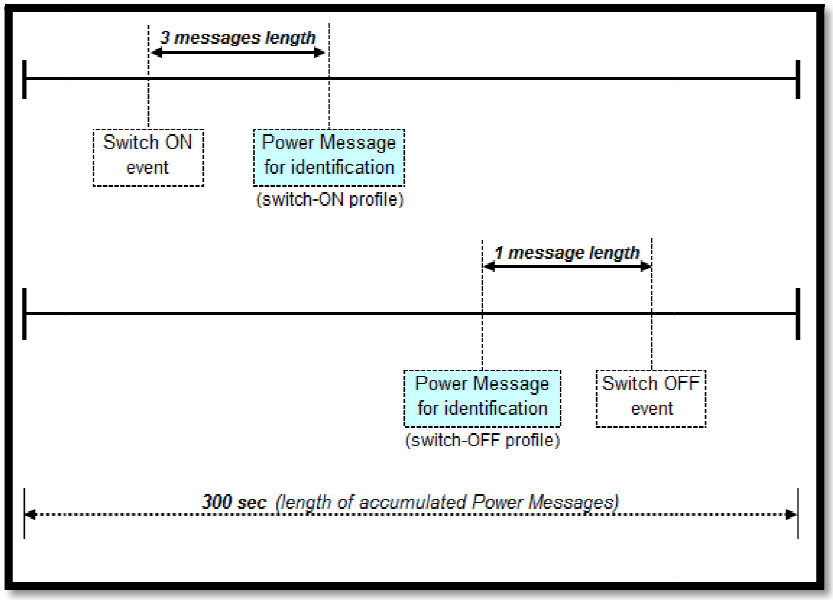

Figure 4.10: *Switch-on profile* and *switch-off profile* occurring within a single accumulation time

– If no match is found, then the user will be prompted to name the appliance and accordingly the load library will be updated with the new information (i.e., a new entry will be created using the appliance name and its switch-on profile, which is equivalent to its steady-state profile).

– The quantity of detected switch-on events can be used as an indicator of the appliance's nature from an operation point-of-view; this approach was discussed earlier in Subsection 3.3.1. The possible cases are:

- **continuous / long-cyclic / short-cyclic**

  Appliances with *short-cyclic* operation generate a number of switch-on events within a single accumulation time as shown in Figure 4.11,

whereas for those appliances with *continuous* (Figure 4.12) or *long-cyclic* (refer back to Figure 4.9) operations, there will be at most one switch-on event.

- **multi-mode / single-mode**

  Appliances such as dishwashers switch from one operating state to another as their operation transits between sequences of tasks. It is probable that multiple transitions can take place within a single accumulation time. However, for appliances with a single task, there will be at most one switch-on event (exceptions are single-task appliances with short-cyclic operations).

- **multi-state / two-state**

  Multi-state appliances can possibly operate in short succession at two different switch-on states, for instance, due to user interaction as in the case of a cooking plate or a table fan (Figure 4.13). On the other hand, two-state appliances have only one switch-on state such as the toaster in Figure 4.12, which means they usually generate at most one switch-on event within a single accumulation time (exceptions are two-state appliances with short-cyclic operations).

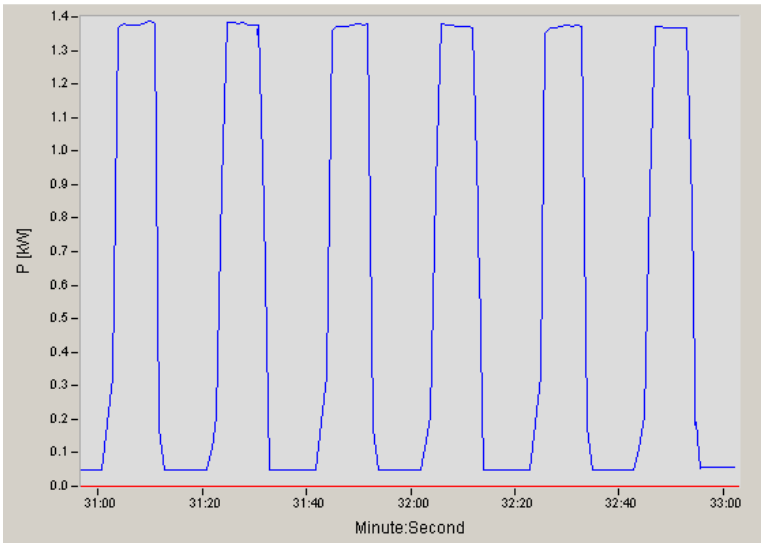

Figure 4.11: Microwave oven operation – several changes of states in a short interval (from measurement report)

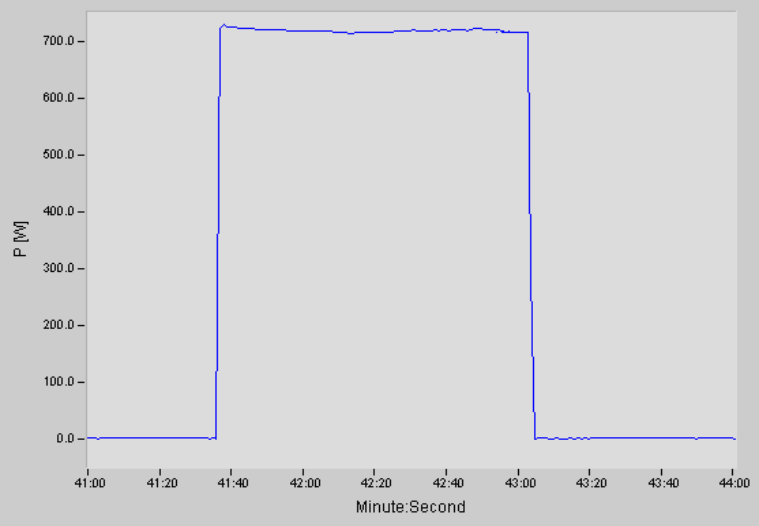

Figure 4.12: Toaster operation – continuous, single-mode, two-state operation (from measurement report)

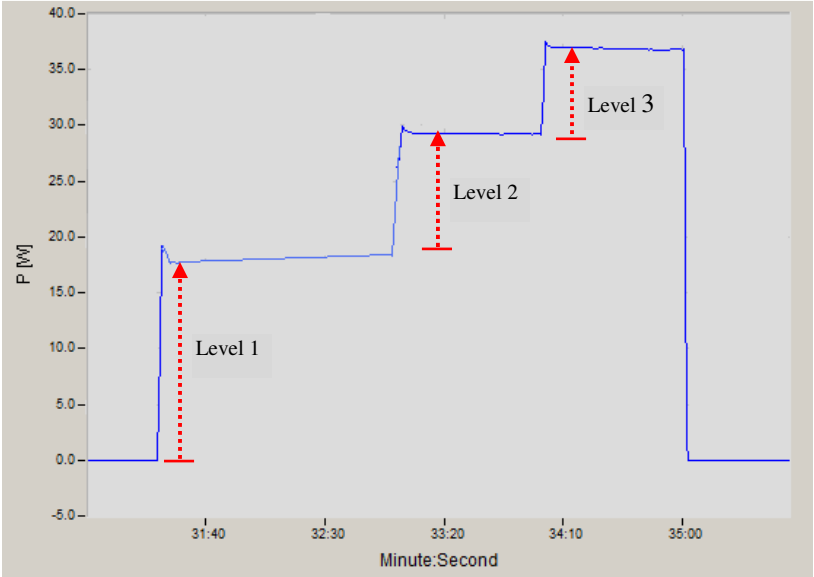

Figure 4.13: Table fan operation – multi-state changes (from measurement report)

– After appliance identification, the switch-on profile (with its appliance ID) is entered into a list of "active" switch-on profiles until a corresponding switch-off profile is found.

- Next, the analysis of switch-off events is carried out. In a similar way, an 8-element vector '*switch-off profile*' (Figure 4.10) is created using attributes from the $(n-1)^{th}$ Power Message (i.e., assuming the first switch-off event was detected in the n^{th} Power Message).
- The quantity of detected switch-off events can also be used as an indicator of the appliance's nature, particularly to provide a distinction between short-cyclic operations and long-cyclic/continuous operations. As can be seen in Figure 4.11, appliances with short-cyclic operations generate a number of switch-off events within a single accumulation time.
- The switch-off profile is then compared with an "active" switch-ON profile ("active" refers to a profile for which a matching switch-off profile is yet to be found):
  - If there is no stored "active" switch-on profile, it means an appliance was in operation without its switch-on event being detected. In this case, the '*appliance ID recovery*' function will be run to identify the appliance type using its switch-off profile. This information can also be passed for investigation to check why the switch-on event was missed and to estimate the length of operation and energy consumption.
  - If there is only a single "active" switch-on profile, then it is directly compared with the switch-off profile.
  - On the other hand, if there are a number of active switch-on profiles belonging to the same appliance (e.g., multi-state appliance), then the most likely combination of the stored profiles needs to be formed (i.e., in terms of *active power consumption*, which is the only addable attribute) and then compared with the switch-off profile. However, if these multiple active switch-on profiles belong to different appliances, it indicates that the older ones had their switch-off events missed (not detected) and hence they also need to be investigated further.

- If a match is found in one of these scenarios, the last step is to compute the *length of operation time* and also the corresponding *energy consumption*, which concludes the switch-off events analysis.

The scheme discussed above is one possible way of actualizing the appliance fingerprinting process. A project-wide design and implementation of this process for a real world application will involve a number of complexities including:

- Handling the different varities of household appliances that keep on getting operationally sophisticated due to continuous technological innovations.
- Consumer interference and its impact on events generation (note that all the experiments done in this work were performed in a controlled manner for testing purposes).
- Presence of aging and abnormally operating appliances.
- The need for systematic collection of load signatures to form a comprehensive load library.

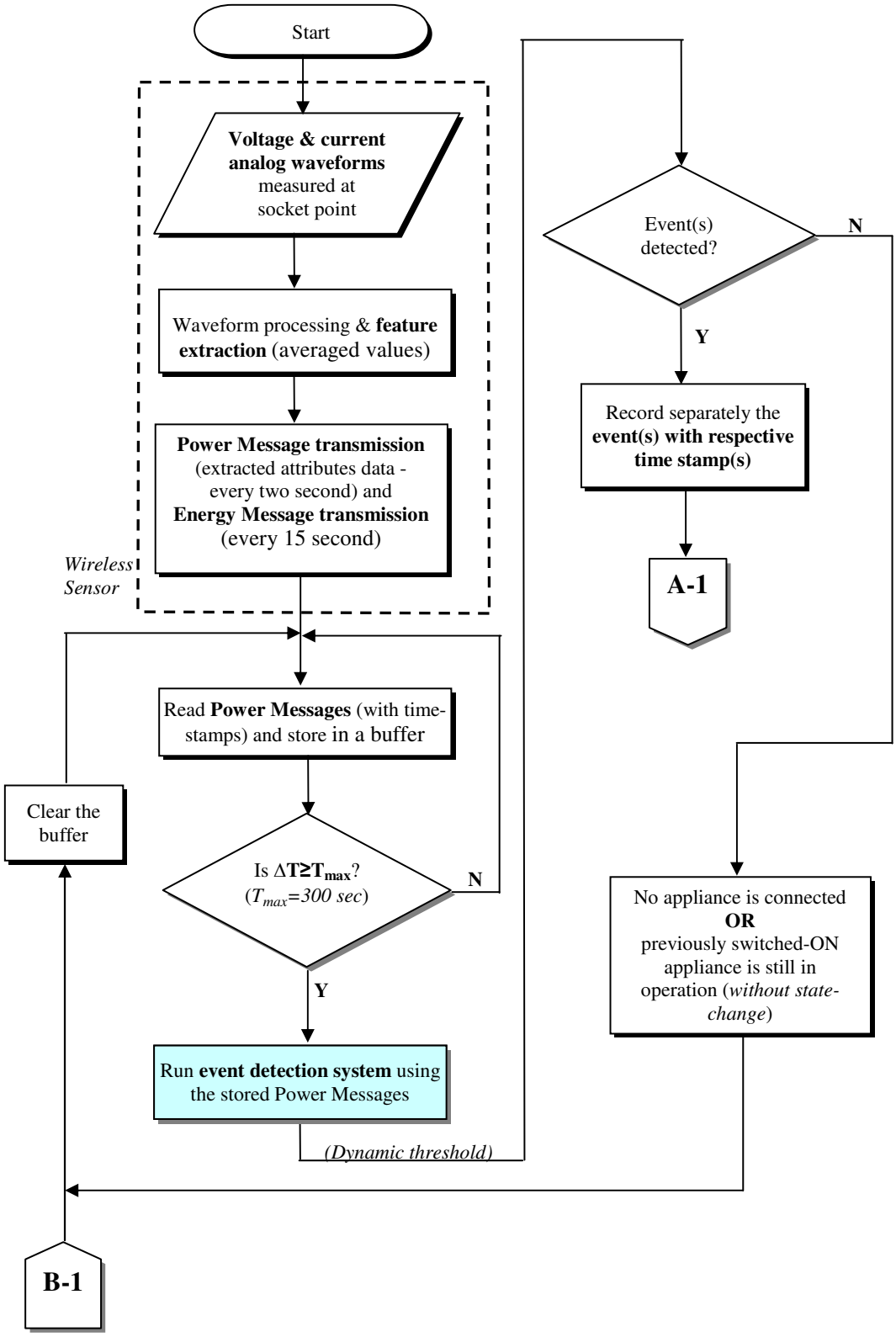
Start
Voltage & current analog waveforms measured at socket point
Waveform processing & feature extraction (averaged values)
Power Message transmission (extracted attributes data - every two second) and Energy Message transmission (every 15 second)
Wireless Sensor
Read Power Messages (with time-stamps) and store in a buffer
Clear the buffer
Is ΔT≥T_max? (T_max=300 sec)
N
Y
Run event detection system using the stored Power Messages
(Dynamic threshold)
B-1
Event(s) detected?
N
Y
Record separately the event(s) with respective time stamp(s)
A-1
No appliance is connected OR previously switched-ON appliance is still in operation (without state-change)

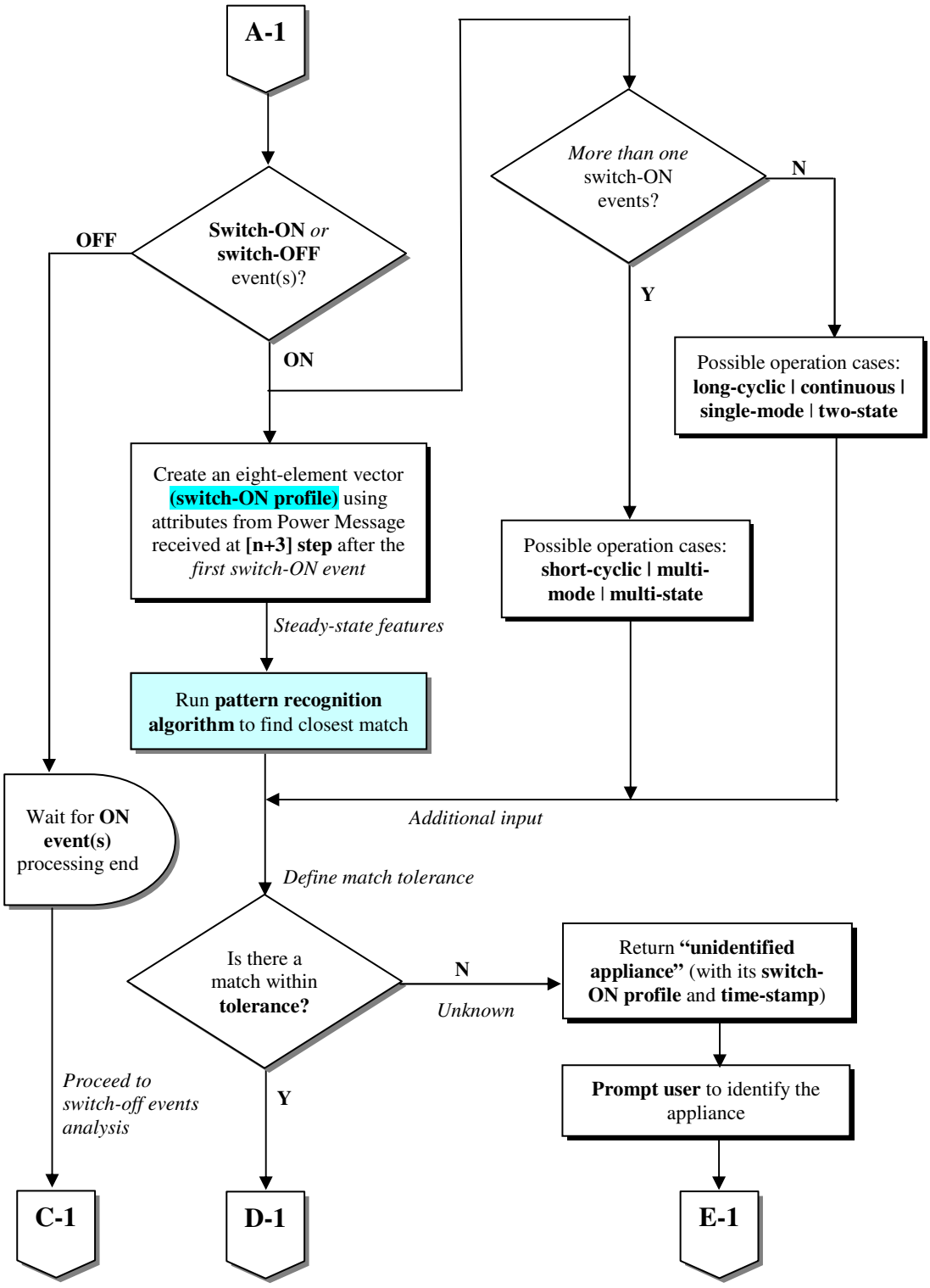
A-1
Switch-ON or switch-OFF event(s)?
OFF
ON
More than one switch-ON events?
N
Y
Possible operation cases: long-cyclic | continuous | single-mode | two-state
Create an eight-element vector (switch-ON profile) using attributes from Power Message received at [n+3] step after the first switch-ON event
Possible operation cases: short-cyclic | multi-mode | multi-state
Steady-state features
Run pattern recognition algorithm to find closest match
Wait for ON event(s) processing end
Additional input
Define match tolerance
Is there a match within tolerance?
N
Unknown
Return "unidentified appliance" (with its switch-ON profile and time-stamp)
Prompt user to identify the appliance
Proceed to switch-off events analysis
Y
C-1
D-1
E-1

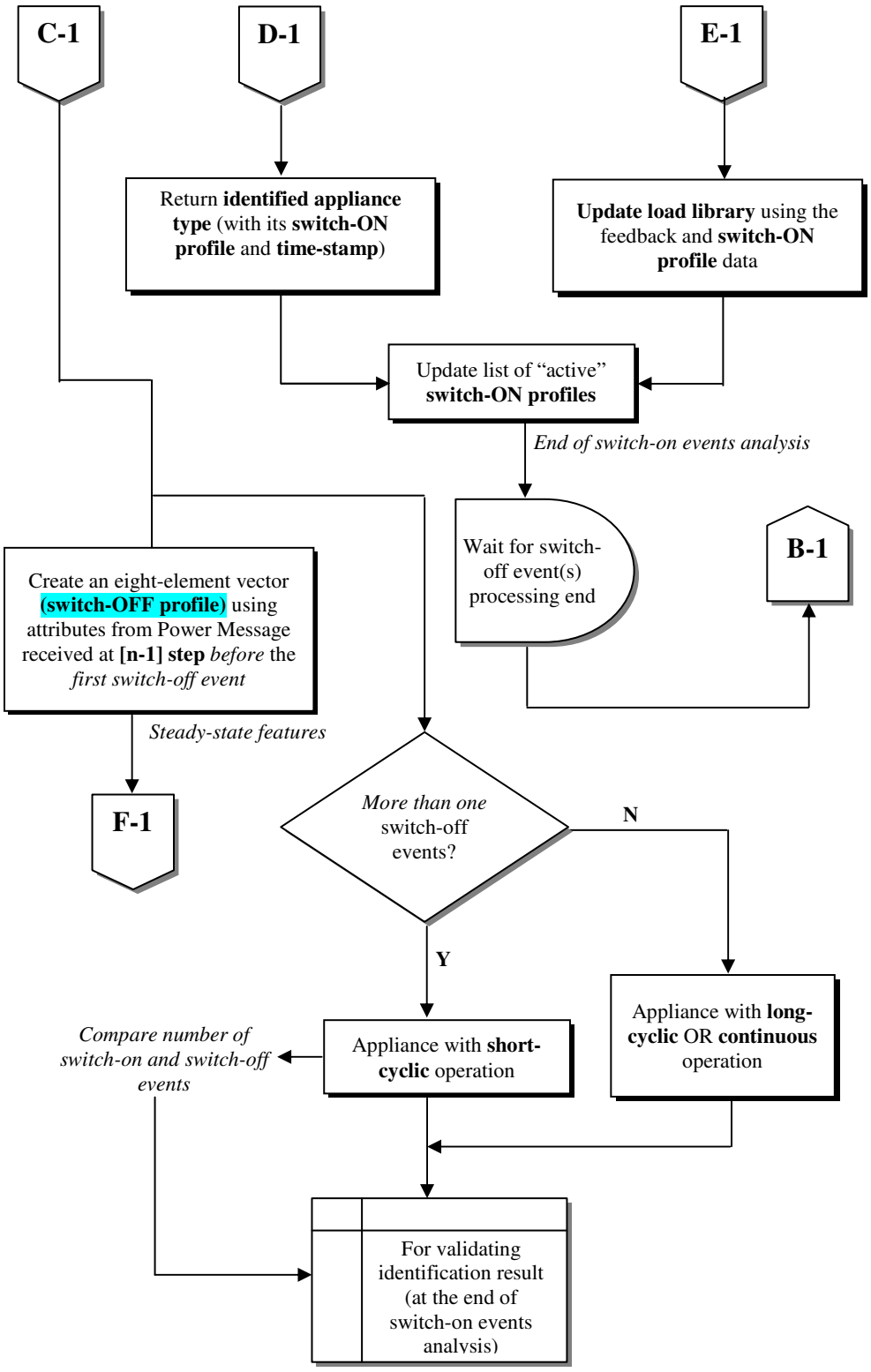
C-1
D-1
E-1
Return **identified appliance type** (with its **switch-ON profile** and **time-stamp**)
Update load library using the feedback and **switch-ON profile** data
Update list of "active" **switch-ON profiles**
End of switch-on events analysis
Wait for switch-off event(s) processing end
B-1
Create an eight-element vector **(switch-OFF profile)** using attributes from Power Message received at **[n-1] step** *before* the *first switch-off event*
Steady-state features
F-1
More than one switch-off events?
N
Y
Appliance with **long-cyclic** OR **continuous** operation
Compare number of switch-on and switch-off events
Appliance with **short-cyclic** operation
For validating identification result (at the end of switch-on events analysis)

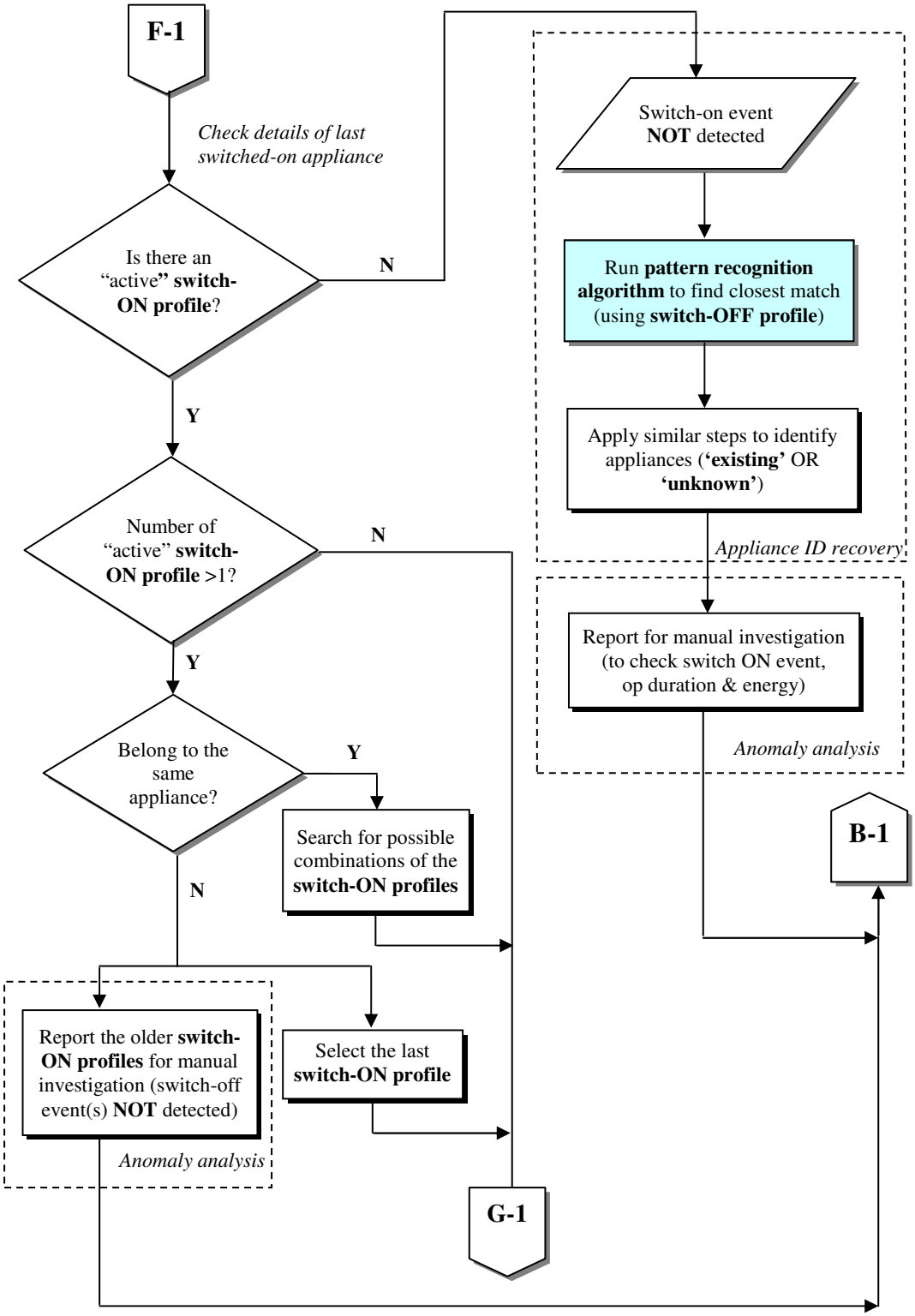
F-1
Check details of last switched-on appliance
Is there an "active" switch-ON profile?
N
Y
Number of "active" switch-ON profile >1?
N
Y
Belong to the same appliance?
Y
N
Search for possible combinations of the switch-ON profiles
Report the older switch-ON profiles for manual investigation (switch-off event(s) NOT detected)
Select the last switch-ON profile
Anomaly analysis
G-1
Switch-on event NOT detected
Run pattern recognition algorithm to find closest match (using switch-OFF profile)
Apply similar steps to identify appliances ('existing' OR 'unknown')
Appliance ID recovery
Report for manual investigation (to check switch ON event, op duration & energy)
Anomaly analysis
B-1

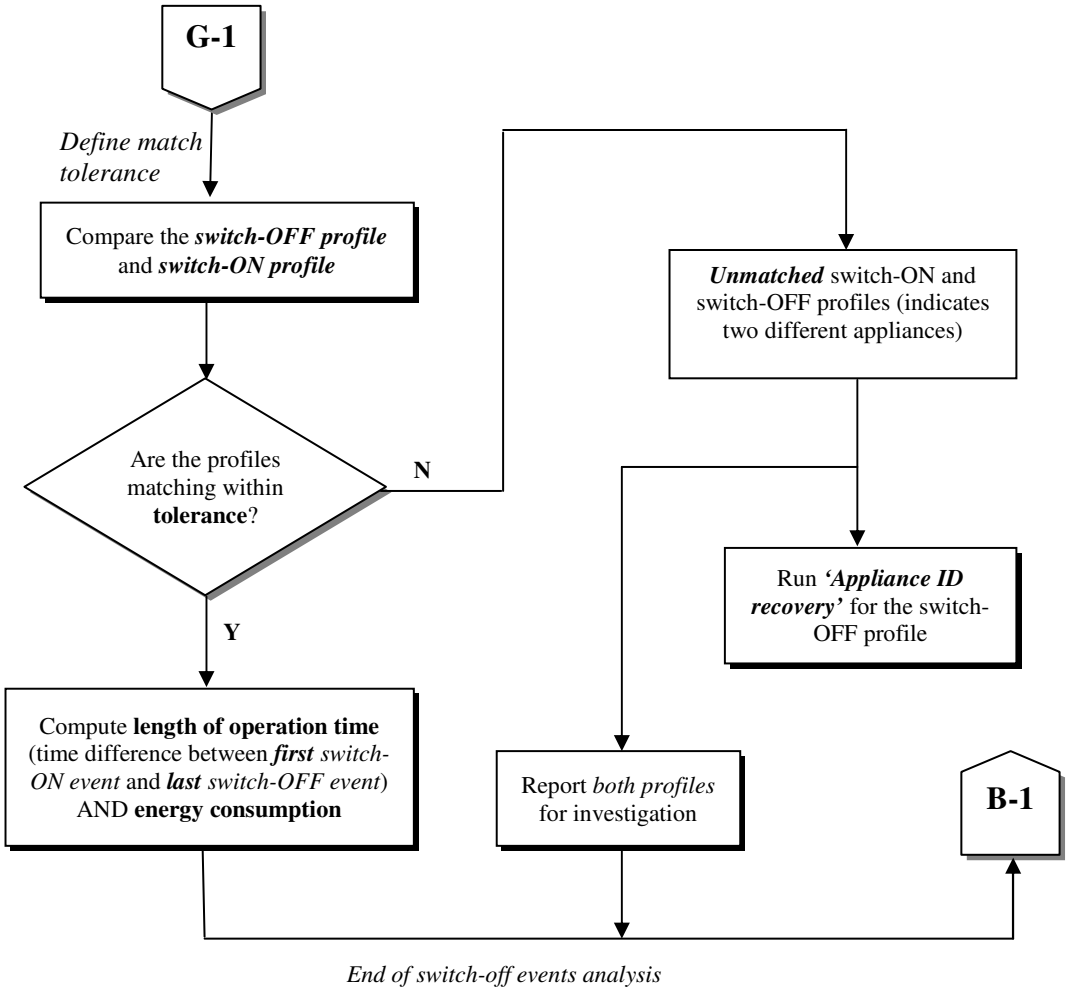

Figure 4.14: Flow chart for the proposed automatic appliance recognition process

4.4 APPLICATION IN ULTRA SMART ADVICES

With the present set up, the BeAware sensor is expected to monitor the operation of individual appliances precisely. This allows the creation of a feedback system to inform consumers about energy-saving methods in the form of advice tips. *Ultra smart advices* are one category of such feedback mechanisms and require accurate measurement and analysis [78].

Among the different ultra smart advices planned for implementation in the project, the monitoring of 'refrigerator door opening action' was studied in

connection with advice tips for managing refrigerator/freezer energy consumption. Refrigerators are major energy consumers and in many households that do not have air conditioning, they use as much and sometimes even more electric energy than all other consumptions put together [79]. This consumption is further incremented by user actions, such as frequent door openings [80] and storage of warm meals [79][80], which temporarily alter the appliance's steady-state cycle of operation.

A specific test was done to investigate the attributes that allow the detection of the door opening actions. It was observed that the small change in active power recording, due to the compartment light turning on when the door is opened, can be used as an indicator. Figure 4.15 below illustrates the changes in active power consumption at four different instances during the test.

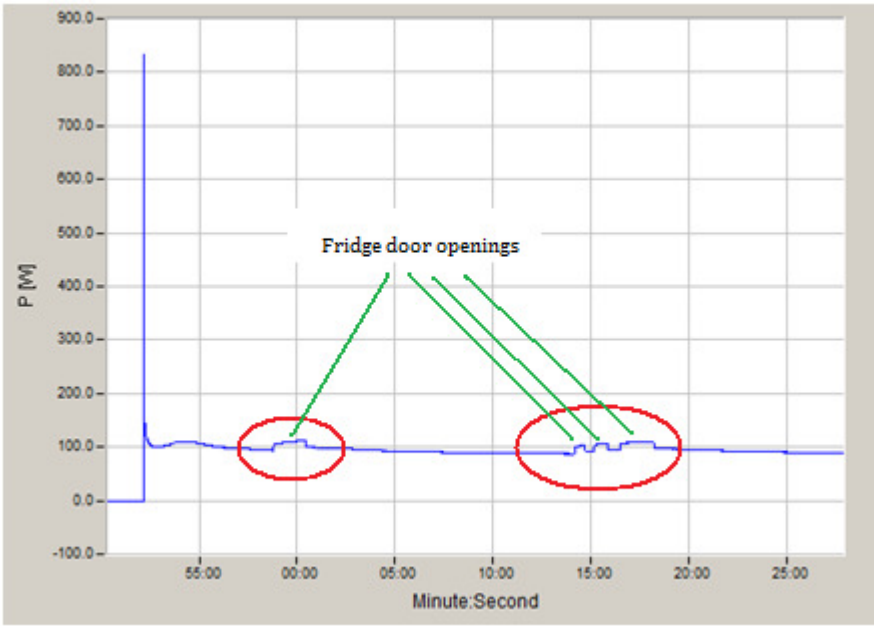

Figure 4.15: Refrigerator door opening detection test

The change in active power reading at the moment of door opening is approximately 12 W in this example. Figure 4.16 shows the detected events (related to the door openings) using the event detector in [61].

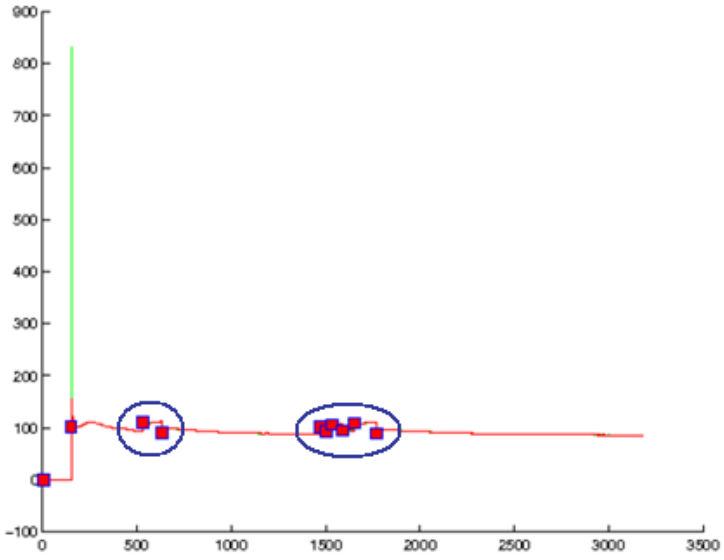

Figure 4.16: Detected events during refrigerator door opening test [61]

By tracking these changes[3] in active power, it shall be possible to associate the number of events with refrigerator door opening actions and then generate the intended advice tips.

[3] The magnitude of change is ideally in the range 12-15 W; most online retailers sell 15 W small Edison screw (SES) type fridge bulbs.

5. CONCLUSION

This thesis studied previous works done in Non-intrusive Appliance Load Monitoring System (NIALMS), analyzed measurement data that were collected during the operation of different household appliances and proposed a generic classifaction for residential loads as well as technique for appliance fingerprinting.

The fingerprinting technique fundamentally differs from previous works in two key areas:

1. Appliance operation measurement is performed at socket outlet level as opposed to most NIALMS techniques, which usually disaggregate the total load measured at the power entry point, and
2. The detection of events and appliance types is done within a short delay after the occurence of the actual events, in contrast to the operation of most NIALMS techniques, which work on data accumulated over a longer period of time.

The measurement work was performed on common household appliances to record their operational behavior during turning on, steady-state operation and turning off. The proposed load classification categorizes appliances into one of three generic classes – *resistive loads*, *power electronic loads* or *motive (inductive) loads*.

The proposed appliance fingerprinting consists of three main stages – *feature extraction*, *event detection* and *appliance type identification*. The feature extraction stage is carried out by the BeAware sensor and it involves the extraction of electrical attributes related to the operation of the appliance such as active power consumption and harmonics content. In the event detection stage, changes in the extracted features are detected and classified as events. Finally in the appliance identification stage, a set of attributes (captured after the occurence of a corresponding event) is processed to find its match from a load library that consists of known appliance signatures. The load library is formed

using 8 selected electrical attributes that are extracted from the respective steady-state operating region of every appliance in the test domain.

Necessary improvements to the proposed system and related further works are discussed below:

- Explore other electrical attributes that can be used for enhancing the pattern recognition stage – for instance, an alternative approach can be sought for the experiment that was done in this work on *current harmonics phase shift from the fundamental frequency voltage*.
- Verify with tests if the event detection system in [61] can be applied to aggregate loads and, if required, make necessary modifications – this is in anticipation that the current BeAware sensor version will be scaled up to measure the consumption at the main power entry point.
- Improve the reliability of the pattern recognition system with regard to the operation of more complex appliances that go through different cycles (states) to complete a certain task. Hidden Markov Model is introduced in [61] as one possible techinque to model such types of appliances. Besides, more samples per appliance type need be collected during the project trial phase so as to enhance the load library and thus improve classification accuracy.
- Work on the integration of appliance fingerprinting and balance sheet[4] applications to arrive at a unified solution.
- Develop additional applications to take advantage of the readily available data – possible applications include *power quality monitoring* using harmonics measurement data, load scheduling (for utilities) based on historical data and tracking of appliance performance through the course of its lifetime (normally, degradation of efficiency is expected to occur with time).

[4] In parallel to this work, a '*balance sheet' application* is being developed in the project in order to keep track of the consumption that is not directly monitored by the BeAware sensor (mainly the consumption of larger loads that are directly connected to the electric supply system).

REFERENCES

[1] ABB Group R&D and Technology, *Smart grids*. ABB Review, January 2010.

[2] International Energy Agency, *Key world energy statistics 2009*. Available: http://www.iea.org/textbase/nppdf/free/2009/key_stats_2009.pdf

[3] International Energy Agency, *World energy outlook 2009*. Available: http://www.worldenergyoutlook.org/docs/weo2009/WEO2009_es_english.pdf

[4] BeAware Project, *Annual report,* June 2009. Available: http://wiki.hiit.fi/pages/worddav/preview.action?fileName=BeAware-Annual+Report-all20090624.doc

[5] S.N. Patel et al., *At the flick of a switch: Detecting and classifying unique electrical events on the residential power line*. Proceedings of 9th International Conference on Ubiquitous Computing, Springer-Verlag, Sept. 2007, pp. 271-288.

[6] BeAware Project, *Public summary of sensing infrastructure,* May 2010. Available: http://wiki.hiit.fi/download/attachments/4063347/Beaware-D3.7-BASEN-V1.0.pdf

[7] D. York and M. Kushler, *Exploring the relationship between demand and response and energy efficiency: A review of experience and discussion of key issues*. American Council for an Energy-Efficient Economy (ACEEE), Report U052, March 2005.

[8] A.I. Cole and A. Albicki, *Algorithm for non-intrusive identification of residential appliances.* Proceedings of the 1998 IEEE International Symposium on Circuits and Systems, vol. 3, May 31- June 3, 1998, pp. 338 – 341.

[9] W.K. Lee et al., *Exploration on load signatures*. Proceedings of the International Conference on Electrical Engineering, Sapporo, Japan, vol. 2, July 4-8, 2004, pp. 690-694.

[10] J.W.M. Cheng, G. Kendall and J. S. K. Leung, *Electric-Load Intelligence (E-LI): concept and applications*. Proceedings of the IEEE Region 10 Conference, Hong Kong, November 14-17, 2006, Paper CI 1.1

[11] BeAware Project, *Specification and interfaces to and from the sensing platform,* September 2008. Available: http://wiki.hiit.fi/download/attachments/4063347/BeAware-D3.1-Basen-V1.0-20080930.pdf

[12] Electric Power Research Institute (EPRI), *Nonintrusive appliance load monitoring system (NIALMS) beta-test results*. Final Report TR-108419, September 1997.

[13] H. Pihala, *Non-intrusive appliance load monitoring system based on a modern kWh-meter*. VTT Publications, no. 356, May 1998.

[14] L. Farinaccio and R. Zmeureanu, *Using a pattern recognition approach to disaggregate the total electricity consumption in a house into the major end-uses*. Energy and Buildings, no. 30, 1999, pp. 245-259.

[15] T.R. Sharp, *Nonintrusive load monitoring systems: Considerations for use and potential applications*. US Department of Energy, Office of Scientific and Technical Information, Paper submitted to ACEEE Journal for publication.

[16] BFM136 feeder monitor application note. Available: http://www.satec-global.com/eng/bfm136_application_note.aspx (accessed 22.05.2010).

[17] G.W. Hart, *Nonintrusive appliance load monitoring*. Proceedings of the IEEE Computer Applications in Power, vol. 80, no. 12, December 1992, pp. 1870-1891.

[18] L.K. Norford and R.D. Tabors, *Non-intrusive electrical load monitoring technique for reduced-cost load research and energy management*. Proceedings of the ACEEE Summer Study on Energy Efficiency in Building, vol. 3, 1992, pp. 3187-3198.

[19] J. Liang et al., *Load signature study—Part I: Basic concept, structure, and methodology*. IEEE Transactions on Power Delivery, vol. 25, no. 2, April 2010, pp. 551-560.

[20] C. Laughman et al., *Power signature analysis*. IEEE Power and Energy Magazine, vol. 1, no. 2, March/April 2003, pp. 56-63.

[21] H. Najmeddine et al., *State of art on load monitoring methods*. Proceedings of 2nd IEEE International Conference on Power and Energy, December 1-3, 2008, Johor Baharu, Malaysia, pp. 1256-1258.

[22] A.J. Bijker, X. Xia and J. Zhang, *Active power residential non-intrusive appliance load monitoring system*. Proceedings of IEEE AFRICON 2009, September 23-25, 2009, Nairobi, Kenya, pp. 1-6.

[23] G.W. Hart, *Residential energy monitoring and computerized surveillance via utility power flows*. IEEE Technology and Society Magazine, vol. 8, no. 2, June 1989, pp. 12-16.

[24] D.D. Sabin, D.L. Brooks and A. Sundaram, *Indices for assessing harmonic distortion from power quality measurements: definitions and benchmark data*. IEEE Transactions on Power Delivery, vol. 14, no. 2, April 1999, pp. 489-496.

[25] A. Nassif, *Modeling, measurement and mitigation of power system harmonics.* PhD thesis, University of Alberta, Fall 2009.

[26] BeAware Project, *Prototypes of wireless sensing,* April 2009. Available: http://wiki.hiit.fi/download/attachments/4063347/BeAware-D3.3-TKK-V1.0-20090429.pdf

[27] D. Srinivasan, W.S. Ng and A.C. Liew, *Neural-network-based signature recognition for harmonic source identification*. IEEE Transactions on Power Delivery, vol. 21, no. 1, January 2006, pp. 398-405.

[28] S. Leeb et al., *Development and validation of a transient event detector*. AMP Journal of Technology, vol. 3, November 1993.

[29] M.R. Brambley, *A novel, low-cost, reduced-sensor approach for providing smart remote monitoring and diagnostics for packaged air conditioners and heat pumps*. US Department of Energy. Available: http://www.pnl.gov/main/publications/external/technical_reports/PNNL-18891.pdf

[30] S.B. Leeb, S.R. Shaw and J.L. Kirtley Jr., *Transient event detection in spectral envelope estimates for nonintrusive load monitoring*. IEEE Transactions on Power Delivery, vol. 10, no. 3, July 1995, pp. 1200-1210.

[31] K.H. Ting et al., *A taxonomy of load signatures for single-phase electric appliances*. Paper submitted to IEEE Power Electronics Specialist Conference, June 12-15, 2005, Brazil.

[32] G.W. Hart, E.C. Kern and F.C. Schweppe, *US Patent 4858141-Nonintrusive appliance monitoring apparatus*, August 1989.

[33] Electric Power Research Institute, *Low cost NIALMS technology: technical assessment*. Final Report TR-108918-V2, November 1997.

[34] J.G. Roos et al., *Using neural networks for nonintrusive monitoring of industrial electrical loads*. Proceedings of the 10th IEEE Instrumentation and Measurement Technology Conference, May 10-12, 1994, Hamamatsu, South Africa, vol. 3, pp. 1115-1118.

[35] M.L. Marceau and R. Zmeureanu, *Nonintrusive load disaggregation computer program to estimate the energy consumption of major end uses in residential buildings*. Energy Conversion and Management, vol. 41, 2000, pp.1389-1403.

[36] A.I. Cole and A. Albicki, *Nonintrusive identification of electrical loads in a three-phase environment based on harmonic content.* Proceedings of the 17th IEEE Instrumentation and Measurement Technology Conference, May 01-04, 2000, Baltimore, USA, vol. 1, pp. 24-29.

[37] S.B. Leeb et al., *US Patent 5483153-Transient event detector for use in nonintrusive load monitoring systems*, January 1996.

[38] S.R. Kamat, *Fuzzy logic based pattern recognition technique for nonintrusive load monitoring*. Proceedings of IEEE Regional 10 Conference, IEEE Press, vol.3, Nov. 2004, pp. 528-530.

[39] Y. Nakano et al., *Nonintrusive electric appliances load efficient monitoring system using harmonic pattern recognition - performance test results at real households*. The 4th International Conference on Energy

Efficiency in Domestic Appliances and Lighting, London, UK, June 2006.

[40] F. Kupzog, T. Zia and A.A. Zaidi, *Automatic electric load identification in self-configuring micro-grids*. Proceedings of IEEE AFRICON 2009, September 23-25, 2009, Nairobi, Kenya, pp. 1-5.

[41] K. Suzuki et al., *Nonintrusive appliance load monitoring based on integer programming*. Proceedings of SICE Annual Conference, IEEE Press, Aug. 2008, pp. 2742 – 2747.

[42] J. Liang et al., *Load signature study—Part II: Disaggregation framework, simulations and applications.* IEEE Transactions on Power Delivery, vol. 25, no. 2, April 2010, pp. 561-569.

[43] LEM Norma GmbH, *TOPAS 1000 power quality analyzer*. Operating Instructions, 2003, A 5505 1 GA 3 E Rev. A.

[44] L. Wuidart, *Understanding power factor*. Application note, STMicroelectronics, 2003. Available: http://www.st.com/stonline/books/pdf/docs/4042.pdf

[45] W.M. Grady and R.J. Gilleskie, *Harmonics and how they relate to power factor*. Proceedings of EPRI Power Quality Issues and Opportunities Conference, November 1993, San Diego, USA.

[46] H.Y. Lam et al., *Building a vector-based load taxonomy using electrical load signatures*. Proceedings of the International Conference on Electrical Engineering, July 10-14, 2005, Kunming, China.

[47] F. Sultanem, *Using appliance signatures for monitoring residential loads at meter panel level.* IEEE Transactions on Power Delivery, vol. 6, no. 4, October 1991, pp. 1380-1385.

[48] IEEE task force on harmonic simulation and modeling, *Impact of aggregate linear load modeling on harmonic analysis: A comparison of common practice and analytical models*. IEEE Transactions on Power Delivery, vol. 18, no. 2, April 2003, pp. 625-630.

[49] M. Akbar and D.Z.A. Khan, *Modified nonintrusive appliance load monitoring for nonlinear devices*. Proceedings of IEEE Multitopic Conference, December 28-30, 2007, Lahore, Pakistan, pp. 1-5.

[50] H.Y. Lam, G.S.K. Fung and W.K. Lee, *A novel method to construct taxonomy of electrical appliances based on load signature*. IEEE Transactions on Consumer Electronics, vol. 53, no. 2, May 2007, pp. 653-660.

[51] A. Testa and R. Langella, *Harmonic pollution in Italian distribution networks in coincidence with important sport events*. Proceedings of IEEE Power Engineering Society General Meeting, June 24-28, 2007, Tampa, USA, pp. 1-7.

[52] Copper Developement Association, *Harmonics: Causes and effects*. Power Qualty Appliction Guide, version 0b, November 2001.

[53] A. Prudenzi, *A neuron nets based procedure for identifying domestic appliances pattern-of-use from energy recordings at meter panel*. Proceedings of IEEE Power Engineering Society Winter Meeting, vol. 2, August 2002, pp. 941-946.

[54] J. Arrillaga and N.R. Watson, *Power system harmonics*. John Wiley & Sons, West Sussex, 2003.

[55] S.M. Halpin, *Harmonics in power systems*. Taylor & Francis Group, 2006. Available:
http://www.scribd.com/doc/25545204/Power-Quality
(accessed 15.2.2010)

[56] H.S. Matthews et al., *Automatically disaggregating the total electrical load in residential buildings: A profile of the required solution*. Proceedings of Intelligent Computing in Engineering, July 2008, Plymouth, pp. 381-389.

[57] F.C. De La Rosa, *Harmonics and power systems*. CRC Press, Taylor & Francis Group, Florida, 2006.

[58] S.R. Gomez, D. Culler and J. Ortiz, *Load disaggregation for increased coverage in a building energy auditing network*. Index of Programs, University of California, Berkeley, August 2009.

[59] C.E. Efstathiou, *Signal smoothing algorithms*. Available: http://www.chem.uoa.gr/applets/appletsmooth/appl_smooth2.html (accessed 02.06.2010)

[60] C.A.V. Aguilera, *Moving average v3.1*. Available: http://www.mathworks.com/matlabcentral/fileexchange/12276-movingaverage-v3-1-mar-2008 (accessed 13.06.2010)

[61] Arto Merilainen, *Algorithms for event detection and fingerprinting of electrical appliances*. BeAware Project Internal Report, June 23, 2010.

[62] M. Berges et al., *Training load monitoring algorithms on highly sub-metered home electricity consumption data*. Tsinghua Science & Technology, vol. 13, 2008, pp. 406-411.

[63] L. Soibelman et al., *Automatic disaggregation of total electrical load from nonintrusive appliance load monitoring*. Carnegie Mellon University, February 2009.
Available: dodfuelcell.cecer.army.mil/rd/NZE_Workshop/7d_Soibelman.pdf

[64] H.H. Chang, C.L. Lin and H.T. Yang, *Load recognition for different loads with the same real power and reactive power in a non-intrusive load-monitoring system*. Proccedings of the 12th International Conference on Computer Supported Cooperative Work in Design, April 16-18, 2008, Xi'an, China, pp. 1122-1127.

[65] M. Berges et al., *Learning systems for electric consumption of buildings*. Proceedings of the 2009 ASCE International Workshop on Computing in Civil Engineering, June 24-27, 2009, Austin, USA, pp. 1-10.

[66] T.M. Cover and P.E. Hart, *Nearest neighbor pattern classification*. IEEE Transactions on Information Theory, vol. 13, no. 1, Jan. 1967, pp. 21-27.

[67] M. Moradian and A. Baraani, *k-Nearest-neighbor-based-association-algorithm*. Journal of Theoretical and Applied Information Technology, vol. 6, Dec. 2009, pp 123-129.

[68] Toby Segaran, *Programming collective intelligence: Building smart web 2.0 applications*. O'Reilly Media Inc., California, 2007.

[69] Stanford University Department of Statistics, *Correspondence analysis and related methods*. Available: http://www.econ.upf.edu/~michael/stanford/maeb4.pdf (accessed 26.03.2010)

[70] L.E.Peterson, *k-Nearest neighbor*. Scholarpedia, 2009, revision #63491. Available: http://www.scholarpedia.org/article/K-nearest_neighbor (accessed 29.03.2010)

[71] J.D. Kelly, Jr. and L. Davis, *A hybrid genetic algorithm for classification*. Proceedings of the 12th International Joint Conference on Artificial Intelligence, 1991, pp. 645-650.

[72] L. Zhang, F. Coenen and P. Leng, *Setting attribute weights for k-NN based binary classification via quadratic programming*. Intelligent Data Analysis, vol. 7, no. 5, October 2003, pp. 427-441.

[73] B. Sun, J. Du and T. Gao, *Study on the improvement of k-Nearest-Neighbor algorithm*. International Conference on Artificial Intelligence and Computational Intelligence, vol. 4, 2009, pp. 390-393.

[74] L. Jiang et al., *Survey of improving k-Nearest-Neighbor for classification*. 4th International Conference on Fuzzy Systems and Knowledge Discovery, vol. 1, 2007, pp. 679-683.

[75] *k*-Nearest neighbor classifier. Available: http://www.cs.aau.dk/~tdn/itev/uploads/media/DM-KNN.pdf (accessed 24.04.2010)

[76] P. Cunningham and S.J. Delany, *k-Nearest neighbor classifier*. Technical Report, UCD-CSI-2007-4, March 27, 2007.

[77] H. Serra et al., *Domestic power consumption measurement and automatic home appliance detection*. Proceedings of IEEE Workshop on Intelligent Signal Processing, September 1-3 2005, Faro, Portugal, pp. 128-132.

[78] Topi Mikkola, *BeAware WP3 Review 2*. BeAware Project Presentation. Available: http://wiki.hiit.fi/pages/worddav/preview.action?pageId=14943956&fileName=beaware_wp3_review2_presentation.ppt (accessed 20.07.2010)

[79] J. Cavallo and J. Mapp, *Targeting refrigerators for repair and replacement*. Available: http://www.doa.state.wi.us/docs_view2.asp?docid=59 (accessed 17.07.2010)

[80] Beaware Project Ultrasmart advice list. Available: http://wiki.hiit.fi/pages/viewpageattachments.action?pageId=4063372&highlight=smart-ultrasmart_20091111.xls#Workpackage+2+Cognition+and+Practices+of+Energy+Consumption-attachment-smart-ultrasmart_20091111.xls (accessed 24.07.2010)

APPENDIX A

NIALMS performance during the EPRI beta test program –

Appliance Type	NIALMS Identification Success Rate	Average Performance Ratio	Standard Deviation of Performance Ratio	Minimum, Maximum Monthly Performance Ratio	Average % Difference of NIALMS to Parallel
Two-State Appliances					
Central Air Conditioner	100%	0.88	0.030	0.00, 1.04	13.2%
Water Heater	100%	0.96	0.047	0.75, 1.11	3.5%
Pump (well or sewage)	83%	0.99	0.072	0.76, 1.14	3.3%
Furnace Blower	0%	--	--	--	--
Water Bed Heater	100%	0.96	0.109	0.72, 1.11	3.7%
Multi-State Appliances					
Heat Pump	100%	0.81	0.280	0.00, 1.51	23.9%
Electric Space Heat	0%	--	--	--	--
Clothes Dryer	88%	0.96	0.206	0.28, 1.28	10.4%
Refrigerator/Freezer	100%	0.96	0.128	0.65, 1.64	13.9%
Dishwasher	0%	--	--	--	--
Range/Oven	0%	--	--	--	--

Table A-1: Results published at the end of the EPRI beta test period [12]

Average Performance Ratio – sum of the energy estimated by NIALMS during the test period divided by sum of parallel-metered (reference) energy during the same period

Minimum, Maximum Performance Ratios – the monthly minimum and maximum performance ratios during the test period

Average Percentage Difference of NIALMS to Parallel –

$$\left[\frac{(Parallel\ metered\ energy) - (NIALMS\ energy)}{(Parallel\ metered\ energy)}\right] \cdot (100\%)$$

APPENDIX A (contd.)

n	Appliance	m	Operating mode	C_n
1	Fluorescent lamp (Room 1,2,3)	1 2	50W 68W	3
2	Fluorescent lamp (Sink)	1	On (50W)	1
3	Incandescent lamp (Bathroom, Toilet)	1	ON(50/54W)	2
4	Incandescent lamp (Entrance)	1	On (60W)	1
5	Incandescent lamp (Lavatory, Mirror stand)	1	ON(100/120W)	2
6	Air fan (Lavatory)	1	On	1
7	Air fan (Bathroom)	1	On	1
8	Air fan (Toilet)	1	On	1
9	Air fan (Room 3)	1	On	1
10	Air fan (Kitchen)	1	On	1
11	Washing machine	1 2 3 4 5 6 7	15A 13A 9A 5A 4A Idling 1 Idling 2	1

Table A-2: Appliances used for NIALMS based on integer programming [41]

$$
\begin{aligned}
0 \le c_1(1), c_1(2), c_2(1), c_3(1), c_4(1), c_5(1), c_6(1), \\
c_7(1), c_8(1), c_9(1), c_{10}(1), c_{11}(1), c_{11}(2), c_{11}(3), \\
c_{11}(4), c_{11}(5), c_{11}(6), c_{11}(7) \in \mathbb{Z}, \\
c_1(1) + c_1(2) \le 3, \\
c_3(1) \le 2, \\
c_5(1) \le 2, \\
c_k(1) \le 1 \text{ for } k = \{2, 4, 6, \cdots, 10\}, \\
c_{11}(1) + c_{11}(2) + c_{11}(3) + c_{11}(4) \\
+ c_{11}(5) + c_{11}(6) + c_{11}(7) \le 1.
\end{aligned}
$$

Eq. A-1: Constraint conditions derived from the appliance operating states shown in Table A-2 above (input to optimization tool) [41]

APPENDIX B

Specifications of *voltage* and *current sensors* of TOPAS 1000 Power Quality Analyzer:

Voltage sensor 400 V

Measuring range	4...680 V
Accuracy / phase angle	0.11% / 0.005^0 (45 Hz…65 Hz)
	0.15% / 0.034° (65 Hz ...1 kHz)
	0.2% / 0.125° (1 kHz…3 kHz)
Frequency range	45 Hz ...3 kHz

Clip-on current sensor 100/10 A

Measuring range	100 mA...120 A / 100 mA...12 A
Accuracy / phase angle	0.5% / 3.50
Frequency range	45 Hz ...10 kHz

Clip-on current sensor 5/1 A

Measuring range	50 mA…14 A / 50 mA...2.8 A
Accuracy / phase angle	0.5% / 3^0
Frequency range	40 Hz ...5 kHz

APPENDIX B (contd.)

	Appliance name	No. of samples
1	Desktop PC (processor)	4
2	CRT PC monitor	2
3	LCD PC monitor	2
4	Laptop	3
5	Printer	1
6	Scanner	1
7	Energy-saving/CFL lamp	4
8	Fluorescent lamp with conventional ballast	4
9	Fluorescent lamp with electronic ballast	2
10	LED lamp	4
11	Incandescent lamp	2
12	Halogen lamp	2
13	Microwave oven	2
14	Toaster	1
15	Freezer	1
16	Dishwasher	2
17	Refrigerator	1
18	Coffee maker	2
19	CRT television	2
20	LCD television	2
21	Plasma television	1
22	Electric space heater	2
23	Table fan	2
24	Washing machine	1
25	Vacuum cleaner	2

Table B-1: Types of appliances and number of samples used in the measurement work

APPENDIX C

Flow chart for computing:

- Phase shift between *fundamental voltage* and *current harmonics*,
- Phase shift betweeen corresponding *harmonic voltage* and *current*,
- *Crest factor*

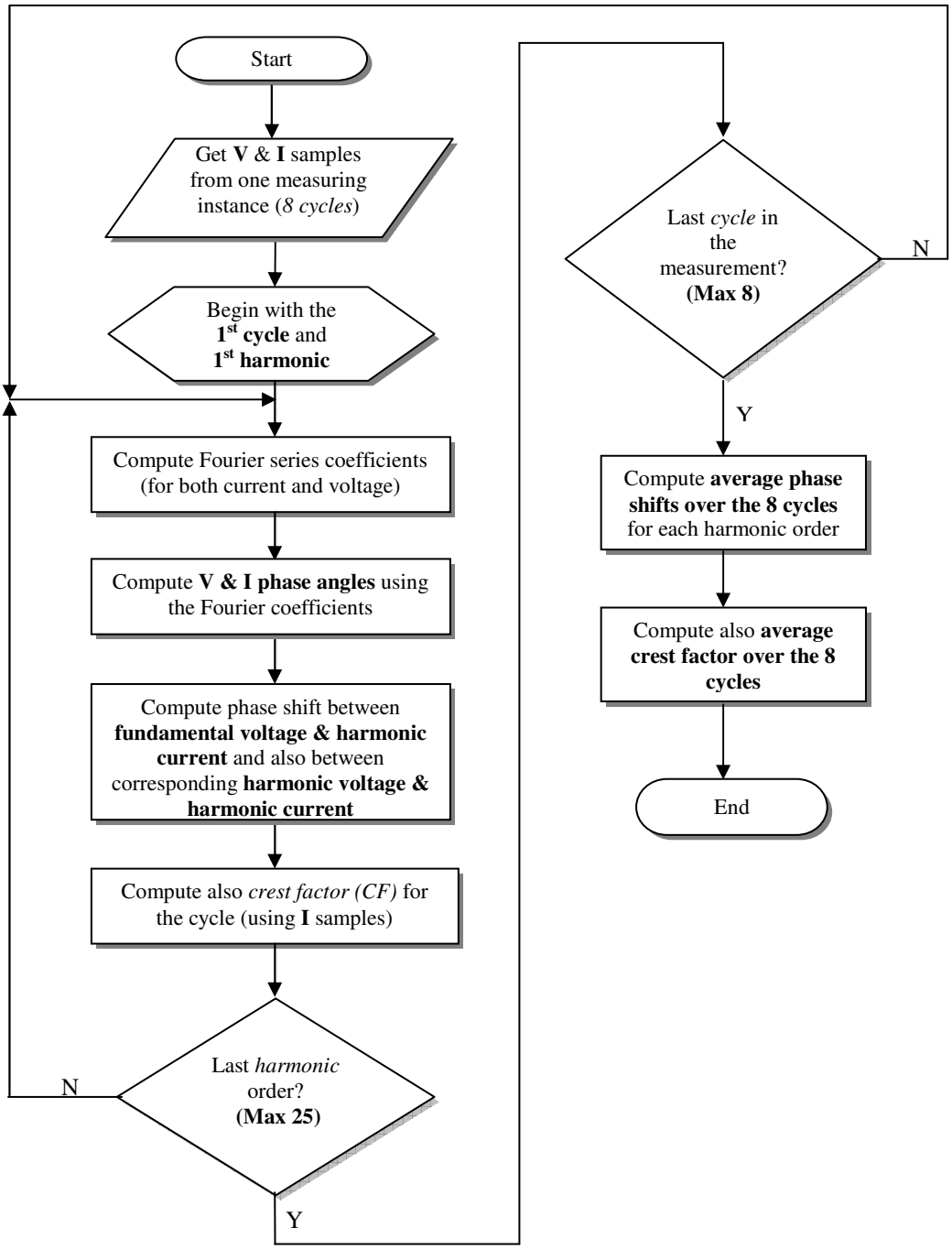

APPENDIX C (contd.)

Harmonic currents phase shift calculation

Results obtained for *vacuum cleaner* and *LCD television* samples (phase shifts of harmonic currents up to 25th order from the fundamental frequency voltage over a *10-minute interval*).

Current harmonic order	1st sample @20:01:29	2nd sample @20:02:29	3rd sample @20:03:29	4th sample @20:04:29	5th sample @20:05:29	6th sample @20:06:29	7th sample @20:07:29	8th sample @20:08:29	9th sample @20:09:29	10th sample @20:10:29
1	**-26.71**	**-26.70**	***153.52***	**-26.45**	***153.51***	***153.79***	**-26.44**	**-26.35**	**-26.09**	**-26.13**
2	47.77	-79.54	85.40	-27.90	75.80	36.54	81.93	-9.59	0.57	69.52
3	**1.10**	**-119.95**	**126.69**	**73.91**	**124.89**	**124.19**	**-13.97**	**-65.54**	**-77.00**	**-8.54**
4	55.43	-92.86	43.05	-23.75	111.65	102.99	41.14	-29.31	-5.20	66.07
5	**65.58**	**3.40**	**136.73**	**31.30**	**133.21**	**131.86**	**35.68**	**-67.61**	**-90.46**	**46.59**
6	41.48	-59.35	68.81	7.89	63.89	36.53	88.54	-16.26	-5.07	70.37
7	-32.77	-36.16	164.24	5.38	158.21	155.84	102.00	-51.30	-86.71	119.42
8	75.11	-70.23	80.03	23.06	98.15	85.68	38.08	-39.50	-13.53	86.59
9	85.49	-38.71	48.46	15.75	39.77	36.00	26.04	2.07	-44.00	50.43
10	9.28	-86.15	80.97	15.95	98.67	68.55	48.19	-7.93	12.72	42.42
11	57.22	-9.67	143.74	60.72	134.99	132.71	-16.25	-86.98	33.00	17.59
12	58.82	-76.72	98.00	10.81	41.64	48.38	66.73	-6.11	-0.59	35.26
13	113.28	-73.35	147.79	10.58	136.59	131.17	23.91	-7.80	11.33	65.86
14	16.59	-127.41	129.87	31.95	77.90	59.50	72.09	18.70	9.15	44.87
15	-7.95	-131.72	151.35	-38.70	140.53	131.39	64.61	67.85	-16.60	101.80
16	83.24	-28.46	35.05	18.49	118.00	95.51	29.98	15.55	-4.58	76.81
17	83.08	-87.19	52.14	-6.99	69.26	42.67	40.32	-63.64	26.20	35.39
18	51.31	-87.08	153.75	-9.24	101.10	76.73	32.51	-21.11	-57.82	41.97
19	35.37	-71.17	77.72	-34.96	62.13	55.91	76.91	-30.91	47.10	118.11
20	11.35	-70.27	135.79	-14.35	81.31	79.23	36.43	13.09	-7.06	12.33
21	89.63	5.63	131.21	-38.91	111.77	99.56	-19.32	10.03	69.85	36.12
22	34.03	-43.55	59.62	-23.04	82.26	78.27	37.51	-20.08	-58.71	14.83
23	64.28	-7.50	4.28	-37.66	95.76	151.14	74.18	45.66	-60.52	128.38
24	70.23	-107.79	117.52	-35.03	50.41	75.94	64.64	-17.92	-14.40	69.90
25	-18.89	-31.91	47.08	-47.25	24.45	11.19	-23.00	-9.40	-60.33	41.12

Table C-1: Harmonic currents phase shift (in degrees) – *vacuum cleaner sample*

APPENDIX C (contd.)

Current harmonic order	1st sample @20:06:29	2nd sample @20:07:29	3rd sample @20:08:29	4th sample @20:09:29	5th sample @20:10:29	6th sample @20:11:29	7th sample @20:12:29	8th sample @20:13:29	9th sample @20:14:29	10th sample @20:15:29
1	**19.35**	**-160.60**	**19.44**	**19.53**	***19.49***	***19.59***	**19.58**	**19.62**	**19.67**	**19.69**
2	85.60	-74.38	-36.88	98.84	52.67	64.01	10.70	5.34	-49.12	-96.93
3	**116.79**	**-162.94**	**-75.04**	**50.50**	**-31.38**	**66.92**	**87.61**	**-74.73**	**59.11**	**-18.81**
4	32.02	-146.53	-61.47	83.27	17.83	35.85	77.88	-66.81	12.37	-24.32
5	**58.18**	**-142.12**	**35.13**	**105.60**	**-12.15**	**138.55**	**0.89**	**34.50**	**-58.33**	**-34.21**
6	61.30	-50.31	-51.02	106.92	23.38	147.81	34.55	-26.07	5.37	-64.79
7	118.59	-3.29	-95.76	99.41	34.46	147.05	34.50	-94.79	-53.87	-107.66
8	57.77	-109.92	-70.12	64.04	-3.14	51.83	76.05	-68.92	-29.93	-72.37
9	50.56	-170.07	3.19	144.30	-0.95	30.07	113.15	4.38	-0.13	-132.29
10	78.70	-64.29	-30.37	94.06	45.04	84.55	96.11	-40.89	-48.84	-77.01
11	82.88	-56.42	22.90	112.46	60.55	11.49	119.23	29.45	-26.81	-52.24
12	102.26	-77.51	-67.67	111.48	95.33	76.60	93.52	-54.17	13.51	-105.10
13	97.55	-141.66	29.52	62.72	113.65	92.86	102.50	28.76	-69.22	1.37
14	77.28	-84.89	-7.68	22.00	40.63	79.04	110.11	-34.08	-6.48	-58.70
15	77.10	-83.83	-7.30	150.48	74.86	83.88	52.36	-4.19	29.40	24.30
16	85.55	-96.18	-88.05	40.66	-10.48	95.21	41.89	-27.42	-54.22	-10.65
17	-9.54	-68.56	-97.29	4.30	53.70	125.38	104.91	-116.27	44.77	-26.20
18	8.70	-116.24	-25.20	116.26	74.68	70.71	123.75	-18.43	-25.87	-94.25
19	-2.79	-5.01	-110.20	114.64	101.58	80.08	89.34	-114.82	5.89	-20.07
20	60.83	-52.88	-48.98	58.85	19.02	74.27	37.19	-59.29	-25.51	-81.06
21	86.29	-21.08	-41.73	131.46	39.09	114.67	105.75	-31.42	36.25	-18.46
22	43.87	-107.25	-38.25	73.63	3.12	70.74	40.65	-15.01	-3.78	-6.55
23	77.80	-124.28	-52.06	62.44	68.13	59.81	113.39	-54.57	-24.20	17.82
24	28.99	-71.87	-17.04	47.53	71.36	52.20	70.25	-33.85	-29.56	-50.72
25	23.53	-100.50	-118.46	121.85	48.24	134.54	29.48	-118.63	42.74	8.11

Table C-2: Harmonic currents phase shift (in degrees) – *LCD television sample*

APPENDIX D

Flow chart for event detection system based on dynamic threshold:

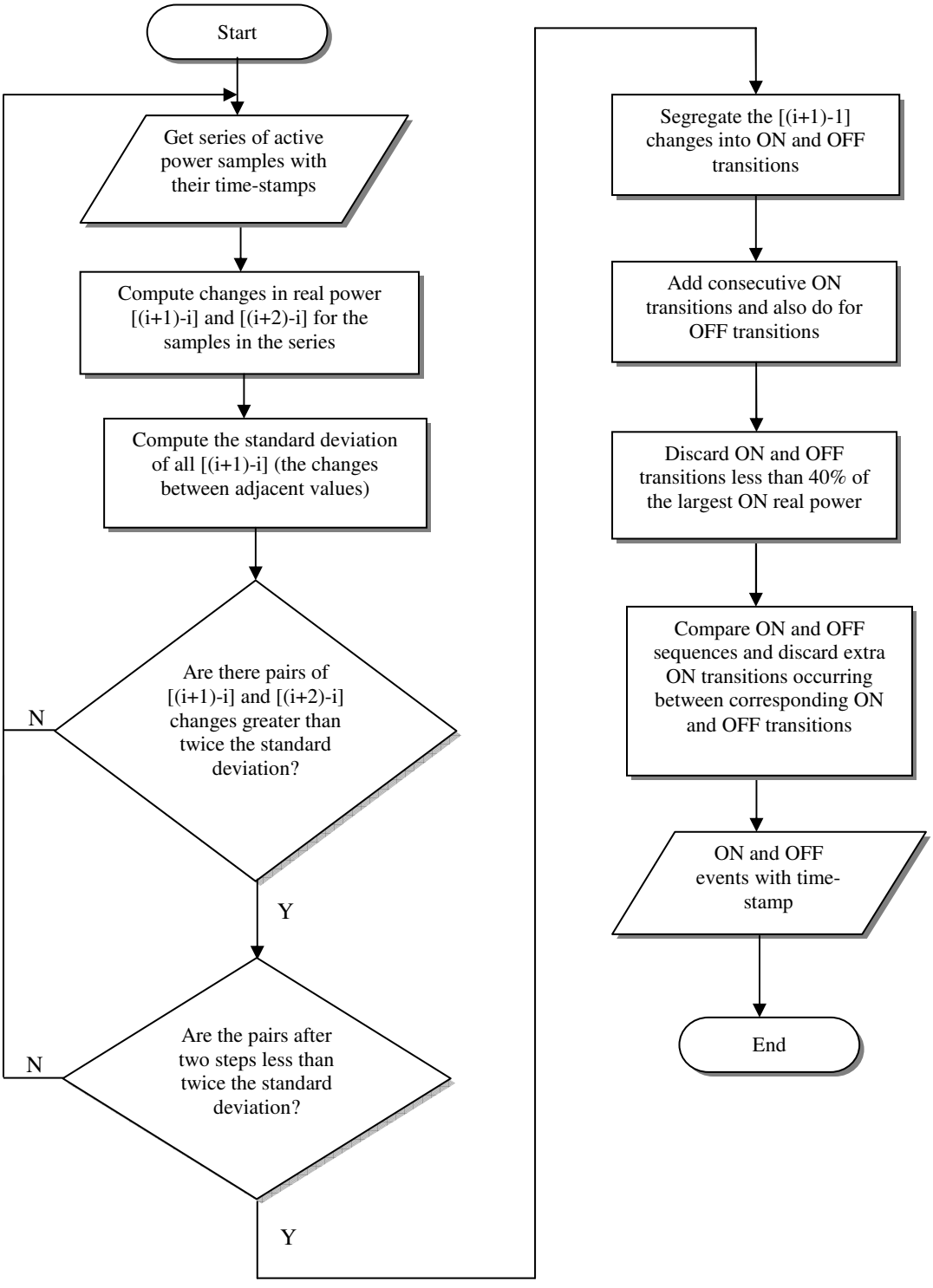

APPENDIX D (contd.)

	Appliance name	Switch ON power [W]		Switch OFF power [W]	
		Test	Actual	Test	Actual
1	Compact fluorescent lamp	12.86	12.86	0.01	0.01
2	Incandescent lamp	101.17	101.17	0.01	0.01
3	Fluorescent lamp (magnetic ballast)	43.77	43.77	0.01	0.01
4	Fluorescent lamp (electronic ballast)	32.24	32.24	0.01	0.01
5	Space heater	860.21	860.21	-0.02	-0.02
6	Toaster	724.10	724.10	*56.82* (1)	0.01
7	Coffee maker (cycle 1)	*994.42* (1)	1032.26	*66.24* (1)	0.30
	Coffee maker (cycle 2)	1012.50	1012.50	0.40	0.40
	Coffee maker (cycle 3)	*907.83* (1)	1004.90	0.40	0.40
	Coffee maker (cycle 4)	1014.60	1014.60	0.30	0.30
8	LCD TV	262.36	262.36	*13.41* (1)	-0.60
9	CRT TV	64.35	64.35	0.02	0.02
10	Desktop PC 1	102.90	102.90	0.55	0.55
	Desktop PC 2	- (2)	114.21	-1.45	-1.45
11	CRT PC monitor 1	124.18	124.18	-0.86	-0.86
	CRT PC monitor 2	314.01	314.01	- (3)	0.16
12	Plasma TV	354.03	354.03	-0.62	-0.62
13	LCD PC monitor	31.02	31.02	-0.09	-0.09
14	Printer	*1326.01* (1)	1432.10	254.60	18.34
15	Laptop 1	52.49	52.49	0.37	0.37
	Laptop 2	- (2)	41.52	*24.79* (1)	0.80
16	Freezer (cycle 1)	552.53	552.53	23.66	23.66
	Freezer (cycle 2)	519.44	519.44	24.32	24.32
	Freezer (cycle 3)	- (2)	378.84	23.79	23.79
	Freezer (cycle 4)	414.45	414.45	24.41	24.41
17	Vacuum cleaner	995.39	995.39	-0.01	-0.01
18	Refrigerator (cycle 1)	- (2)	890.89	- (3)	0.00
19	Microwave oven 500W (cycle 1)	1438.10	1438.10	47.80	47.80
	Microwave oven 500W (cycle 2)	*918.92* (1)	1431.90	47.80	47.80
	Microwave oven 500W (cycle 3)	*918.95* (1)	1493.50	*145.43* (1)	47.70
	Microwave oven 500W (cycle 4)	1407.40	1407.40	47.80	47.80

'Actual' - observed switch-on & switch-off values from the measurement files
'Test' - switch-on & switch-off values from the event detection method

Table D-1: Event detection test results obtained for the appliances monitored during the measurement period.
(1) Accurate within ±2 sec. (2) and (3) undetected events.

APPENDIX E

E.1 – Flow chart for appliance type identification using *distance-weighted k*-NN classifier:

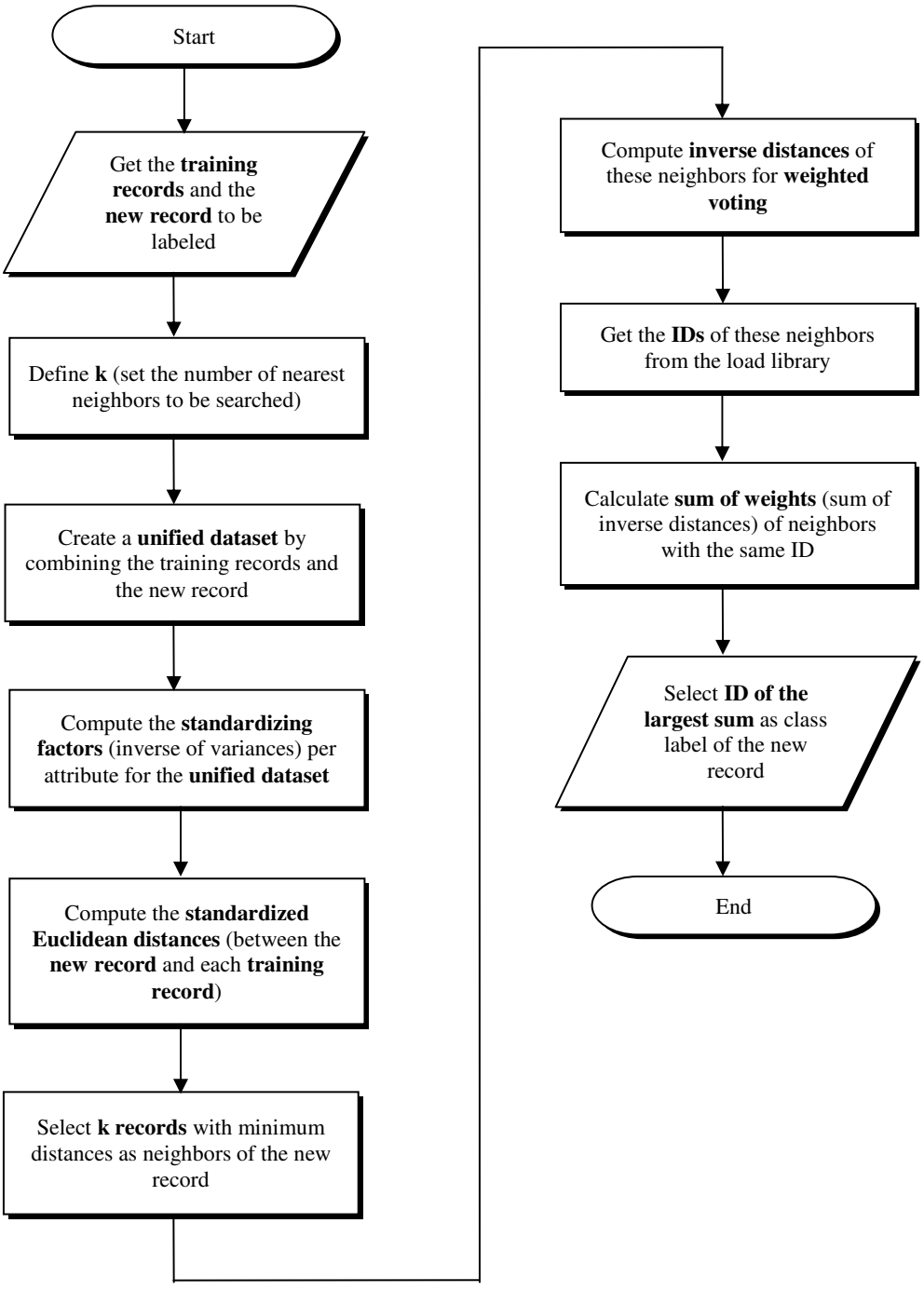

APPENDIX E (contd.)

E.2 – Flow chart for *LEAVE-ONE-OUT-CROSS-VALIDATION* (LOOCV)

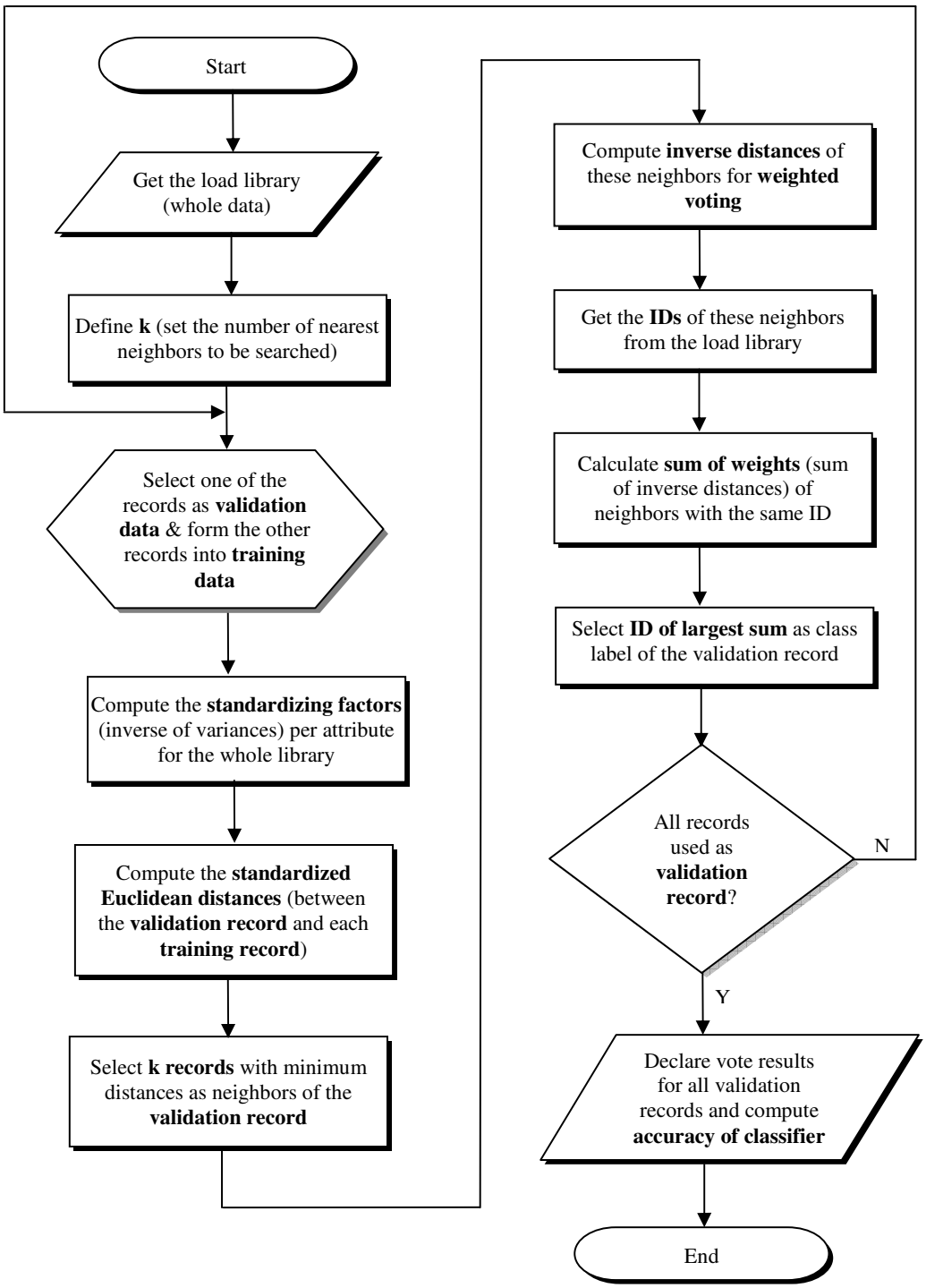

APPENDIX E (contd.)

		k=1	*k=1*	*1*	*2*	*3*	*4*	*5*	*6*	*7*	*8*
APPLIANCE NAME	ID	*result*	*error*(*)	P [W]	PPF	PF	THD	CF	3RD H	5TH H	7TH H
Compact fluorescent (CFL) 1	701	*701*	*0*	14.37	0.863	0.576	110.75	3.38	77.5	45.7	30.1
Compact fluorescent (CFL) 2	701	*713*	*1*	18.09	0.876	0.730	65.05	1.97	52.9	4.5	19.7
Compact fluorescent (CFL) 3	701	*701*	*0*	10.31	0.827	0.519	119.48	4.75	76.3	48.4	28.0
Compact fluorescent (CFL) 4	701	*701*	*0*	10.94	0.847	0.592	101.53	3.07	74.8	41.2	28.6
incandescent lamp 1	702	*702*	*0*	60.83	0.998	0.998	1.35	1.41	0.8	0.1	0.4
incandescent lamp 2	702	*702*	*0*	101.56	0.998	0.998	1.2	1.41	0.4	0.1	0.4
halogen lamp 1	702	*702*	*0*	53.88	0.998	0.997	1.4	1.41	0.8	0.4	0.4
halogen lamp 2	702	*702*	*0*	42.17	0.998	0.997	1.5	1.41	0.9	0.4	0.4
halogen lamp 3 (with integrated transformer)	702	*707*	*1*	29.54	0.979	0.975	8.4	1.44	4.3	3.3	3.7
LED lamp 1	704	*718*	*1*	7.24	0.841	0.798	29.7	1.57	24.2	11.9	4.9
LED lamp 2	704	*701*	*1*	5.94	0.834	0.656	78.0	2.46	62.6	30.3	21.7
LED lamp 3	704	*704*	*0*	16.33	0.975	0.476	178.9	4.85	93.7	82.8	68.7
LED lamp 4	704	*704*	*0*	5.79	0.971	0.469	175.7	4.96	93.8	81.8	66.5
Fluorescent lamp (magnetic ballast) 1	705	*705*	*0*	53.78	0.526	0.523	9.4	1.52	9.1	1.4	2.0
Fluorescent lamp (magnetic ballast) 2	705	*705*	*0*	86.26	0.515	0.512	10.1	1.51	9.7	1.6	1.6
Fluorescent lamp (magnetic ballast with PFC) 1	706	*706*	*0*	45.42	0.968	0.926	29.4	1.58	19.8	4.5	4.7
Fluorescent lamp (magnetic ballast with PFC) 2	706	*706*	*0*	78.78	0.990	0.957	25.5	1.65	20.4	3.7	4.1
Fluorescent lamp (electronic ballast) 1	707	*707*	*0*	34.70	0.991	0.987	9.7	1.52	8.9	2.4	1.3
Fluorescent lamp (electronic ballast) 2	707	*707*	*0*	97.86	0.996	0.992	9.4	1.53	9.0	1.5	1.0
Coffee maker 1	708	*709*	*1*	966.87	0.998	0.996	1.4	1.40	0.2	0.4	0.7
Coffee maker 2	708	*709*	*1*	2079.16	0.999	0.999	1.2	1.42	1.0	0.5	0.4
Coffee maker 3	708	*709*	*1*	1493.93	0.998	0.998	1.7	1.40	0.8	0.9	0.7
Space heater 1 (level 1)	709	*708*	*1*	815.13	0.997	0.997	0.9	1.41	0.5	0.4	0.5
Space heater 1 (level 2)	709	*709*	*0*	1196.09	0.999	0.999	0.9	1.41	0.2	0.4	0.5
Space heater 2	709	*708*	*1*	1013.03	0.999	0.999	2.1	1.38	1.3	1.0	0.8
Space heater 1 (level 1 & 2)	709	*708*	*1*	2010.45	0.998	0.997	0.8	1.41	0.2	0.4	0.4
PC LCD monitor 1	711	*711*	*0*	36.72	1.000	0.580	138.4	3.07	91.5	75.5	55.6
PC LCD monitor 2	711	*711*	*0*	33.93	0.937	0.500	156.9	3.51	90.5	80.9	68.9
Laptop 1	713	*713*	*0*	19.72	0.973	0.380	229.3	4.93	90.8	86.8	84.0
Laptop 2	713	*713*	*0*	23.36	0.966	0.374	233.6	4.92	96.4	93.0	89.1
Laptop 3	713	*720*	*1*	34.32	0.950	0.845	44.9	2.01	41.5	4.5	8.2
Desktop computer 1	718	*723*	*1*	65.24	0.833	0.821	14.99	1.63	13.2	1.6	2.8
Desktop computer 2	718	*719*	*1*	110.35	0.995	0.772	81.60	2.60	70.9	32.1	17.4
Desktop computer 3	718	*719*	*1*	45.98	0.999	0.673	111.03	2.72	86.1	56.7	30.5
Desktop computer 4	718	*720*	*1*	84.25	0.990	0.721	90.86	2.49	78.0	42.8	16.1
CRT TV 1	719	*720*	*1*	84.14	0.969	0.761	79.4	2.34	70.5	32.4	12.4
CRT TV 2	719	*718*	*1*	65.44	0.989	0.630	116.7	2.66	86.3	63.1	37.5
CRT monitor 1	720	*706*	*1*	82.90	0.946	0.903	30.9	1.77	29.5	6.4	2.4
CRT monitor 2	720	*719*	*1*	88.49	0.991	0.762	83.1	2.25	74.1	34.3	11.5
Vacuum cleaner 1 (normal op mode)	721	*725*	*1*	820.70	0.895	0.785	56.1	2.10	52.8	17.5	6.4
Vacuum cleaner 1 (max op mode)	721	*721*	*0*	1119.10	0.990	0.961	24.5	1.67	24.3	1.2	1.6
Vacuum cleaner 2	721	*721*	*0*	1130.37	0.999	0.988	14.4	1.59	14.2	0.8	1.4
Table fan 1 (level 1)	722	*722*	*0*	26.80	0.615	0.610	12.0	1.50	11.9	1.4	0.9
Table fan 1 (level 2)	722	*722*	*0*	33.59	0.615	0.610	13.3	1.50	13.0	2.3	1.1
Table fan 2	722	*726*	*1*	28.38	0.924	0.924	2.7	1.42	0.8	1.1	1.5
Refrigerator 1 (steady op cycle)	723	*723*	*0*	11.20	0.776	0.773	8.1	1.51	7.5	2.0	1.4
Refrigerator 1 (starting op cycle)	723	*723*	*0*	99.50	0.734	0.731	8.1	1.49	7.6	2.1	1.4
Freezer 1	723	*723*	*0*	334.27	0.684	0.681	10.2	1.54	8.7	1.7	1.4
Cloth washer (water filling and pre-wash cycle)	725	*725*	*0*	55.33	0.498	0.318	76.0	2.59	56.9	34.5	16.2
Cloth washer (water heating and washing cycle)	725	*708*	*1*	2100.99	0.997	0.996	12.7	1.37	10.3	5.0	2.1
Cloth washer (washing cycle)	725	*725*	*0*	130.50	0.466	0.321	93.2	2.54	74.9	39.8	13.3
Cloth washer (water draining cycle)	725	*725*	*0*	132.25	0.532	0.404	82.2	2.50	65.0	35.5	14.8
Cloth washer (re-wash cycle)	725	*725*	*0*	156.84	0.500	0.353	74.7	2.51	61.9	27.5	10.2
Cloth washer (spinning cycle)	725	*721*	*1*	420.85	0.859	0.799	47.0	2.47	42.0	9.9	8.5
Dish washer (water filling cycle)	726	*726*	*0*	76.23	0.897	0.883	5.3	1.56	0.8	1.3	0.9
Dish washer (water heating cycle)	726	*726*	*0*	1874.41	1.000	1.000	0.7	1.42	0.2	0.1	0.4
Dish washer (pre-wash & re-filling cycle)	726	*726*	*0*	83.85	0.928	0.927	8.6	1.60	1.5	2.1	2.0
Dish washer (heating)	726	*726*	*0*	1873.19	1.000	1.000	0.7	1.41	0.2	0.2	0.4
Dish washer (washing)	726	*726*	*0*	76.18	0.930	0.893	6.1	1.64	1.2	1.2	1.3
Microwave oven 1 (at 500 W)	727	*727*	*0*	796.87	0.990	0.731	27.9	1.66	23.6	12.3	5.0
Microwave oven 1 (at 350 W)	727	*727*	*0*	589.69	0.981	0.630	29.5	2.16	25.1	12.8	5.1
classification accuracy **62.30%**											

Table E-1: Classification result using *k*-NN at *k*=1

(**Legend**: $Error = \mathbf{0}$ – *correct classification*; $Error = \mathbf{1}$ – *misclassification*)

APPENDIX F

Electronic copies of the followng documents are available on CDROM at the Power Systems Laboratory:

- Measurement data for each appliance in the test domain (in TOPAS file format)
- Appliance-wise measurement reports (in MS-Excel format)